

UC Santa Barbara

UC Santa Barbara Electronic Theses and Dissertations

Title

Network Science of Teams: Dynamics, Algorithms, and Implications

Permalink

<https://escholarship.org/uc/item/2b17v2v5>

Author

mohagheghi, Shadi

Publication Date

2020

Peer reviewed|Thesis/dissertation

University of California
Santa Barbara

Network Science of Teams: Dynamics, Algorithms, and Implications

A dissertation submitted in partial satisfaction
of the requirements for the degree

Doctor of Philosophy
in
Electrical and Computer Engineering

by

Shadi Mohagheghi

Committee in charge:

Francesco Bullo, Chair
Professor João P. Hespanha,
Professor Jason R. Marden
Professor Ambuj K. Singh

March 2020

The Dissertation of Shadi Mohagheghi is approved.

Professor João P. Hespanha,

Professor Jason R. Marden

Professor Ambuj K. Singh

Francesco Bullo, Committee Chair

March 2020

Network Science of Teams: Dynamics, Algorithms, and Implications

Copyright © 2020

by

Shadi Mohagheghi

To Monique and Frida

Acknowledgements

I would like to extend my sincere gratitude to my advisor, Francesco Bullo, for his unrelenting support, guidance, and encouragement throughout my graduate studies. Francesco nurtured my ideas and aspirations, and his valuable insights played a decisive role in my experience. I gratefully acknowledge the assistance of my committee members. Special thanks to Professor Ambuj Singh for his support, advice, and belief in my work.

I very much appreciate the opportunity to work with Professors Sandro Zampieri and Noah Friedkin. I also wish to thank Dr. Wenjun Mei, Dr. Pushkarini Agharkar, and Professor Jingying Ma for their contributions. I would like to recognize the assistance that I received from all of our lab members, as well as my colleagues in the MURI and IGERT programs, who never hesitated to help.

I am also grateful for the opportunity to work with UCSB CSEP and SRA programs. I particularly thank Dr. Lina Kim for supporting my work and for her invaluable career advice. I must also thank Angela Zhang and Rachel Redberg for assisting me in fulfilling my educational ambitions.

I have been fortunate to have had great friends throughout my academic life whose support cannot be overestimated, among whom I particularly would like to thank Manie for always encouraging me to reach new heights, and from whom I learned integrity and dedication to work; and Angela, Nazanin, and Anokina for their continued support and kindness.

I am deeply appreciative of my family: my mother, Monique, for her unconditional dedication, support, and strength, and for being my role model. I'm deeply indebted to my aunt, Frida, without whose support none of my achievements, great or small, would have been possible. Many thanks to my caring uncle and aunt, Ali and Manijeh.

Curriculum Vitæ

Shadi Mohagheghi

Education

- 2020 Ph.D. in Electrical and Computer Engineering, University of California, Santa Barbara.
- 2015 BS in Electrical Engineering, University of California, Los Angeles

Professional Experience

- 2015-2020 **Graduate Student Researcher**
University of California, Santa Barbara
Developing community detection algorithms for identifying the structure of organizational networks. Designed algorithms for generating organizational network models, analyzed different dynamics on them, and developed dynamic game-theoretic models for such models formation (supported by the US ARL). Studied epidemic diffusion dynamics over arbitrary graph topologies; proposed novel results on system behavior. Designing and Implementing coverage and formation control schemes on non-convex environments
- 2019-2020 **Computer Vision Intern**
Toyon Research Corporation
Implementing deep learning algorithms (semantic and instance segmentation) for 3D model reconstruction and low-shot detection in satellite imagery through various neural net architectures.
- Feb.-Sep. 2015 **Software Engineer Intern**
SurfX Technologies
Developed the software and User Interface for the company's plasma system: Designing, implementing, testing, and debugging the algorithms in Python for serial port communications (RS-232) and micro-controllers
- 2014-2015 **Research Assistant**
Adaptive Systems Laboratory at UCLA
Developed an interactive educational mobile app demonstrating DSP concepts, edited Dr. Sayed's Digital Signal Processing textbook
- Summer 2014 **Summer Research Intern**
Center for Domain Specific Computing at UCLA
Implemented and simulated a number of error correction codes to study the different aspects of currently available ECC schemes in terms of effectiveness

Teaching/Mentorship Experience

Summer 2019	Lecturer , <i>UCSB Summer Sessions</i> Social Networks: Data Analysis, and Artificial Intelligence
Fall 2018	Instructor , <i>UCSB School for Scientific Thought</i> Course on Networks
Winter 2018	Teaching assistant , <i>UCSB Electrical and Computer Engineering Department</i>
Summer 2017	Instructor and project mentor , <i>UCSB Summer Institute in Mathematics and Science</i>
Summers 2016/2017	Bootcamp instructor and mentor , <i>UCSB Network Science Graduate Program</i>

Honors and Awards

Fall 2015	NSF-funded Network Science (IGERT) fellowship at UCSB
Winter 2015	Katehi-Tseregounis Endowed Scholarship in Electrical Engineering
Fall 2013	UCLA Faculty Women's Scholarship
Fall 2013	UCLA Luckenbach and Stout Memorial Scholarships
June 2012	R. Luke Scholarship for excellence in mathematics and Excellence in Physics Awards
June 2012	JPLUS (JPL Undergraduate Scholar) Award

Publications

- W. Mei, S. Mohagheghi, S. Zampieri, and F. Bullo. On the dynamics of deterministic epidemic propagation models over networks. *Annual Reviews in Control*, Jan. 2017.
- S. Mohagheghi, P. Agharkar, N. E. Friedkin, and F. Bullo. Multi-Group Connectivity Structures and their Implications. *Network Science*, June 2019.
- S. Mohagheghi, J. Ma, F. Bullo. Stable and Efficient Structures in Multigroup Network Formation. *IEEE Transactions on Computational Social Systems*, Dec. 2019 (Submitted).

Abstract

Network Science of Teams: Dynamics, Algorithms, and Implications

by

Shadi Mohagheghi

The scientific world has witnessed a significant paradigm shift in recent years: that the networks should not be studied in isolation from the processes taking place over them and the large amounts of data derived and generated by them. Science has now embraced a systems approach that captures the effect of the interconnections between individual units and the behavior of a network system. This dissertation provides modeling and analysis of dynamical phenomena over interconnected network systems.

In chapter 1, we review a class of deterministic nonlinear models for the propagation of infectious diseases over contact networks with strongly-connected topologies. We consider network models for susceptible-infected (SI), susceptible-infected-susceptible (SIS), and susceptible-infected-recovered (SIR) settings. In each setting, we provide a comprehensive nonlinear analysis of equilibria, stability properties, convergence, monotonicity, positivity, and threshold conditions.

The recent convergence of research in social sciences, dynamic modeling, and network science has encouraged reexamining the collective team behavior from a quantitative perspective. Research shows that teams cannot be understood fully by studying their members in isolation. To study the coordination and control features of a group task, the multiple subgroups' performances must be fitted together. On such decomposed tasks, group performance is more than a simple union of subgroup performances. This work aims to understand how patterns of interactions among teams impact performance.

In chapter 2, we investigate the implications of different forms of multi-group connec-

tivity. Four multi-group connectivity modalities are considered: co-memberships, edge bundles, bridges, and liaison hierarchies. We propose generative models to generate these four modalities. Our models are variants of planted partition or stochastic block models conditioned under certain topological constraints. We report findings of a comparative analysis in which we evaluate these structures, controlling for their edge densities and sizes, on mean rates of information propagation, convergence times to consensus, and steady state deviations from the consensus value in the presence of noise as network size increases.

In chapter 3, we present a strategic network formation model predicting the emergence of multigroup structures. Individuals decide to form or remove links based on the benefits and costs those connections carry; we focus on bilateral consent for link formation. We are interested in structures that arise to resolve coordination issues and, specifically, structures in which groups are linked through bridging, redundant, and co-membership interconnections. We characterize the conditions under which certain structures are stable and study their efficiency as well as the convergence of formation dynamics.

Contents

Curriculum Vitae	vi
Abstract	viii
1 Dynamics of Epidemic Propagation over Networks	1
1.1 Introduction	1
1.2 Model Set-Up and Notations	8
1.3 Susceptible-Infected Model	10
1.4 Susceptible-Infected-Susceptible model	15
1.5 Network Susceptible-Infected-Recovered Model	25
1.6 Conclusion	37
2 Multi-group Connectivity Structures and Their Implications	39
2.1 Introduction	39
2.2 Methods	46
2.3 Results	51
2.4 Discussion	58
2.5 Permissions and Attributions	62
3 Stable and Efficient Structures in Multigroup Network Formation	66
3.1 Introduction	66
3.2 Multigroup Network Formation Model	72
3.3 Results on Formation of Disjoint Cliques	77
3.4 Two Group Connectivity Structure	80
3.5 Multigroup Connectivity Structure	94
3.6 Conclusion	101
3.7 Permissions and Attributions	102
A Algorithm Specifications	107
Bibliography	109

Chapter 1

Dynamics of Epidemic Propagation over Networks

1.1 Introduction

Problem motivation and description

Propagation phenomena appear in numerous disciplines. Examples include the spread of infectious diseases in contact networks, the transmission of information in communication networks, the diffusion of innovations in competitive economic networks, cascading failures in power grids, and the spreading of wild-fires in forests.

One important class of models of propagation phenomena are scalar deterministic models. These models have been widely studied, e.g., see the survey [1]. These models qualitatively capture some dynamic features, including phase transitions and asymptotic states. However, shortcomings of scalar models are also prominent: for example, scalar models are typically based on the assumption that individuals in the population have the same chances of interacting with each other. This assumption overlooks the internal

structure of the network over which the propagation occurs, as well as the heterogeneity of individuals in the network. Both these aspects play critical roles in shaping the dynamical behavior of the propagation processes.

In a general formulation, propagation is a dynamical process on a complex network. Each network node has a state taking value in a discrete set and state changes are influenced by the nodes' neighbors in the network. Many relevant research questions arise naturally, including: how to model the local dynamics at each node, how to identify model parameters, how to estimate the state of such a dynamical system, and how to analyze the system transient and asymptotic properties.

Various types of models have been proposed to describe propagation processes over complex networks; one key distinguishing feature of these models is whether the propagation dynamics is assumed to be stochastic or deterministic. Deterministic network epidemic models were originally proposed in the late 1970's in the seminal works [2, 3]. These models are of great research value, as attested by the large literature focusing on them (see below). Moreover, they can be considered as approximations of certain Markov-chain models, e.g., see [4].

In this chapter, we review three key continuous-time deterministic models for epidemic propagation over networks. Depending upon the nodal dynamics, i.e., the disease propagation behavior, deterministic epidemic propagation models are classified as: the *Susceptible-Infected* (SI) model, the *Susceptible-Infected-Susceptible* (SIS) model and the *Susceptible-Infected-Recovered* (SIR) model; basic representations of these models are illustrated in Figure 1.1. In this work we focus on transient and asymptotic behavior of these three continuous-time dynamical models over networks. It is our key objective to relate the structure of the network to the function of the network (i.e., the transient and asymptotic behavior of the propagation phenomenon).

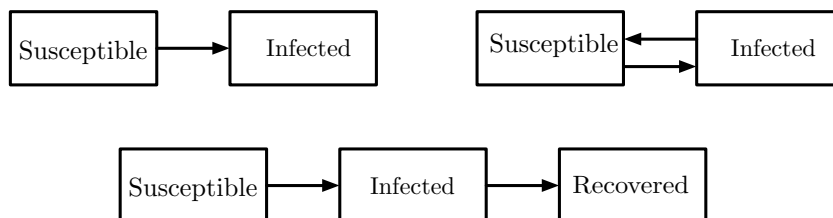


Figure 1.1: Three basic models of infectious diseases: SI, SIS and SIR.

Literature review on deterministic epidemic models over networks

The literature on epidemic propagation is exceedingly vast. This chapter focuses on deterministic models over networks and on their dynamical behavior. Accordingly, this subsection reviews the literature on deterministic epidemic models. Unless specified, the works and results reviewed in what follows are all for the deterministic models. For readers interested in Markov-chain models and in the mean-field approximation method, we refer to [4, 5, 6, 7] and [8, Chapter 17]. (Note that Markov-chain network epidemic models and their deterministic approximating models are different in some of the dynamical properties, such as the epidemic threshold and the asymptotic behavior.)

The dynamics of several classic scalar epidemic models, i.e., the population models without network structure, are surveyed in detail by Hethcote in [1]. Among the different metrics discussed, identifying the *effective reproduction number* R is of particular interest to researchers; R is the expected number of individuals that a randomly infected individual can infect during its infection period. In these scalar models, whether an epidemic outbreak occurs or the disease dies down depends upon whether $R > 1$ or $R < 1$, i.e., upon whether the system is above or below the so-called *epidemic threshold*. Here by epidemic outbreak we mean an exponential growth of the fraction of the infected population for small time. The *basic reproduction number* R_0 is the effective reproduction number in a fully-healthy susceptible population. In what follows we focus our review

on deterministic network models.

The earliest work on the (continuous-time heterogeneous) SIS model on networks is [2]. This work proposes an n -dimensional model on a contact network and analyzes the system's asymptotic behavior. This article proposes a rigorous analysis of the threshold for the epidemic outbreak, which depends on both the disease parameters and the spectral radius of the contact network. For the case when the basic reproduction number is above the epidemic threshold, this chapter establishes the existence and uniqueness of a nonzero steady-state infection probability, called the endemic state. In what follows we refer to the model by [2] as the *network SIS model*; it is also known as the multi-group or multi-population SIS model.

Allen [9] proposes and analyzes a discrete-time network SIS model. This work appears to be the first to revisit and formally reproduce, for the discrete-time case, the earlier results by [2]; see also the later [10]. This work confirms the existence of an epidemic threshold, as a function of the spectral radius of the contact network. Further recent results on the discrete-time model are obtained by Ahn and Hassibi [11] and by Azizan Ruhi and Hassibi [5].

Van Mieghem et al. [12] argue that the (continuous-time) network SIS model is in fact the mean-field approximation of the original Markov-chain SIS model of exponential dimension; this claim is rigorously proven in [4]. Van Mieghem et al. [12] refer to this model as the intertwined SIS model and write the endemic state as a continued fraction.

The works [13] and [14] discuss the continuous-time network SIS model in a more modern language. Fall et al. [13] refer to this model as the n -group SIS model and apply Lyapunov techniques and Metzler matrix theory to establish existence, uniqueness, and stability of the equilibrium points below and above the epidemic threshold. Khanafer et al. [14] use positive system theory in their analysis and extend the existence, uniqueness, and stability results to the setting of weakly connected digraphs.

Numerous extensions of these basic results on the network SIS model and other related works have appeared over the years. For example, the estimation of the epidemic threshold in contact networks with power-law degree distributions has been studied both by mathematically rigorous analysis, see [15], and by numerical simulation, see [16]. The deterministic network SIS models without mean-field approximation and with second-order mean-field approximation have been analyzed in [17] and [18], respectively.

An early work by Hethcote [3] proposes a general multi-group SIR model with birth, death, immunization, and de-immunization. The epidemic threshold and the equilibria below/above the threshold are characterized. For the simplified model without birth/death and de-immunization, [3] proves that the system converges asymptotically to an all-healthy state. Guo et al. consider a generalized network SIR model with vital dynamics, that is, with birth and death in [19]. They characterize the basic reproduction number and, through a careful Lyapunov analysis, show the existence and global asymptotic stability of an endemic state above the threshold. Youssef and Scogli [20] study a special case of the network SIR model under the name of individual-based SIR model over undirected networks. Through a simulation-based analysis, the epidemic threshold is given as a function of the spectral radius of the network.

There are also some extensions and related studies regarding the network SIR model. Sharkey investigates the deterministic network SIR model without mean-field approximation in [21]. Castellano and Pastor-Satorras [16] point out that the (mean-field) network SIR predicts a vanishing threshold for a certain class of power-law distributed networks, which is inconsistent with the corresponding stochastic SIR model. Sharkey et al. [22] show that, different from the network SIR model with mean-field approximation, the so-called pair-based approach gives an exact description of the stochastic SIR process for the tree topology.

To the best of our knowledge, no works have comprehensively characterized the prop-

erties of the network SI model.

We conclude by mentioning other surveys and textbook treatments. In [23], the stability of equilibria for the SEIR model is reviewed through Lyapunov and graph theory. The additional state E represents the exposed population, i.e., the individuals who are infected but not infectious. Various heterogeneous epidemic models are reviewed in [24, Chapter 17], [25, Chapter 21], and [26, Chapter 9]. The recent survey by Nowzari et al. [7] presents various epidemic models and addresses many solved and open problems in the control of epidemic spreading.

Statement of Contribution

This chapter reviews, in a comprehensive and coherent manner, deterministic models and dynamical behavior of SI, SIS and SIR epidemic phenomena over networks. This review includes known results from the literature as well as several novel results. We discuss SI, SIS and SIR models in three subsequent corresponding sections. Each section starts by reviewing the well-known results for the corresponding scalar models; these are the models in which variables represent an entire "well-mixed" population or nodes of an all-to-all unweighted graph. The core of each section is a discussion about multi-group network models. We provide a tutorial treatment with comprehensive statements and proofs for the deterministic network SI, SIS and SIR models.

We first analyze the network SI model. We analyze its asymptotic convergence, positivity of infection probabilities, initial and asymptotic growth rates, and the stability of equilibria. We show that in the network SI model, the system does not display a threshold and, with the exception of the trivial no-epidemics equilibrium, all the trajectories converge to the full contagion state. While these results are not technically difficult, they are novel here in the sense that, to the best of our knowledge, the properties of the

network SI model have never before been formally characterized.

Next we focus on the network SIS model. Our presentation includes known results from [2] (see also [13, 14]) regarding the epidemic threshold, the system's behavior below the epidemic threshold, the existence and uniqueness of the endemic state for systems above the epidemic threshold, and the asymptotic stability of the endemic state. Moreover, we provide a novel provably-correct iterative algorithm for computing the fraction of infected individuals converging to the endemic state. This algorithm also provides an alternative proof for the existence and uniqueness of the endemic state for systems above the epidemic threshold. We argue that this alternative proof is more concise than the those proposed in the previous works [2, 13, 14]. In addition, we present novel Taylor expansions for the endemic state near the epidemic threshold and in the limit of high infection rates. These novel Taylor expansions shed light on these previously poorly-understood regimes. Finally, we show that the spread of infection takes place instantaneously upon infecting at least one node in the network.

Finally, for the network SIR model, we review some known results on the monotonicity of the individuals' susceptible probabilities and the system's asymptotic behavior from [3]. More importantly, we provide the several novel results: We present novel transient behavior and system properties. First, we propose new threshold conditions above which the epidemic grows initially, and below which it exponentially dies down. The initial rate of growth above the threshold is given in terms of network characteristics, initial conditions, and infection parameters. Moreover, we show that our proposed weighted average of the infected population, obtained by the entries of dominant eigenvector of an irreducible quasi-positive matrix, captures information regarding the distribution of infection in the system. We also establish positivity of the infection probabilities. Finally, we provide a novel iterative algorithm to compute the asymptotic state of the network SIR model, with any arbitrary initial condition. For the iterative algorithm, the existence

and uniqueness of the fixed point, and the convergence of the iteration are rigorously proved. Our results are analogous to the scalar SIR model properties and are valid for any arbitrary network topologies. In comparison with [20], our treatment builds on their numerical results but our result is more general in that it does not depend upon specific initial conditions and graph topologies, and establishes numerous properties, including the novel characterization of epidemic threshold.

Organization

Section 1.2 introduces our model set-up and some preliminary notations. The SI, SIS and SIR models are presented, respectively, in Sections 1.3, 1.4, and 1.5. Section 6 is the conclusion.

1.2 Model Set-Up and Notations

For the scalar models, we use the notation $x(t)$ ($s(t)$ and $r(t)$ resp.) for the fraction of infected (susceptible and recovered resp.) individuals in the population at time t . The rest of this section is about the notations and basic model set-up for the network epidemic model.

a) Contact Network: The epidemics are assumed to propagate over a weighted digraph $G = (V, E)$, where $V = \{1, \dots, n\}$ and E is the set of directed links. Nodes of G can be interpreted as either single individuals in the contact network or as homogeneous populations of individuals at each location/node in the contact network. $A = (a_{ij})_{n \times n}$ denotes the adjacency matrix associated with G . For any $i, j \in V$, a_{ij} characterizes the contact strength from node j to node i . For $(i, j) \in E$, $a_{ij} > 0$ and for $(i, j) \notin E$, $a_{ij} = 0$. In this chapter, G is assumed to be strongly connected.

b) Node States and Probabilities: For different epidemic propagation models, the set

of possible node states are distinct. For network SI or SIS models, each node can be in either the “susceptible” or “infected” state, while in the network SIR model, there is an additional possible node state: “recovered.” For a graph in which the nodes are single individuals, let $s_i(t)$ ($x_i(t)$ and $r_i(t)$ resp.) be the probability that individual i is in the susceptible (infected and recovered resp.) state at time t . Alternatively, if the nodes are considered to be the populations, then $s_i(t)$ ($x_i(t)$ and $r_i(t)$ resp.) is interpreted as the fraction of susceptible (infected and recovered resp.) individuals in population i . In this chapter without loss of generality, we adopt the interpretation of nodes as single individuals.

c) Frequently Used Notations: The symbol \mathbb{R} denotes the set of real numbers, while $\mathbb{R}_{\geq 0}$ denotes the set of non-negative real numbers. The symbol ϕ denotes the empty set. For any two vectors $x, y \in \mathbb{R}^n$, we write

$$\begin{aligned} x \ll y, & \quad \text{if } x_i < y_i \text{ for all } i \in \{1, \dots, n\}, \\ x \leq y, & \quad \text{if } x_i \leq y_i \text{ for all } i \in \{1, \dots, n\}, \text{ and} \\ x < y, & \quad \text{if } x \leq y \text{ and } x \neq y. \end{aligned}$$

We adopt the shorthand notations $\mathbb{1}_n = [1, \dots, 1]^\top$ and $\mathbb{0}_n = [0, \dots, 0]^\top$. Let I_n denote the $n \times n$ identity matrix. Given $x = [x_1, \dots, x_n]^\top \in \mathbb{R}^n$, let $\text{diag}(x)$ denote the diagonal matrix whose diagonal entries are x_1, \dots, x_n . For an irreducible nonnegative matrix A , let $\lambda_{\max}(A)$ denote the dominant eigenvalue of A that is equal to the spectral radius $\rho(A)$. Moreover, we let $v_{\max}(A)$ ($u_{\max}(A)$ resp.) denote the corresponding entry-wise strictly positive left (right resp.) eigenvector associated with $\lambda_{\max}(A)$, normalized to satisfy $\mathbb{1}_n^\top v_{\max}(A) = 1$ (resp. $\mathbb{1}_n^\top u_{\max}(A) = 1$). The Perron-Frobenius Theorem for irreducible matrices guarantees that $\lambda_{\max}(A)$, $v_{\max}(A)$ and u_{\max} are well defined and unique. Where

not ambiguous, we will drop the (A) argument and, for example, write

$$v_{\max}^\top A = \lambda_{\max} v_{\max}^\top \quad \text{and} \quad Au_{\max} = \lambda_{\max} u_{\max},$$

with $v_{\max} \gg \mathbb{0}_n$ and $\mathbb{1}_n^\top v_{\max} = 1$; $u_{\max} \gg \mathbb{0}_n$ and $\mathbb{1}_n^\top u_{\max} = 1$.

1.3 Susceptible-Infected Model

In this section, we first review the classic scalar susceptible-infected (SI) model, and then present and characterize the network SI model.

1.3.1 Scalar SI model

The scalar SI model assumes that the growth rate of the fraction of the infected individuals is proportional to the fraction of the susceptible individuals, multiplied by a so-called *infection rate* $\beta > 0$. The model is given by

$$\dot{x}(t) = \beta s(t)x(t) = \beta(1 - x(t))x(t). \quad (1.1)$$

This is the well-established logistic equation. The following results can be found for example in the textbook [27].

Lemma 1.3.1 (Dynamical behavior of the SI model) *Consider the scalar SI model (1.1) with $\beta > 0$. The solution from initial condition $x(0) = x_0 \in [0, 1]$ is*

$$x(t) = \frac{x_0 e^{\beta t}}{1 - x_0 + x_0 e^{\beta t}}. \quad (1.2)$$

All initial conditions $0 < x_0 < 1$ result in the solution $x(t)$ being monotonically increasing

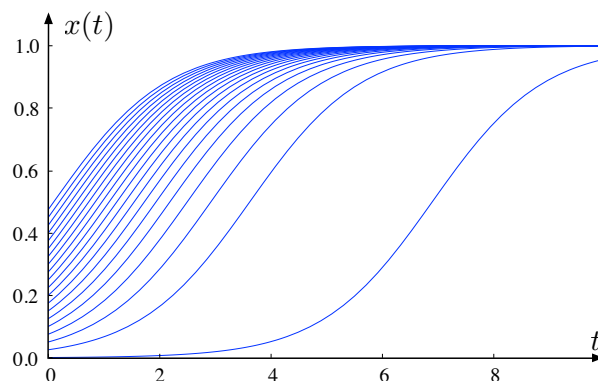


Figure 1.2: Evolution of the (lumped deterministic) SI model ($\beta = 1$) from small initial fraction of infected individuals.

and converging to the unique equilibrium 1 as $t \rightarrow \infty$.

Solutions to equation (1.1) with different initial conditions are plotted in Figure 1.2. The SI model (1.1) results in an evolution akin to a logistic curve, and is also called the logistic equation for population growth.

1.3.2 Network SI model

The network SI model on a weighted digraph with the adjacency matrix $A \in \mathbb{R}_{\geq 0}^{n \times n}$ is given by

$$\dot{x}_i(t) = \beta(1 - x_i(t)) \sum_{j=1}^n a_{ij}x_j(t), \quad (1.3)$$

or, in equivalent vector form,

$$\dot{x}(t) = \beta \left(I_n - \text{diag}(x(t)) \right) A x(t), \quad (1.4)$$

where $\beta > 0$ is the infection rate. Alternatively, in terms of the fractions of susceptible individuals $s(t) = \mathbb{1}_n - x(t)$, the network SI model is

$$\dot{s}(t) = -\beta \text{diag}(s(t)) A (\mathbb{1}_n - s(t)). \quad (1.5)$$

The network SI model is a particular case of the widely-studied network SIS model, which is to be discussed in the next section. The dynamical properties of the network SI model are not difficult to analyze, but, to the best of our knowledge, have not been formally presented in any previous literature. We present the results on the transient and asymptotic behavior of the network SI model, as well as the proof, in the following theorem.

Theorem 1.3.2 (Dynamical behavior of network SI model) *Consider the network SI model (2.4) with $\beta > 0$. For strongly connected graph with adjacency matrix A , the following statements hold:*

- (i) *if $x(0), s(0) \in [0, 1]^n$, then $x(t), s(t) \in [0, 1]^n$ for all $t > 0$. Moreover, $x(t)$ is monotonically non-decreasing (here by monotonically non-decreasing we mean $x(t_1) \leq x(t_2)$ for all $t_1 \leq t_2$). Finally, if $x(0) > \mathbb{0}_n$, then $x(t) \gg \mathbb{0}_n$ for all $t > 0$;*
- (ii) *the model (2.4) has two equilibrium points: $\mathbb{0}_n$ (no epidemic), and $\mathbb{1}_n$ (full contagion);*
 - (a) *the linearization of model (2.4) about the equilibrium point $\mathbb{0}_n$ is $\dot{x} = \beta Ax$ and it is exponentially unstable;*
 - (b) *let $D = \text{diag}(A\mathbb{1}_n)$ be the degree matrix. The linearization of model (1.5) about the equilibrium $\mathbb{0}_n$ is $\dot{s} = -\beta Ds$ and it is exponentially stable;*
- (iii) *each trajectory with initial condition $x(0) \neq \mathbb{0}_n$ converges asymptotically to $\mathbb{1}_n$, that is, the epidemic spreads monotonically to the entire network.*

Proof:

- (i) The fact that, if $x(0), s(0) \in [0, 1]^n$, then $x(t), s(t) \in [0, 1]^n$ for all $t > 0$ means that $[0, 1]^n$ is an invariant set for the differential equation (2.4). This is the consequence of

Nagumo's Theorem (see [28, Theorem 4.7]), since for any x belonging on the boundary of the set $[0, 1]^n$, the vector $\beta(I_n - \text{diag}(x))Ax$ is either tangent, or points inside the set $[0, 1]^n$.

Observe that the invariance of the set $[0, 1]^n$ implies that $\dot{x}(t) \geq 0_n$ and so $x(t_1) \leq x(t_2)$ for all $t_1 \leq t_2$.

We want to prove now that, if $x(0) > 0_n$, then $x(t) \gg 0_n$ for all $t > 0$. If by contradiction there is $i \in \{1, \dots, n\}$ and $T > 0$ such that $x_i(T) = 0$, then the monotonicity of $x_i(t) = 0$ would imply that $x_i(t) = 0$ for all $t \in [0, T]$, which would yield $\dot{x}_i(t) = 0$ for all $t \in [0, T]$. By (1.3) this would imply that $x_j(t) = 0$ for all $t \in [0, T]$ for all j such that $a_{ij} > 0$. We could iterate this argument and using the irreducibility of A we would get the contradiction that $x(t) = 0$ for all $t \in [0, T]$ concluding in this way the proof of (i).

(ii) Regarding statement (ii), note that 0_n and 1_n are clearly equilibrium points. Let $\bar{x} \in [0, 1]^n$ be an equilibrium and assume that $\bar{x} \neq 1_n$. Then there is i such that $\bar{x}_i \neq 1$. Since $\beta(1 - \bar{x}_i) \sum_{j=1}^n a_{ij} \bar{x}_j = 0$, then $\sum_{j=1}^n a_{ij} \bar{x}_j = 0$ which implies that $\bar{x}_j = 0$ for all j such that $a_{ij} > 0$. By iterating this argument and using the irreducibility of A we get that $\bar{x} = 0$ concluding only 0_n and 1_n are equilibrium points. Statements (ii)a and (ii)b are obvious. Exponential stability of the linearization $\dot{s} = -\beta Ds$ is obvious, and the Perron-Frobenius Theorem implies the existence of the unstable positive eigenvalue $\rho(A) > 0$ for the linearization $\dot{x} = \beta Ax$.

(iii) Consider the function $V(x) = 1_n^\top(1_n - x)$; this is a smooth function defined over the compact and forward invariant set $[0, 1]^n$ (see statement (i)). Since $\dot{V} = -\beta 1_n^\top(I_n - \text{diag}(x))Ax$, we know that $\dot{V} \leq 0$ for all x and $\dot{V}(x) = 0$ if and only if $x \in \{0_n, 1_n\}$. The LaSalle Invariance Principle implies that all trajectories with $x(0)$ converge asymptotically to either 1_n or 0_n . Additionally, note that $0 \leq V(x) \leq n$ for all $x \in [0, 1]^n$, that $V(x) = 0$ if and only if $x = 1_n$ and that $V(x) = n$ if and only if $x = 0_n$. Therefore, all trajectories with $x(0) \neq 0_n$ converge asymptotically to 1_n . ■

In the next two paragraphs we present the “initial-time” (“final-time” resp.) approximation of the solution to the network SI model, i.e., the approximated solution to equation (2.4), or equation (1.5) equivalently, when t is sufficiently small (large resp.). These results are novel.

For the adjacency matrix A , there exists a non-singular matrix T such that $A = TJT^{-1}$, where J is the Jordan normal form of A . Since A is non-negative and irreducible, according to Perron-Frobenius theorem, the first Jordan block $J_1 = (\lambda_{\max})_{1 \times 1}$ and $\lambda_{\max} > \operatorname{Re}(\lambda_i)$ for any other eigenvalue λ_i of A . Consider now the onset of an epidemic in a large population characterized by a small initial infection $x(0) = x_0$ much smaller than $\mathbb{1}_n$. The system evolution is approximated by $\dot{x} = \beta Ax$. This “initial-times” linear evolution satisfies

$$x(t) = e^{\beta At}x(0) = Te^{\beta Jt}T^{-1}x(0) = e^{\beta \lambda_{\max}t}(T\mathbf{e}_1\mathbf{e}_1^\top T^{-1}x(0) + o(1)),$$

where \mathbf{e}_1 is the first standard basis vector in \mathbb{R}^n and $o(1)$ denotes a time-varying vector that vanishes as $t \rightarrow +\infty$. Let u_1 denote the first column of T and let v_1^\top denote the first row of T^{-1} . Since $AT = TJ$ and $T^{-1}A = JT^{-1}$, one can check that u_1 (v_1 resp.) is the right (left resp.) eigenvector of A associated with the eigenvalue λ_{\max} . Since $T^{-1}T = I_n$, we have $v_1^\top u_1 = 1$. therefore,

$$\begin{aligned} x(t) &= e^{\beta \lambda_{\max}t}(u_1 v_1^\top x(0) + o(1)) \\ &= e^{\beta \lambda_{\max}t}\left(\frac{v_{\max}^\top x(0)}{v_{\max}^\top u_{\max}}u_{\max} + o(1)\right). \end{aligned} \tag{1.6}$$

That is, the epidemic initially experiences exponential growth with rate $\beta \lambda_{\max}$ and with distribution among the nodes given by the eigenvector u_{\max} .

Now suppose that at some time T , for all i we have that $x_i(T) = 1 - \epsilon_i$, where each ϵ_i

is much smaller than 1. Then, for time $t > T$, the approximated system for $s(t)$ is given by:

$$\dot{s}_i(t) = -\beta d_i s_i(t) \implies s_i(t) = \epsilon_i e^{-\beta d_i(t-T)},$$

where, for any $i \in \{1, \dots, n\}$, $d_i = \sum_{j=1}^n a_{ij}$ denotes the out-degree of node i in the network. From the discussion above, we conclude that the initial infection rate is proportional to the eigenvector centrality, and the final infection rate is proportional to the degree centrality.

1.4 Susceptible-Infected-Susceptible model

In this section we review the Susceptible-Infected-Susceptible (SIS) epidemic model. In addition to the existence of an infection process with rate $\beta > 0$, this model assumes that the infected individuals recover to the susceptible state at so-called *recovery rate* $\gamma > 0$.

1.4.1 Scalar SIS model

In the scalar SIS model, the population is divided into two fractions: the infected $x(t)$ and the susceptible $s(t)$, with $x(t) + s(t) = 1$, obeying the following dynamics:

$$\dot{x}(t) = \beta s(t)x(t) - \gamma x(t) = (\beta - \gamma - \beta x(t))x(t). \quad (1.7)$$

The dynamical behavior of system (1.7) given below can be found in [1].

Lemma 1.4.1 (Dynamical behavior of the SIS model) *For the SIS model (1.7) with $\beta > 0$ and $\gamma > 0$:*

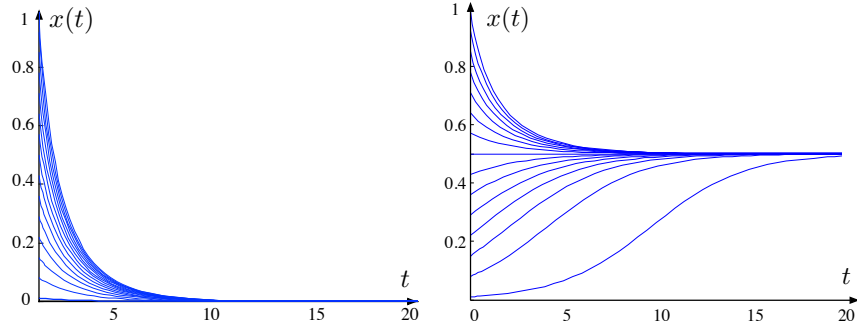


Figure 1.3: Evolution of the scalar SIS model with varying initial fraction of infected individuals. Top figure: $\beta = 0.5 < \gamma = 1$. Bottom figure: $\beta = 0.8 > \gamma = .4$.

- (i) the closed-form solution to equation (1.7) from initial condition $x(0) = x_0 \in [0, 1]$, for $\beta \neq \gamma$, is

$$x(t) = \frac{(\beta - \gamma)x_0}{\beta x_0 - e^{-(\beta - \gamma)t}(\gamma - \beta(1 - x_0))}; \quad (1.8)$$

- (ii) if $\beta \leq \gamma$, all trajectories converge to the unique equilibrium $x = 0$ (i.e., the epidemic disappears);
- (iii) if $\beta > \gamma$, then each trajectory from an initial condition $x(0) > 0$ converges to the exponentially stable equilibrium $x^* = (\beta - \gamma)/\beta$, which is called the endemic state.

Case (iii) corresponds to the case in which epidemic outbreaks take place and a steady-state epidemic contagion persists. The basic reproduction number in this deterministic scalar SIS model is given by $R_0 = \beta/\gamma$. Simulations regarding to Lemma 1.4.1(ii) and (iii) are shown in Figure 1.3.

1.4.2 Network SIS Model

In this section we study the network SIS model which is closely related to the original “multi-group SIS model” proposed by [2]; see also the intertwined SIS model in [12].

The network SIS model with infection rate β and recovery rate γ is given by:

$$\dot{x}_i(t) = \beta(1 - x_i(t)) \sum_{j=1}^n a_{ij}x_j(t) - \gamma x_i(t), \quad (1.9)$$

or, in equivalent vector form,

$$\dot{x}(t) = \beta(I_n - \text{diag}(x(t)))Ax(t) - \gamma x(t). \quad (1.10)$$

In the rest of this section we study the dynamical properties of this model. We start by defining the monotonically-increasing functions

$$f_+(y) = y/(1 + y), \quad \text{and} \quad f_-(z) = z/(1 - z),$$

for $y \in \mathbb{R}_{\geq 0}$ and $z \in [0, 1[$. Note that $f_+(f_-(z)) = z$ for all $z \in [0, 1)$. For vector variables $y \in \mathbb{R}_{\geq 0}^n$ and $z \in [0, 1)^n$, we write $F_+(y) = (f_+(y_1), \dots, f_+(y_n))$, and $F_-(z) = (f_-(z_1), \dots, f_-(z_n))$.

Behavior of System Below the Threshold In this subsection, we characterize the behavior of the network SIS model in a regime we describe as “below the threshold.” The results presented in the theorem below can be found in [2, 13, 14]. Historically, it is meaningful to attribute this theorem to [2], even if the language adopted here is more modern.

Theorem 1.4.2 (Dynamical behavior of the network SIS model: Below the threshold)

Consider the network SIS model (2.5), with $\beta > 0$ and $\gamma > 0$, over a strongly connected digraph with adjacency matrix A . Let λ_{\max} and v_{\max} be the dominant eigenvalue of A and the corresponding normalized left eigenvector respectively. If $\beta\lambda_{\max}/\gamma < 1$, then

- (i) if $x(0), s(0) \in [0, 1]^n$, then $x(t), s(t) \in [0, 1]^n$ for all $t > 0$. Moreover, if $x(0) > \mathbb{0}_n$, then $x(t) \gg \mathbb{0}_n$ for all $t > 0$;
- (ii) there exists a unique equilibrium point $\mathbb{0}_n$, the linearization of (2.5) about $\mathbb{0}_n$ is $\dot{x} = (\beta A - \gamma I_n)x$ and it is exponentially stable;
- (iii) from any $x(0) \neq \mathbb{0}_n$, the weighted average $t \mapsto v_{\max}^\top x(t)$ is monotonically and exponentially decreasing, and all the trajectories converge to $\mathbb{0}_n$.

Proof: (i) As in Theorem 1.3.2 the first part is the consequence of Nagumo's Theorem. Then define $y(t) := e^{\gamma t}x(t)$. Notice that this variable satisfies the differential equation $\dot{y}(t) = \beta \text{diag}(s(t))Ay(t)$. From the same arguments used in the proof of the point (i) of Theorem 1.3.2 we argue that $y(t) \gg \mathbb{0}_n$ for all $t > 0$. From this it follows that also $x(t) \gg \mathbb{0}_n$ for all $t > 0$.

(ii) Assume that x^* is an equilibrium point. It is easy to see that $x^* \ll \mathbb{1}_n$. Let $\hat{A} = \beta A / \gamma$. Observe moreover that x^* is an equilibrium point if and only if $\hat{A}x^* = F_-(x^*)$ or, equivalently, if and only if $F_+(\hat{A}x^*) = x^*$. This means that x^* is an equilibrium if and only if it is a fixed point of \mathcal{F} , where $\mathcal{F}(x) := F_+(\hat{A}x)$. For $x \in [0, 1]^n$, note $F_+(\hat{A}x) \leq \hat{A}x$ because $f_+(z) \leq z$. Moreover, $\mathbb{0}_n \leq x \leq y$ implies that $\mathbb{0}_n \leq \mathcal{F}(x) \leq \hat{A}y$. Therefore, if $\mathbb{0}_n \leq x$, then $\mathcal{F}^k(x) \leq \hat{A}^k x$, for all k . Since \hat{A} is Schur stable, then $\lim_{k \rightarrow \infty} \mathcal{F}^k(x) = 0$. This shows that the only fixed point of \mathcal{F} is zero.

Next, the linearization of equation (1.10) is verified by dropping the second-order terms. The linearized system is exponentially stable at $\mathbb{0}_n$ for $\beta \lambda_{\max} - \gamma < 0$ because λ_{\max} is larger, in real part, than any other eigenvalue of A by the Perron-Frobenius Theorem for irreducible matrices.

(iii) Finally, regarding statement (iii), define $y(t) = v_{\max}^\top x(t)$ and note that $(I_n -$

$\text{diag}(z))v_{\max} \leq v_{\max}$ for any $z \in [0, 1]^n$. Therefore,

$$\dot{y}(t) \leq \beta v_{\max}^{\top} A x(t) - \gamma v_{\max}^{\top} x(t) = (\beta \lambda_{\max} - \gamma) y(t) < 0.$$

By the Grönwall-Bellman Comparison Lemma, $y(t)$ is monotonically decreasing and satisfies $y(t) \leq y(0)e^{(\beta \lambda_{\max} - \gamma)t}$ from all initial conditions $y(0)$. This concludes our proof of statement (iii). ■

Behavior of System Above the Threshold We present the dynamical behavior of the network SIS model above the threshold as follows. Statement (i) of the theorem below is a straightforward result from equation (1.10). Historically, the existence of a unique endemic state and its global attractivity properties, i.e., statements (ii), (iii), (iii)a and (iv) in the theorem below, are due to [2], and can be found in [13] and [14]. To the best of our knowledge, the Taylor expansions in parts (iii)b and (iii)c and the algorithm in part (iii)d are novel. In addition, compared with the previous works [2, 13, 14], construction of the algorithm in part (iii)d provides an alternative and more concise proof for the existence and uniqueness of the endemic state, and the convergence of any solution starting with $x(0) \in (0, 1)^n$ to this endemic state.

Theorem 1.4.3 (Dynamical behavior of the network SIS model: Above the threshold)

Consider the network SIS model (2.5), with $\beta > 0$ and $\gamma > 0$, over a strongly connected digraph with adjacency matrix A . Let λ_{\max} be the dominant eigenvalue of A and let v_{\max} and u_{\max} be the corresponding normalized left and right eigenvectors respectively. Let $d = A\mathbf{1}_n$. If $\beta \lambda_{\max} / \gamma > 1$, then

- (i) *if $x(0), s(0) \in [0, 1]^n$, then $x(t), s(t) \in [0, 1]^n$ for all $t > 0$. Moreover, if $x(0) > \mathbb{0}_n$, then $x(t) \gg \mathbb{0}_n$ for all $t > 0$;*

(ii) \mathbb{O}_n is an equilibrium point, the linearization of system (1.10) at \mathbb{O}_n is unstable due to the unstable eigenvalue $\beta\lambda_{\max} - \gamma$ (i.e., there will be an epidemic outbreak);

(iii) besides the equilibrium \mathbb{O}_n , there exists a unique equilibrium point x^* , called the endemic state, such that

(a) $x^* \gg \mathbb{O}_n$,

(b) $x^* = \delta a u_{\max} + O(\delta^2)$ as $\delta \rightarrow 0^+$, where $\delta := \beta\lambda_{\max}/\gamma - 1$ and

$$a = \frac{v_{\max}^T u_{\max}}{v_{\max}^T \text{diag}(u_{\max}) u_{\max}},$$

(c) $x^* = \mathbb{1}_n - (\gamma/\beta) \text{diag}(d)^{-1} \mathbb{1}_n + O(\gamma^2/\beta^2)$, at fixed A , as $\gamma/\beta \rightarrow 0^+$, where $d = A\mathbb{1}_n$,

(d) define a sequence $\{y(k)\}_{k \in \mathbb{N}} \subset \mathbb{R}^n$ by

$$y(k+1) := F_+ \left(\frac{\beta}{\gamma} A y(k) \right). \quad (1.11)$$

If $y(0) \geq 0$ is a scalar multiple of u_{\max} and satisfies either $0 < \max_i y_i(0) \leq 1 - \gamma/(\beta\lambda_{\max})$ or $\min_i y_i(0) \geq 1 - \gamma/(\beta\lambda_{\max})$, then

$$\lim_{k \rightarrow \infty} y(k) = x^*.$$

Moreover, if $\max_i y_i(0) \leq 1 - \gamma/(\beta\lambda_{\max})$, then $y(k)$ is monotonically non-decreasing; if $\min_i y_i(0) \geq 1 - \gamma/(\beta\lambda_{\max})$, then $y(k)$ is monotonically non-increasing.

(iv) the endemic state x^* is locally exponentially stable and its domain of attraction is $[0, 1]^n \setminus \mathbb{O}_n$.

Note: statement (ii) means that, near the onset of an epidemic outbreak, the exponential growth rate is $\beta\lambda_{\max} - \gamma$ and the outbreak tends to align with the dominant eigenvector u_{\max} ; for more details see the discussion leading up to the approximate evolution (1.6). The basic reproduction number for this deterministic network SIS model is given by $R_0 = \beta\lambda_{\max}/\gamma$. The network SI model discussed in Section 3 describes the limit behavior of the network SIS model as $\gamma/\beta \rightarrow 0^+$. Statement (iii)c in Theorem 1.4.3 indicates that $x^* \rightarrow \mathbb{1}_n$ as $\gamma/\beta \rightarrow 0^+$, which is consistent with statement (iii) in Theorem 1.3.2.

Proof: [Proof of selected statements in Theorem 1.4.3]

(i) This point can be proved as done in point (i) of Theorem 1.3.2.

(ii) This follows from the same analysis of the linearized system as in the proof of Theorem 1.4.2(ii).

(iii) We begin by establishing two properties of the map $x \mapsto F_+(\hat{A}x)$, for $\hat{A} = \beta A/\gamma$. First, we claim that, $y \gg z \geq \mathbb{0}_n$ implies $F_+(\hat{A}y) \gg F_+(\hat{A}z)$. Indeed, note that G being connected implies that the adjacency matrix A has at least one strictly positive entry in each row. Hence, $y - z \gg \mathbb{0}_n$ implies $\hat{A}(y - z) \gg \mathbb{0}_n$ and, since f_+ is monotonically increasing, $\hat{A}y \gg \hat{A}z$ implies $F_+(\hat{A}y) \gg F_+(\hat{A}z)$.

Second, we observe that, for any $0 < \alpha < 1$ and $z > 0$, we have $f_+(\alpha z) \geq z$ if and only if $z \leq 1 - 1/\alpha$. Suppose $y(0)$ is a scalar multiple of u_{\max} and $0 < \max_i y_i(0) \leq 1 - \gamma/(\beta\lambda_{\max})$. We have

$$F_+(\hat{A}y(0))_i = f_+\left(\frac{\beta\lambda_{\max}}{\gamma}y_i(0)\right) \geq y_i(0).$$

Therefore, the sequence $\{y(k)\}_{k \in \mathbb{N}}$ defined by equation (1.11) satisfies $y(1) \geq y(0)$, which in turn leads to $y(2) = F_+(\hat{A}y(1)) \geq F_+(\hat{A}y(0)) = y(1)$, and by induction, $y(k+1) = F_+(\hat{A}y(k)) \geq y(k)$ for any $k \in \mathbb{N}$. Such sequence $\{y(t)\}$ is monotonically non-decreasing

and entry-wise upper bounded by $\mathbb{1}_n$. Therefore, as k diverges, $y(k)$ converges to some $x^* \gg \mathbb{0}_n$ such that $F_+(\hat{A}x^*) = x^*$. This proves the existence of an equilibrium $x^* = \lim_{k \rightarrow \infty} y(k) \gg \mathbb{0}_n$ as claimed in statements (iii)a and (iii)d.

Similarly, for any $0 < \alpha < 1$ and $z > 0$, $f_+(\alpha z) \leq z$ if and only if $z \geq 1 - 1/\alpha$. Following the same line of argument in the previous paragraph, one can check that the $\{y(k)\}_{k \in \mathbb{N}}$ defined by equation (1.11) is monotonically non-increasing and converges to some x^* , if $y(0)$ is a scalar multiple of u_{\max} and satisfies $\min_i y_i(0) \geq 1 - \gamma/(\beta\lambda_{\max})$.

Now we establish the uniqueness of the equilibrium $x^* \in [0, 1]^n \setminus \{\mathbb{0}_n\}$. First, we claim that an equilibrium point with an entry equal to 0 must be $\mathbb{0}_n$. Indeed, assume y^* is an equilibrium point and assume $y_i^* = 0$ for some $i \in \{1, \dots, n\}$. The equality $y_i^* = f_+(\sum_{j=1}^n a_{ij}y_j^*)$ implies that also any node j with $a_{ij} > 0$ must satisfy $y_j^* = 0$. Because G is connected, all entries of y^* must be zero. Second, by contradiction, we assume there exists another equilibrium point $y^* \gg \mathbb{0}_n$ distinct from x^* . Let $\alpha := \min_j \{y_j^*/x_j^*\}$ and let i such that $\alpha = y_i^*/x_i^*$. Then $y^* \geq \alpha x^* \gg \mathbb{0}_n$ and $y_i^* = \alpha x_i^*$. Notice that we can assume with no loss of generality that $\alpha < 1$ otherwise we exchange x^* and y^* . Observe now that

$$\begin{aligned} (F_+(\hat{A}y^*) - y^*)_i &= f_+((\hat{A}y^*)_i) - \alpha x_i^* \\ &\geq f_+(\alpha(\hat{A}x^*)_i) - \alpha x_i^* && (\hat{A} \geq \mathbb{0}_{n \times n}) \\ &> \alpha f_+((\hat{A}x^*)_i) - \alpha x_i^* && (0 < \alpha < 1 \text{ and } z > 0) \\ &= \alpha(F_+(\hat{A}x^*) - x^*)_i = 0. && (x^* \text{ is an equilibrium}) \end{aligned}$$

Therefore, $(F_+(\hat{A}y^*) - y^*)_i > 0$, which contradicts the fact that y^* is an equilibrium.

Now we prove (iii)b. Observe first that, since taking

$$y(0) = \left(1 - \frac{\gamma}{\beta\lambda_{\max}}\right) \frac{u_{\max}}{\max_i \{u_{\max,i}\}} = \frac{\delta}{\delta + 1} \frac{u_{\max}}{\max_i \{u_{\max,i}\}}$$

then $y(k)$ is monotonically non-decreasing and converges to x^* , and since taking instead

$$y(0) = \left(1 - \frac{\gamma}{\beta\lambda_{\max}}\right) \frac{u_{\max}}{\min_i\{u_{\max,i}\}} = \frac{\delta}{\delta + 1} \frac{u_{\max}}{\min_i\{u_{\max,i}\}}$$

then $y(k)$ is monotonically non-increasing and converges to x^* , we can argue that

$$\frac{\delta}{\delta + 1} \frac{u_{\max}}{\max_i\{u_{\max,i}\}} \leq x^* \leq \frac{\delta}{\delta + 1} \frac{u_{\max}}{\min_i\{u_{\max,i}\}}$$

This implies that x^* is infinitesimal as a function of δ . Consider the expansion $x^*(\delta) = x_1\delta + x_2\delta^2 + O(\delta^3)$. Since the equilibrium x^* satisfies the equation

$$(\delta + 1)(I_n - \text{diag}(x^*))Ax^* - \lambda_{\max}x^* = 0$$

by substituting the expansion and equating to zero the coefficient of the term δ we obtain the equation

$$Ax_1 - \lambda_{\max}x_1 = 0$$

which proves that x_1 is a multiple of u_{\max} , namely $x_1 = au_{\max}$ for some constant a . By equating to zero the coefficient of the term δ^2 we obtain instead the equation

$$Ax_1 + Ax_2 - \text{diag}(x_1)Ax_1 - \lambda_{\max}x_2 = 0$$

Using the fact that $x_1 = au_{\max}$ we argue that

$$a\lambda_{\max}u_{\max} + Ax_2 - a^2\lambda_{\max}\text{diag}(u_{\max})u_{\max} - \lambda_{\max}x_2 = 0$$

By multiplying on the left by v_{\max}^T we obtain

$$a\lambda_{\max}v_{\max}^T u_{\max} - a^2\lambda_{\max}v_{\max}^T \text{diag}(u_{\max})u_{\max} = 0$$

which proves that

$$a = \frac{v_{\max}^T u_{\max}}{v_{\max}^T \text{diag}(u_{\max})u_{\max}}$$

Point (iii)c can be proved in a similar way. Indeed, define $\epsilon := \gamma/\beta$. Since

$$\left(1 - \frac{\epsilon}{\lambda_{\max}}\right) \frac{u_{\max}}{\max_i \{u_{\max,i}\}} \leq x^* \leq \left(1 - \frac{\epsilon}{\lambda_{\max}}\right) \frac{u_{\max}}{\min_i \{u_{\max,i}\}}$$

we can argue that the expansion $x^*(\epsilon) = x_0 + x_1\epsilon + O(\epsilon^2)$ as ϵ tends to zero is such that $x_0 \gg \mathbb{0}_n$. Since the equilibrium x^* satisfies the equation

$$(I_n - \text{diag}(x^*))Ax^* - \epsilon x^* = 0$$

by substituting the expansion and equating to zero the coefficient of the term ϵ^0 we obtain the equation

$$Ax_0 - \text{diag}(x_0)Ax_0 = 0$$

which proves that $x_0 = \text{vectorones}[n]$. By equating to zero the coefficient of the term ϵ^1 we obtain instead the equation

$$Ax_1 - \text{diag}(x_1)Ax_0 - \text{diag}(x_0)Ax_1 - x_0 = 0$$

Using the fact that $x_0 = \mathbb{1}_n$ we argue that

$$\text{diag}(A\mathbb{1}_n)x_1 + \mathbb{1}_n = 0$$

which yields the thesis.

(iv) For this point we refer to [2, 13] or [14, Theorems 1 and 2] in the interest of brevity. ■

Remark 1.4.4 *The network SI model can be regarded as the limit case of the network SIS model with vanishing curing rate $\gamma \rightarrow 0^+$. According to Theorem 1.4.2 and 1.4.3, for any strongly connected digraph and any fixed infection rate $\beta > 0$, the quantity $\beta\lambda_{\max}/\gamma$ is always above the threshold in the limit $\gamma \rightarrow 0^+$. Moreover, statement (iii)(c) indicates that, as $\gamma \rightarrow 0^+$, the endemic state x^* satisfies $x^* \rightarrow \mathbb{1}_n$. Therefore, the behavior of the network SI model is the same as that for the network SIS model in the limit $\gamma \rightarrow 0^+$.*

1.5 Network Susceptible-Infected-Recovered Model

In this section we review the Susceptible-Infected-Susceptible (SIR) epidemic model.

1.5.1 Scalar SIR model

In this model individuals who recover from infection are assumed not susceptible to the epidemic any more. In this case, the population is divided into three distinct groups: $s(t)$, $x(t)$, and $r(t)$, denoting the fraction of susceptible, infected, and recovered individuals, respectively, with $s(t) + x(t) + r(t) = 1$. We write the (Susceptible–Infected–Recovered) SIR model as:

$$\begin{aligned}\dot{s}(t) &= -\beta s(t)x(t), \\ \dot{x}(t) &= \beta s(t)x(t) - \gamma x(t), \\ \dot{r}(t) &= \gamma x(t).\end{aligned}\tag{1.12}$$

The following results on the dynamical behavior of the scalar SIR model can be found in [1].

Lemma 1.5.1 (Dynamical behavior of the SIR model) *Consider the SIR model (1.12).*

From each initial condition $s(0) + x(0) + r(0) = 1$ with $s(0) > 0$, $x(0) > 0$ and $r(0) \geq 0$, the resulting trajectory $t \mapsto (s(t), x(t), r(t))$ has the following properties:

- (i) $s(t) > 0$, $x(t) > 0$, $r(t) \geq 0$, and $s(t) + x(t) + r(t) = 1$ for all $t \geq 0$;
- (ii) $t \mapsto s(t)$ is monotonically decreasing and $t \mapsto r(t)$ is monotonically increasing;
- (iii) $\lim_{t \rightarrow \infty} (s(t), x(t), r(t)) = (s_\infty, 0, r_\infty)$, where r_∞ is the unique solution to the equality

$$1 - r_\infty = s(0)e^{-\frac{\beta}{\gamma}(r_\infty - r(0))}; \quad (1.13)$$

- (iv) if $\beta s(0)/\gamma < 1$, then $t \mapsto x(t)$ monotonically and exponentially decreases to zero as $t \rightarrow \infty$;
- (v) if $\beta s(0)/\gamma > 1$, then $t \mapsto x(t)$ first monotonically increases to a maximum value and then monotonically decreases to 0 as $t \rightarrow \infty$; the maximum fraction of infected individuals is given by:

$$x_{\max} = x(0) + s(0) - \frac{\gamma}{\beta} \left(\log(s(0)) + 1 - \log\left(\frac{\gamma}{\beta}\right) \right).$$

As mentioned before, we describe the behavior in statement (v) as an epidemic outbreak, an exponential growth of $t \mapsto x(t)$ for small times.) The effective reproduction number in the deterministic scalar SIR model is $R = \beta s(t)/\gamma$. Note that the basic reproduction number $R_0 = \beta/\gamma$ does not have predict power in this model.

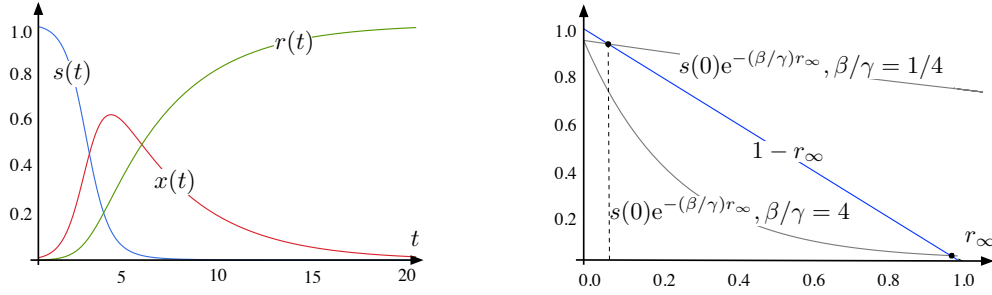


Figure 1.4: Left figure: evolution of the scalar SIR model from small initial fraction of infected individuals (and zero recovered); parameters $\beta = 2$, $\gamma = 1/4$ (case (iv) in Lemma 1.5.1). Right figure: intersection between the two curves in equation (1.13) with $s(0) = 0.95$, $r(0) = 0$ and $\beta/\gamma \in \{1/4, 4\}$. If $\beta/\gamma = 1/4$, then $.05 < r_\infty < .1$. If $\beta/\gamma = 4$, then $.95 < r_\infty$.

1.5.2 Network SIR model

The network SIR model on a graph with adjacency matrix A is given by

$$\begin{aligned}\dot{s}_i(t) &= -\beta s_i(t) \sum_{j=1}^n a_{ij} x_j(t), \\ \dot{x}_i(t) &= \beta s_i(t) \sum_{j=1}^n a_{ij} x_j(t) - \gamma x_i(t), \\ \dot{r}_i(t) &= \gamma x_i(t),\end{aligned}$$

where $\beta > 0$ is the infection rate and $\gamma > 0$ is the recovery rate. Note that the third equation is redundant because of the constraint $s_i(t) + x_i(t) + r_i(t) = 1$. Therefore, we regard the dynamical system in vector form as:

$$\dot{s}(t) = -\beta \text{diag}(s(t))Ax(t), \quad (1.14a)$$

$$\dot{x}(t) = \beta \text{diag}(s(t))Ax(t) - \gamma x(t). \quad (1.14b)$$

We state our main results of this section below. Weaker versions of statements (i)a and (i)b are due to [3]. To the best of our knowledge, statements (i)c, (ii), (iii), (iv) and (v) are novel.

Theorem 1.5.2 (Dynamical behavior of the network SIR model) *Consider the network SIR model (1.14), with $\beta > 0$ and $\gamma > 0$, over a strongly connected digraph with adjacency matrix A . For $t \geq 0$, let $\lambda_{\max}(t)$ and $v_{\max}(t)$ be the dominant eigenvalue of the non-negative matrix $\text{diag}(s(t))A$ and the corresponding normalized left eigenvector, respectively. The following statements hold:*

(i) *if $x(0) > \mathbb{0}_n$, and $s(0) \gg \mathbb{0}_n$, then*

(a) *$t \mapsto s(t)$ and $t \mapsto x(t)$ are strictly positive for all $t > 0$,*

(b) *$t \mapsto s(t)$ is monotonically decreasing, and*

(c) *$t \mapsto \lambda_{\max}(t)$ is monotonically decreasing;*

(ii) *the set of equilibrium points is the set of pairs $(s^*, \mathbb{0}_n)$, for any $s^* \in [0, 1]^n$, and the linearization of model (1.14) about $(s^*, \mathbb{0}_n)$ is*

$$\begin{aligned}\dot{s}(t) &= -\beta \text{diag}(s^*)Ax, \\ \dot{x}(t) &= \beta \text{diag}(s^*)Ax - \gamma x;\end{aligned}\tag{1.15}$$

(iii) *(behavior below the threshold) let the time $\tau \geq 0$ satisfy $\beta \lambda_{\max}(\tau) < \gamma$. Then the weighted average $t \mapsto v_{\max}(\tau)^\top x(t)$, for $t \geq \tau$, is monotonically and exponentially decreasing to zero;*

(iv) *(behavior above the threshold) if $\beta \lambda_{\max}(0) > \gamma$ and $x(0) > \mathbb{0}_n$, then,*

(a) *(epidemic outbreak) for small time, the weighted average $t \mapsto v_{\max}(0)^\top x(t)$ grows exponentially fast with rate $\beta \lambda_{\max}(0) - \gamma$, and*

(b) *there exists $\tau > 0$ such that $\beta \lambda_{\max}(\tau) < \gamma$;*

(v) *each trajectory converges asymptotically to an equilibrium point, that is, $\lim_{t \rightarrow \infty} x(t) = \mathbb{0}_n$ so that the epidemic asymptotically disappears.*

The effective reproduction number in the deterministic network SIR model is $R(t) = \beta \lambda_{\max}(t) / \gamma$. When $R(0) > 1$, we have an epidemic outbreak, i.e., an exponential growth of infected individual for short time. In any case, the theorem guarantees that, after at most finite time, $R(t) < 1$ and the infected population decreases exponentially fast to zero.

Proof: Regarding statement (i)a, $s(t) \gg 0_n$ is due to the fact that Ax is bounded and $s(t)$ is continuously differentiable to t . The statement that $x(t) \gg 0_n$ for all $t > 0$ is proved in the same way as Theorem 1.4.2 (i). Statement (i)b is the immediate consequence of $\dot{s}_i(t)$ being strictly negative. From statement (i)a we know that each $s_i(t)$ is positive, and from A being irreducible and $x(0) \neq 0_n$ we know that $\sum_{j=1}^n a_{ij}x_j$ is positive. Therefore, $\dot{s}_i(t) = -\beta s_i(t) \sum_{j=1}^n a_{ij}x_j(t) < 0$ for all $i \in V$ and $t \geq 0$.

For statement (i)c, we start by recalling the following property from [29, Example 7.10.2]: for B and C nonnegative square matrices, if $B \leq C$, then $\rho(B) \leq \rho(C)$. Now, pick two time instances t_1 and t_2 with $0 < t_1 < t_2$. Let $\alpha = \max_i s_i(t_2) / s_i(t_1)$ and note $0 < \alpha < 1$ because $s(t)$ is strictly positive and monotonically decreasing. Now note that,

$$\text{diag}(s(t_1))A > \alpha \text{diag}(s(t_1))A \geq \text{diag}(s(t_2))A,$$

so that, using the property above, we know

$$\rho(\text{diag}(s(t_1))A) > \alpha \rho(\text{diag}(s(t_1))A) \geq \rho(\text{diag}(s(t_2))A).$$

This concludes the proof of statement (i)c.

Regarding statement (ii), note that a point (s^*, x^*) is an equilibrium if and only if:

$$\mathbb{O}_n = -\beta \operatorname{diag}(s^*)Ax^*, \quad \text{and}$$

$$\mathbb{O}_n = \beta \operatorname{diag}(s^*)Ax^* - \gamma x^*.$$

Therefore, each point of the form (s^*, \mathbb{O}_n) is an equilibrium. On the other hand, summing the last two equalities we obtain $\mathbb{O}_n = \gamma x^*$ and thus x^* must be \mathbb{O}_n . As a straightforward result, the linearization of model (1.14) about any equilibrium point $(s^*, \mathbb{O}_n, \mathbb{1}_n - s^*)$ is given by equation (1.15).

Regarding statement (iii), multiplying $v_{\max}(\tau)^\top$ from the left on both sides of equation (1.14b) we obtain:

$$\begin{aligned} \frac{d}{dt}(v_{\max}(\tau)^\top x(t)) &= v_{\max}(\tau)^\top \left(\beta \operatorname{diag}(s(t))Ax(t) - \gamma x(t) \right) \\ &\leq v_{\max}(\tau)^\top \left(\beta \operatorname{diag}(s(\tau))Ax(t) - \gamma x(t) \right) = (\beta \lambda_{\max}(\tau) - \gamma)v_{\max}(\tau)^\top x(t). \end{aligned}$$

Therefore, we obtain

$$v_{\max}(\tau)^\top x(t) \leq (v_{\max}(\tau)^\top x(0))e^{(\beta \lambda_{\max}(\tau) - \gamma)t}.$$

The right-hand side exponentially decays to zero when $\beta \lambda_{\max}(\tau) < \gamma$. Therefore, $v_{\max}(\tau)^\top x(t)$ also decreases monotonically and exponentially to zero for all $t > \tau$.

Regarding statement (iv)a, note that based on the argument in (i)a, we only need to consider the case when $x(0) \gg \mathbb{O}_n$. Left-multiplying $v_{\max}(0)^\top$ on both sides of equation (1.14b), we obtain:

$$\left. \frac{d}{dt}(v_{\max}(0)^\top x(t)) \right|_{t=0} = v_{\max}(0)^\top \left(\beta \operatorname{diag}(s(t))Ax(t) - \gamma x(t) \right) \Big|_{t=0} = (\beta \lambda_{\max}(0) - \gamma)v_{\max}(0)^\top x(0).$$

Since $\beta\lambda_{\max}(0) - \gamma > 0$, the initial time derivative of $v_{\max}(0)^\top x(t)$ is positive. Since $t \mapsto v_{\max}(0)^\top x(t)$ is a continuously differentiable function, there exists $\tau' > 0$ such that $\frac{d}{dt}(v_{\max}(0)^\top x(t)) > 0$ for any $t \in [0, \tau']$.

Regarding statement (iv)b, since $\dot{s}(t) \leq \mathbb{0}_n$ and is lower bounded by $\mathbb{0}_n$, we conclude that the limit $\lim_{t \rightarrow +\infty} s(t)$ exists. Moreover, since $s(t)$ is monotonically non-increasing, we have $\lim_{t \rightarrow +\infty} \dot{s}(t) = 0$, which implies either $\lim_{t \rightarrow +\infty} s(t) = \mathbb{0}_n$ or $\lim_{t \rightarrow +\infty} x(t) = \mathbb{0}_n$. If $s(t)$ converges to $\mathbb{0}_n$, then $\dot{x}(t)$ converges to $-\gamma x(t)$. Therefore, there exists $T > 0$ such that $\beta\lambda_{\max}(T) < \gamma$, which leads to $x(t) \rightarrow \mathbb{0}_n$ as $t \rightarrow +\infty$; If $s(t)$ converges to some $s^* > \mathbb{0}_n$, then $x(t)$ still converges to $\mathbb{0}_n$. Therefore, for any $(s(0), x(0))$, the trajectory $(s(t), x(t))$ converges to some equilibria with the form $(s^*, \mathbb{0}_n)$, where $s^* \geq \mathbb{0}_n$. Let

$$s(t) = s^* + \delta_s(t), \quad \text{and } x(t) = \mathbb{0}_n + \delta_x(t).$$

We know that $\delta_s(t) \geq 0$ and $\delta_x(t) \geq 0$ for all $t \geq 0$. Moreover, $\delta_s(t)$ is monotonically non-increasing and converges to $\mathbb{0}_n$, and there exists $\tilde{T} > 0$ such that, for any $t \geq T$, $\delta_x(t)$ is monotonically non-increasing and converges to $\mathbb{0}_n$.

Let λ^* and v^* denote the dominant eigenvalue and the corresponding normalized left eigenvector of matrix $\text{diag}(s^*)A$, respectively, that is, $v^{*\top} \text{diag}(s^*)A = \lambda^* v^{*\top}$. First let us suppose $\beta\lambda^* - \gamma > 0$, then the linearized system of (1.12) around $(s^*, \mathbb{0}_n)$ is written as

$$\begin{aligned} \dot{\delta}_s &= -\beta \text{diag}(s^*)A \delta_x, \\ \dot{\delta}_x &= \beta \text{diag}(s^*)A \delta_x - \gamma \delta_x. \end{aligned}$$

Since $\beta\lambda^* - \gamma > 0$, the linearized system is exponentially unstable, which contradicts the fact that $(\delta_s(t), \delta_x(t)) \rightarrow (\mathbb{0}_n, \mathbb{0}_n)$ as $t \rightarrow +\infty$. Alternatively, suppose $\beta\lambda^* - \gamma = 0$. By

left multiplying $v^{*\top}$ on both sides of the equation for $\dot{x}(t)$ in (1.12), we obtain

$$v^{*\top} \dot{\delta}_x = (\beta\lambda^* - \gamma)(v^{*\top} \delta_x) + \beta v^{*\top} \text{diag}(\delta_s) A \delta_x = \beta v^{*\top} \text{diag}(\delta_s) A \delta_x \geq \mathbb{0}_n,$$

which contradicts $\delta_x(t) \rightarrow \mathbb{0}_n$ as $t \rightarrow +\infty$. Therefore, we conclude that $\beta\lambda^* - \gamma < 0$. Since $\lambda_{\max}(t)$ is continuous on t , we conclude that there exists $\tau < +\infty$ such that $\beta\lambda_{\max}(t) - \gamma < 0$. ■

Remark 1.5.3 *Consider the network SIR model as a parameterized dynamical system, with the curing rate γ as the parameter. The network SI model can be regarded the network SIR dynamics with $\gamma = 0$ and zero initial fraction of recovered individuals. However, due to the specific bifurcation behavior of the network SIR model at $\gamma = 0$, the dynamical properties of the network SIR model with $\gamma = 0$ are qualitatively different from the case when $\gamma > 0$. When $\gamma = 0$, the set given by statement (ii) of Theorem 1.5.2 is only a subset of the equilibrium set. Points in the set of pairs $(\mathbb{0}_n, x^*)$ are also the equilibria of the network SIR with $\gamma = 0$. In addition, while statement (iv)a of Theorem 1.5.2 on the initial epidemic outbreak is still true, statements (iv)b and (v) on the eventual decay no longer hold for $\gamma = 0$.*

In what follows, we present a novel result on an iterative algorithm that computes the limit state $\lim_{t \rightarrow \infty} (s(t), 0, r(t))$ of the network SIR model (1.14) as a function of an arbitrary initial condition $(s(0), x(0), r(0))$.

Note that, for the scalar SIR model (1.12), if we define

$$V(s(t), x(t)) := s(t) e^{\frac{\beta}{\gamma} (1 - x(t) - s(t))}.$$

Simple calculations result in $dV(s(t), x(t))/dt = 0$, which implies that the trajectories

are on the level sets of V and in the set $\{(s, x) \in \mathbb{R}^2 \mid s \geq 0, x \geq 0, s + x \leq 1\}$. Here, we apply a similar approach to the network SIR system (1.14). Let

$$V_i(s, r) := s_i e^{\frac{\beta}{\gamma} \sum_{j=1}^n a_{ij} r_j}, \quad \text{for any } i \in \{1, \dots, n\}.$$

One can check that, along any trajectory of dynamics (1.14), $dV_i/dt = 0$ for any $i \in \{1, \dots, n\}$. Therefore, the trajectories $(s(t), r(t))$ lie on the level curves of the functions $V_i(s, r)$ for $i \in \{1, \dots, n\}$.

Let $s(\infty) := \lim_{t \rightarrow +\infty} s(t)$, $x(\infty) := \lim_{t \rightarrow +\infty} x(t)$, and $r(\infty) := \lim_{t \rightarrow +\infty} r(t)$. Notice that $x(\infty) = \mathbb{0}_n$ and so $r(\infty) = \mathbb{1}_n - s(\infty)$. Since $dV_i/dt = 0$ for any $i \in \{1, \dots, n\}$, we have

$$s_i(\infty) = s_i(0) e^{-\frac{\beta}{\gamma} \sum_{j=1}^n a_{ij} (1-r_j(0))} e^{\frac{\beta}{\gamma} \sum_{j=1}^n a_{ij} s_j(\infty)}. \quad (1.16)$$

Given any initial condition $(s(0), r(0))$, the right-hand side of equation (1.16) defines a map

$$H(s) := e^{\frac{\beta}{\gamma} \text{diag}(A(s - \mathbb{1}_n + r(0)))} s(0), \quad (1.17)$$

and $s(\infty)$ is a fixed point of H , that is, $s(\infty) = H(s(\infty))$. The following theorem is novel.

Theorem 1.5.4 (Existence, uniqueness, and algorithm for the asymptotic point)

Consider the network SIR model (1.14), with positive rates β and γ and with initial condition $(s(0), x(0), r(0))$ satisfying $s(0) \gg \mathbb{0}_n$, $x(0) > \mathbb{0}_n$, $r(0) \geq \mathbb{0}_n$ and $s(0) + x(0) + r(0) = \mathbb{1}_n$. Let $(s(\infty), \mathbb{0}_n, r(\infty))$ be the asymptotic state of system (1.14). The map $H : \mathbb{R}^n \rightarrow \mathbb{R}^n$ defined by equation (1.17) has the following properties:

- (i) *there exists a unique fixed point s^* of the map H in the set $\{s \in \mathbb{R}^n \mid \mathbb{0}_n \leq s \leq \mathbb{1}_n - r(0)\}$. Moreover, $s^* = s(\infty)$ and $r(\infty) = \mathbb{1}_n - s^*$; and*

(ii) any sequence $\{y(k)\}_{k \in \mathbb{N}}$ defined by $y(k+1) = H(y(k))$ and initial condition $\mathbb{0}_n \leq y(0) \leq \mathbb{1}_n - r(0)$ converges to the unique fixed point s^* .

Proof: Since A is a non-negative matrix, and $s(0) \leq \mathbb{1} - r(0)$, one can easily observe that, if $\mathbb{0}_n \leq p \leq q \leq \mathbb{1}_n - r(0)$, then $\mathbb{0}_n \leq H(\mathbb{0}_n) \leq H(p) \leq H(q) \leq H(\mathbb{1}_n - r(0)) \leq \mathbb{1}_n - r(0)$. According to the Brower Fixed Point Theorem, the map H has at least one fixed point.

Define the sequence $\{p(k)\}_{k \in \mathbb{N}}$ by $p(k+1) = H(p(k))$ and $p(0) = \mathbb{0}_n$. Since

$$\mathbb{1}_n - r(0) \geq p(1) = H(\mathbb{0}_n) = e^{\frac{\beta}{\gamma} \text{diag}(-A\mathbb{1}_n + Ar(0))} s(0) \geq p(0),$$

we have $\mathbb{1}_n - r(0) \geq p(2) = H(p(1)) \geq H(p(0)) = p(1)$ and, by induction, $\mathbb{1}_n - r(0) \geq p(k+1) \geq p(k)$ for any $k \in \mathbb{N}$. Since $p(k)$ is non-decreasing and upper bounded by $\mathbb{1}_n - r(0)$, we conclude that the limit $p^* = \lim_{k \rightarrow \infty} p(k)$ exists, and p^* is a fixed point of the map H .

Similarly, define a sequence $\{q(k)\}_{k \in \mathbb{N}}$ by $q(k+1) = H(q(k))$ and $q(0) = \mathbb{1}_n - r(0)$. One can check that $q(k)$ is non-increasing and that $q^* = \lim_{k \rightarrow \infty} q(k)$ is a fixed point of map H . Moreover, since $p(0) \leq q(0)$, we have $p(k) \leq q(k)$ for any $k \in \mathbb{N}$ and thereby $p^* \leq q^*$.

If $p^* = q^*$, then, for any $\mathbb{0}_n \leq y(0) \leq \mathbb{1}_n - r(0)$, the sequence $\{y(k)\}_{k \in \mathbb{N}}$ defined by $y(k+1) = H(y(k))$ satisfies $p(k) \leq y(k) \leq q(k)$ for any $k \in \mathbb{N}$. Therefore, $y^* = \lim_{k \rightarrow \infty} y(k)$ exists and $y^* = p^* = q^*$, which implies that the fixed point of map H is unique. According to equation (1.16), $s(\infty)$ is the unique fixed point. This concludes the proof for statement (i) and (ii).

Now we eliminate the case $p^* < q^*$ by contradiction. First of all we prove that $q^* \ll \mathbb{1}_n - r(0)$. Let $N_i = \{j \mid a_{ij} > 0\}$ and $\mathcal{I}(k) = \{i \mid q_i(\tau) < 1 - r_i(0) \text{ for any } \tau \geq k\}$. We have $\mathcal{I}(0) = \emptyset$. Since $x(0) > \mathbb{0}_n$, we have $q(1) = s(0) < 1 - r(0)$, that is, there

exists i such that $q_i(1) < 1 - r_i(0)$. Moreover, since $q(k)$ is non-increasing, we have $q(k) \leq q(1)$ for any $k \geq 1$. Therefore, for any i such that $q_i(1) < 1 - r_i(0)$, it satisfies $q_i(k) \leq q_i(1) < 1 - r_i(0)$ for any $k \geq 1$. Since $j \notin \mathcal{I}(1)$ if $q_j(1) = s_j(0) = 1 - r_j(0)$, we conclude that $\mathcal{I}(1) = \{i \mid s_i(0) < 1 - r_i(0)\}$. Moreover, for any given $k \geq 1$, since, for any i such that $N_i \cap \mathcal{I}(k) \neq \phi$,

$$q_i(k+1) = H(q(k))_i = e^{\frac{\beta}{\gamma} \sum_{j=1}^n a_{ij} (q_j(k) - 1 + r_j(0))} s_i(0) < s_i(0) \leq 1 - r_i(0);$$

and for any i such that $N_i \cap \mathcal{I}(k) = \phi$ and $i \notin \mathcal{I}(k)$,

$$q_i(k+1) = H(q(k))_i = e^{\frac{\beta}{\gamma} \sum_{j=1}^n a_{ij} (q_j(k) - 1 + r_j(0))} s_i(0) = s_i(0) = 1 - r_i(0),$$

we have $\mathcal{I}(k+1) = \{i \mid N_i \cap \mathcal{I}(k) \neq \phi\} \cup \mathcal{I}(k)$ for any $k \geq 1$. Because the graph associated with A is strongly connected, we can argue that $\mathcal{I}(k)$ contains all the indices when k is large enough. Therefore, $q^* \ll \mathbb{1}_n - r(0)$.

Now suppose $p^* < q^*$. Let

$$\alpha = \min_j \frac{1 - r_j(0) - p_j^*}{q_j^* - p_j^*}, \quad \text{and} \quad w = (1 - \alpha)p^* + \alpha q^*.$$

We have $\alpha > 1$, $0_n \leq w < \mathbb{1}_n - r(0)$, and $w_i = 1 - r_i(0)$ for any i such that $\alpha_i = (1 - r_i(0) - p_i^*) / (q_i^* - p_i^*)$. Let $\mu = 1/\alpha$. Thereby $q^* = \mu w + (1 - \mu)p^*$, where $0 < \mu < 1$. This means that q^* is a convex combination of p^* and w . Since $H(s)_i$ is a strictly convex function of s , we obtain that

$$q_i^* = H(\mu w + (1 - \mu)p^*)_i < \mu H(w)_i + (1 - \mu)p_i^* \leq \mu(1 - r_i(0)) + (1 - \mu)p_i^* = q_i^*.$$

In the last inequality, we used the fact that $H(w)_i \leq 1 - r_i(0)$ for any $0 \leq w \leq \mathbb{1}_n - r(0)$.

The previous inequality yields a contradiction. ■

In the rest of this section, we present some numerical results for the network SIR model for the famous Krackhardt's advice network illustrated in Figure 1.5. This network reflects the data collected by Krackhardt [30] on the cognitive social structure of the management personnel in a high-tech machine manufacturing firm. In the network, each node represents an individual, and each directed link (i, j) means that individual i seeks advice from individual j . We refer the interested readers to [30] for more details.

Consider the epidemic spreading process on the Krackhardt's advice network. The associated adjacency matrix A is binary. Unless otherwise stated, the system parameters are set as $\beta = 0.5$ and $\gamma = 0.4$. As for initial condition, we select one node fully infected (the dark-gray node in Figure 1.5, say, with index 1), 16 fully healthy individuals, and zero recovered fraction — corresponding to $x(0) = \mathbf{e}_1$, $r(0) = \mathbf{0}_n$, and $s(0) = \mathbf{1}_n - x(0)$. These parameters lead to an initial effective reproduction number $R(0) = 3.57$.

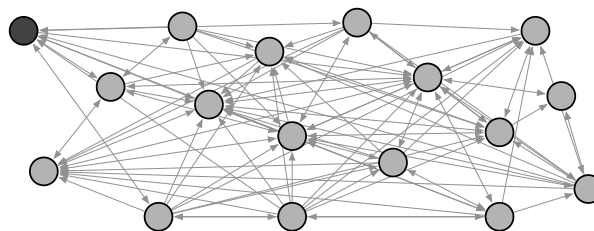


Figure 1.5: Main strongly-connected component of the Krackhardt digraph with 17 nodes

Figure 1.6 illustrates the time evolution of $(\beta/\gamma)\lambda_{\max}(t)$ with varying network parameters. Note that each evolution starts above the threshold, reaches the threshold value 1 in finite time, and converges to a final value below 1.

Figure 1.7 illustrates the behavior of the average susceptible, average infected and average recovered quantities in populations starting from a small initial infection fraction and with an effective reproduction number above 1 at time 0. Note that the evolution of the infected fraction of the population displays a unimodal dependence on time, like in

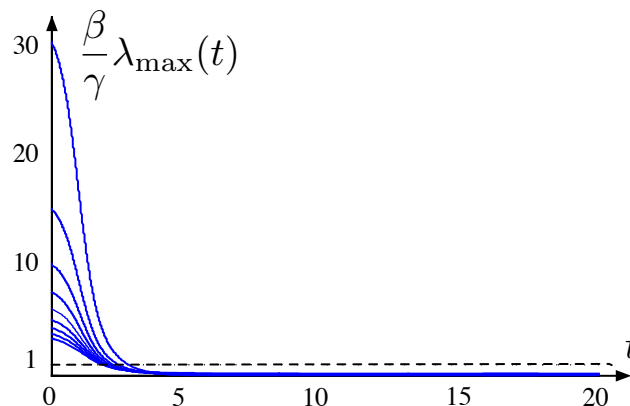


Figure 1.6: Evolution of the spectral radius of $(\beta/\gamma) \text{diag}(s(t))A$ over the strongly connected digraph in Figure 1.5. The parameter γ takes value in $.1, .2, \dots, .9$, corresponding respectively to the curves from up to down in the time interval $[0, 5]$.

the scalar model.

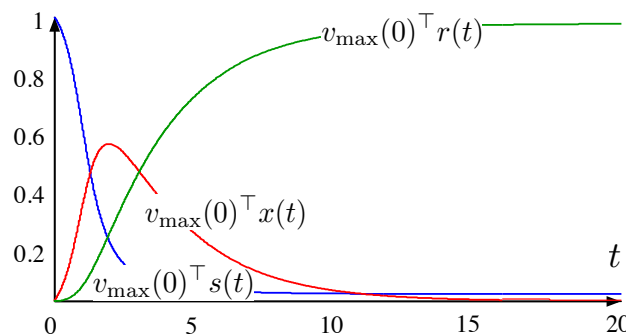


Figure 1.7: Evolution of the network SIR model from initial condition consisting of one node fully infected individual (the dark-gray node in Figure 1.5), 16 fully healthy individuals, and zero recovered fraction. The effective reproduction number satisfies $R(0) = 3.57$.

1.6 Conclusion

This chapter provides a comprehensive and consistent treatment of deterministic non-linear continuous-time SI, SIS, and SIR propagation models over contact networks. We investigated the asymptotic behaviors (vanishing infection, steady-state epidemic, and full contagion). We studied the transient propagation of an epidemic starting from small

initial fractions of infected nodes. We presented conditions under which a possible epidemic outbreak occurs or the infection monotonically vanishes for arbitrary fixed topology graphs. We introduced a network SI model and analyzed its behavior. Network SIS model sections includes improved properties over previously proposed works. New transient behavior, threshold condition, and system properties for the network SIR model were proposed. In addition, for the network SIR model, we provide a novel iterative algorithm to compute the asymptotic state of the system. In all cases, we show the results for network models are appropriate generalizations of those for the respective scalar models.

There are numerous potential future research directions regarding the deterministic network epidemic processes and the literature is still growing rapidly. Recent progress in this area includes but is not limited to the modeling and analysis of epidemic spreading on time-varying networks, e.g., see [31, 32], the optimal immunization strategies, e.g., see [33, 34], and the competitive propagation of multiple virus/memes, e.g., see [35, 36, 37].

Finally, we point out that, although the network SI, SIS, and SIR models have attracted enormous attention by researchers working on network epidemics, they are not the only deterministic models of epidemic spreading processes on networks. For example, there is another class of deterministic network models, referred to as the *multi-city model* or the *epidemic model in a patchy environment*. This class of models considers each node in the network as a city obeying the scalar SIS or SIR dynamics. The disease is spread via the traffic flows between those cities. We refer the interested reader to [38, 39, 40] for detailed treatments.

Chapter 2

Multi-group Connectivity Structures and Their Implications

2.1 Introduction

2.1.1 Motivation and problem description

As the size of a connected social network increases, multi-group formations that are distinguishable clusters of individuals become a characteristic and important feature of network topology. The connectivity of multi-group networks may be based on co-memberships, edge bundles that connect multiple individuals located in two disjoint groups, bridges that connect two individuals in two disjoint groups, or liaison hierarchies of nodes. Fig. 2.1 illustrates each form. A large-scale network may include instances of all four connectivity modalities. The work reported in this chapter is addressed to the implications of these different forms of intergroup connectivity. We set up populations of multiple subgroups and evaluate the implications of different forms of intergroup connectivity structures. We analyze the implications of different forms by adopting standard

models of opinion formation and information propagation that allow a comparative analysis on metrics of mean rates of information propagation, convergence times to consensus, and steady state deviations from the consensus value under conditions of noise.

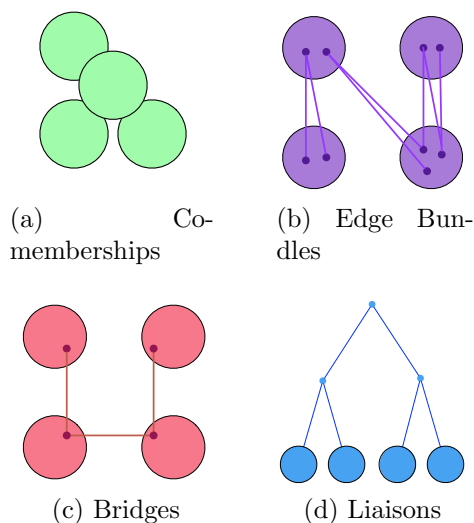


Figure 2.1: Small-scale illustration of the four forms of multi-group connectivity structures

2.1.2 Related literature

Typically, a corporation has formal hierarchical structure and additional informal communication structures [41]. The authority of the large-scale organizations is subject to the well-known problem of control loss, i.e., the cumulative decay of influence of superiors over subordinates along the chain-of-command [42, 43]. Classic and fascinating work on organization cultures [44] points to the importance of the topology of informal communication and influence networks in mitigating and exacerbating coordination and control problems. Other work has emphasized particular types of network typologies (linking-pin, bridge, ridge, co-membership, and hierarchical) that may serve as structural bases of mitigating coordination and control loss [41, 45, 46, 47]. In this work we propose generative network models and provide a comparative analysis for these

typologies, which we believe are lacking in the literature. Among the multitude of possible coordination and control structures for large groups, we study four prototypical structures and corresponding taxonomy shown in Fig. 2.1. Bridge connected structure, in which communication between subgroups are based on single contact edges between subgroups; the coordination and control importance of such bridges is the emphasis of the [46] model. According to Granovetter [46] only weak ties can be bridges and those weak ties are more likely to be sources of novel information making them surprisingly valuable. Additional references include [48, 49, 50, 51]. Ridge connected or redundant ties structure, in which multiple redundant contact edges connect pairs of groups providing a robust basis of subgroup connectivity; the coordination and control importance of such ridges is the emphasis of [45], Chapter 8. Additional references are [52, 53, 54]. Co-membership intersection structures, in which subgroups have common members; the coordination and control importance of such structures is the emphasis of the linking-pin model by Likert [41]. This structure represents an organization as a number of overlapping work units in which a member of a unit can belong to other units. Further references include [55, 56, 57]. Hierarchical connected structure, in which distinct subgroups communicate through liaisons, e.g., a star configuration in which a single individual (who may or may not be in a command role) monitors and facilitates all the work by subgroups and is responsible for all communications among them. Further references are [58, 59, 47, 60].

We relate the generative models for the first three connectivity structures (co-memberships, edge bundles, and bridges) to stochastic block models (SBMs), which were first introduced in statistical sociology by Holland et al. [61] and Fienberg & Wasserman [62]. Also known as planted partition model in theoretical computer science, SBM is a generative graph model that leads to networks with clusters. Conventionally, SBMs are defined for undirected binary graphs and non-overlapping communities. Generalizations of these models to digraphs [63], overlapping memberships [64], weighted graphs [65] and

arbitrary degree distributions [66] have also been studied.

In the field of social network science, the four forms of subgroup connectivity illustrated in Fig. 2.1 are familiar constructs. Comparative research on their implications is limited. Granovetter [46] and Watts & Strogatz [67] have focused on the implications of multi-group connectivity based on bridges. Friedkin [45] focused on co-membership and edge-bundle connectivity constructs, referring to them as “ridge” structures. Reynolds & Johnson [59] focused on the importance of liaisons. It may be that ridge structures provide a more robust basis of influence and information flows than thinly dispersed bridges and liaisons. We are unaware of any comparative analysis of all four forms of inter-group connectivity structures that employs a common set of dynamical-system behavioral metrics.

2.1.3 Statement of contribution

We develop generative-network models that set up sample networks for each form of multi-group connectivity topology and conduct a comparative analysis of them, which we believe is lacking in the literature. Our models, under some additional constraints, can be regarded as stochastic block models. We compare these network topologies on three metrics: (i) spectral radius, that is a metric of the rate of information propagation in a network propagation models, (ii) convergence time to consensus based on the classic French-DeGroot opinion dynamics, and (iii) steady state deviation from the French-DeGroot consensus value in the presence of noise. We perform a regression analysis to obtain an equitable comparison on the performance of these four connectivity structures and to account for the discrepancies among their structural properties. We learned that the development of generative-network models, suitable for this comparative analysis, is non-trivial. We lay out in detail the assumptions of our models. This is the

methodological contribution of the chapter. The comparative analysis of network metrics, over samples of networks of increasing size in the class of each form of multi-group connectivity, is our theoretical contribution to a better understanding of the implications of these different forms.

For network propagation processes, we refer to the classic references [2, 3, 9] and to the recent review [68]. For opinion dynamic processes and the French-DeGroot model, we refer to the classic references [69, 70] and the books [45, 71, 8].

2.1.4 Preliminaries

Graph theory Each graph $\mathcal{G}(\mathcal{V}, \mathcal{E})$ is identified with the pair $(\mathcal{V}, \mathcal{E})$. The set of graph nodes $\mathcal{V} \neq \emptyset$ represents actors or groups of actors in a social network. $|\mathcal{V}| = n$ is the size of the network. The set of graph links \mathcal{E} represents the social interactions or ties among those actors. We denote the set of neighbors of node i with \mathcal{N}_i . In a weighted graph, edge weights represent the frequency or the strength of contact between two individuals, whereas in a binary graph all edge weights are equal to one. The density of \mathcal{G} is given by ratio of the number of its observed to possible edges, $\frac{2|\mathcal{E}|}{n(n-1)}$. Graph \mathcal{G} is called dense if $|\mathcal{E}| = \mathcal{O}(n^2)$ and sparse if $|\mathcal{E}| \ll n^2$. A graph with density of 1 is a *clique*.

A walk of minimum length between two nodes is the shortest path or geodesic. Average geodesic length is defined by $L = \frac{1}{n(n-1)} \sum_{i,j \in \mathcal{V}, i \neq j} d_{ij}$, where d_{ij} is the length of the geodesic from node i to node j . A connected acyclic subgraph of \mathcal{G} spanning all of its nodes is a spanning tree. A uniform spanning tree of size n is a spanning tree chosen uniformly at random in the set of all possible spanning trees of size n . Degree or connectivity of node i is defined as the number of edges incident on it. The degree distribution of a graph $P(k)$ is the number of nodes with degree k , or the probability that a node chosen uniformly at random has degree k . The clustering coefficient of node

i is given by the ratio of existing edges between the neighbors of node i over all the possible edges among those neighbors. Letting $c_i = \frac{2e_{jk} : v_j, v_k \in \mathcal{N}_i, e_{jk} \in \mathcal{E}}{k_i(k_i - 1)}$, $k_i = |\mathcal{N}_i|$, the average clustering coefficient of graph \mathcal{G} is defined as $C = \frac{1}{n} \sum_{i \in \mathcal{V}} c_i$.

An Erdős-Rényi graph [72] is constructed by connecting nodes randomly. Each edge is included in the graph with a fixed probability p independent from every other edge. We represent such graph as $\mathcal{G}_{ER}(n, p)$ where p is the probability that each edge is included in the graph independent from every other edge. The probability distribution of $\mathcal{G}_{ER}(n, p)$ follows a binomial distribution $P(k) = \binom{n-1}{k} p^k (1-p)^{n-1-k}$, and its average clustering coefficient is given as $C = p$.

Linear algebra We denote the adjacency matrix of \mathcal{G} with $A \in \mathbb{R}^{n \times n}$ whose a_{ij} th entry is equal to the weight of the link between nodes i and j when such an edge exists, and zero otherwise. Matrix A is irreducible if the underlying digraph is strongly connected. If digraph \mathcal{G} is aperiodic and irreducible, then A is primitive. (A digraph is aperiodic if the greatest common divisor of all cycle lengths is 1.) A cycle is a closed walk, of at least three nodes, in which no edge is repeated.

We adopt the shorthand notations $\mathbb{1}_n = [1, \dots, 1]^\top$ and $\mathbb{0}_n = [0, \dots, 0]^\top$. Given $x = [x_1, \dots, x_n]^\top \in \mathbb{R}_n$, $\text{diag}(x)$ denotes the diagonal matrix whose diagonal entries are x_1, \dots, x_n . For an irreducible nonnegative matrix A , λ_{\max} denotes the dominant eigenvalue of A which is equal to the spectral radius of A , $\rho(A)$. The left positive eigenvector of A associated with λ_{\max} is called the left dominant eigenvector of A .

Empirical networks properties Our generative-network models attend to three often observed properties of real networks. (i) *Small average shortest path*: in networks with a large number of vertices, the average shortest path lengths are relatively small due to the existence of bridges or shortcuts. (ii) *Heavy tail degree distribution*: in contrast to Erdős-

Rényi graphs with binomial degree distribution, degree distributions of more realistic networks display a power law shape: $P(k) \sim Ak^{-\alpha}$, where typically $2 < \alpha < 3$. (iii) *High average clustering coefficient*: in most real world networks, particularly social networks, nodes tend to create tightly knit groups with relatively high clustering coefficient.

Stochastic block model (SBM) Let $n, k \in \mathbb{Z}^+$ denote the number of vertices and the communities, respectively; $p = (p_1, \dots, p_k)$ be a probability vector (the prior) on the k communities, and $W \in \{0, 1\}^{k \times k}$ be a symmetric matrix of connectivity probabilities. The pair (X, \mathcal{G}) is drawn under the $\text{SBM}(n, p, W)$ if X is an n -dimensional random vector with i.i.d. components distributed under p , and $\mathcal{G}(\mathcal{V}, \mathcal{E})$ is a simple graph where vertices v and u are connected with probability W_{X_v, X_u} , independently of any other pairs. We define the community sets by $\Omega_i = \Omega_i(X) := \{v \in \mathcal{V} : X_v = i\}, i \in \{1, \dots, k\}$.

Note that edges are independently but not identically distributed. Instead, they are conditionally independent, i.e., conditioned on their groups, all edges are independent and for a given pair of groups (i, j) , they are i.i.d. Because each vertex in a given group connects to all other vertices in the same way, vertices in the same community are said to be stochastically equivalent. The distribution of (X, \mathcal{G}) for $x \in \{1, \dots, k\}^n$ is given by:

$$\begin{aligned} \mathbb{P}\{X = x\} &:= \prod_{u=1}^n p_{x_u} = \prod_{i=1}^k p_i^{|\Omega_i(x)|}, \\ \mathbb{P}\{\mathcal{E} = y | X = x\} &:= \prod_{1 \leq u < v \leq n} W_{x_u, x_v}^{y_{uv}} (1 - W_{x_u, x_v})^{(1-y_{uv})}. \end{aligned}$$

The law of large numbers implies that, almost surely, $\frac{1}{n}|\Omega_i| \rightarrow p_i$.

Symmetric SBM (SSBM) If the probability vector p is uniform and W has all diagonal entries equal to q_{in} and all non-diagonal entries equal to q_{out} , then the SBM is

said to be symmetric. We say (X, \mathcal{G}) is drawn under the $\text{SSBM}(n, k, q_{in}, q_{out})$, where the community prior is $p = \{1/k\}^k$, and X is drawn uniformly at random with the constraints $|\{v \in \mathcal{V} : X_v = i\}| = n/k$. The case where $q_{in} > q_{out}$ is called assortative model.

2.2 Methods

To design our four models we first generate a sequence of group sizes, and refer to the appendix for some of the detailed algorithms involved. Secondly, we produce the community structures according to the sequence of group sizes and add the interconnections among them in the four modalities of multi-group connectivity.

2.2.1 Generating subgroup sizes

In this section we describe an algorithm to generate relative subgroup sizes, and introduce the resulting properties of these subgroups. We compute a normalized sequence of group sizes with a heavy tail distribution. We refer to Algorithm 1 in the appendix for a formal description based on pseudocode. Each subgroup is modeled as a connected dense Erdős-Rényi graph. For ϵ substantially smaller than 1 (we shall select it to be 10%), a subgroup of size i is the random graph $\mathcal{G}_{ER}(i, 1 - \epsilon)$.

Each subgroup of size i and edge probability $1 - \epsilon$ has the following properties:

- (i) connectivity threshold of $t(i) = \frac{\ln(i)}{i}$, that is, for $1 - \epsilon > t(i)$, \mathcal{G}_{ER} is almost surely connected (almost any graph in the ensemble \mathcal{G}_{ER} is connected);
- (ii) $(1 - \epsilon) \frac{i(i-1)}{2}$ edges on average;
- (iii) small average shortest path close to 1 and depending at most logarithmically on i ;

- (iv) binomial degree distribution: $P(k) = \binom{i-1}{k}(1-\epsilon)^k(\epsilon)^{i-1-k}$. Note that as ϵ decreases, the standard error becomes smaller and the distribution is more densely concentrated around the mean $(i-1)(1-\epsilon)$; and
- (v) large clustering coefficient close to 1 (conditioned on small ϵ) and equal to $C = 1-\epsilon$.

Given a population of n individuals, Algorithm 1 generates a sequence of relative subgroup sizes, such that, when interpreted as a disconnected graph, the collection of these subgroups exhibits a heavy tail degree distribution. An example of subgroup sizes generated by Algorithm 1 is illustrated in Fig. 2.2.

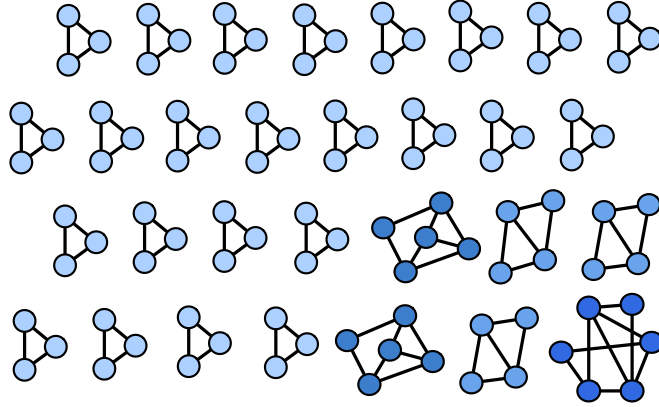


Figure 2.2: A collection of subgroups on 100 individuals.

As part of Algorithm 1, we design the probability distribution for the subgroup size i to be proportional to $\frac{1}{i^3}$. The choice of exponent equal to 3 is based on the following notes: first, in order for $f(i) = \frac{k}{i^\alpha}$ and its mean to be well-defined, one should have $\alpha \geq 2$; second, if one additionally requires the distribution to have a finite variance, then $\alpha \geq 3$. With exponent 3, the outcome of each realization of the algorithm is a collection of mostly small connected subgroups.

2.2.2 Models of multi-group connectivity

In this section we describe the algorithms that generate realizations of the four multi-group connectivity modalities.

For three of the four modalities (bridges, edge bundles, and co-members), we connect the subgroups through a minimal set of pairwise coordination problems among them. Specifically, a minimal set of pairwise coordination problems is modeled through the notion of a random spanning tree among the subgroups. To define the generative algorithms for these three structures, we apply the notion of stochastic block models.

Bridge connectivity model

Here we propose an algorithm to generate the bridge connected model. This structure can be modeled as a stochastic block model where the communities are connected through a uniform randomly generated spanning tree, and the interconnections are through precisely one node of each subgroup. We denote the edge set of this random tree with \mathcal{E}_T . The graph is drawn under the $\text{SBM}(n, p, W^B)$, conditioned under connectivity, where p is calculated by Algorithm 1, and W^B is given by:

$$W_{ij}^B = \begin{cases} 1 - \epsilon, & \text{if } i = j, \\ \frac{1}{n^2 p_i p_j} = \frac{1}{s_i s_j}, & \text{if } i \neq j \text{ and } ij \in \mathcal{E}_T, \\ 0, & \text{otherwise,} \end{cases} \quad (2.1)$$

where $s_i = |\Omega_i|$ denotes the size of group i , and W^B contains a tree structure. Note that given an SBM, a node in community i has $np_j W_{ij}$ neighbors in expectation in community j . We illustrate a realization of our algorithm in Fig. 2.3.

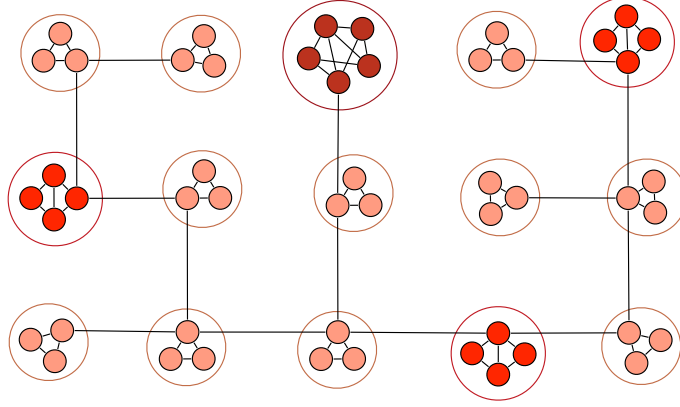


Figure 2.3: Example of a network of 50 individuals in subgroups connected by bridges.

Edge bundle connectivity model

In this section we propose an algorithm to generate the edge bundle connectivity model. Again we apply a random spanning tree as the building block of the interconnections. Here, instead of adding a single edge as the basis of intergroup connectivity, we add multiple edges whose number grows with the size of the subgroups. We illustrate an algorithm realization in Fig. 2.4.

We draw the graph under the $\text{SBM}(n, p, W^{EB})$, conditioned under redundant connectivity. Communities are connected through a uniform randomly generated spanning tree with edge set \mathcal{E}_T . The interconnections involve two or more nodes from neighboring subgroups. p is calculated by Algorithm 1, and W_{EB} is given by:

$$W_{ij}^{EB} = \begin{cases} 1 - \epsilon, & \text{if } i = j, \\ \frac{\alpha_{ij}}{n^2 p_i p_j} = \frac{\alpha_{ij}}{s_i s_j}, & \text{if } i \neq j \text{ and } ij \in \mathcal{E}_T, \\ 0, & \text{otherwise,} \end{cases} \quad (2.2)$$

where W^{EB} contains a tree structure, $\alpha_{ij} = \alpha_{ji} \geq 2$ for all i, j , and α_{ij} scales with $s_i s_j$.

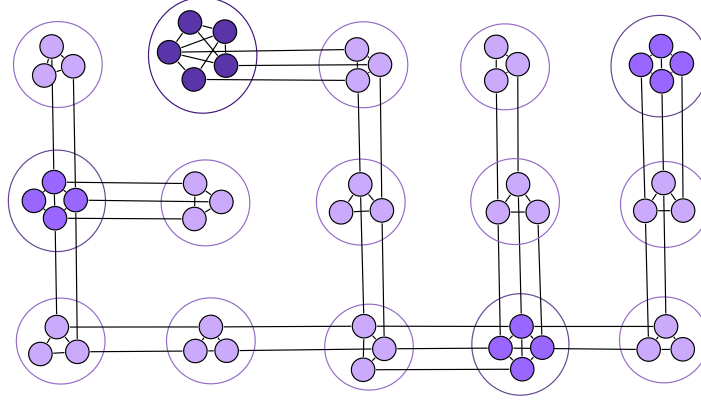


Figure 2.4: Example of a network of 50 individuals in subgroups connected by bundles of edges.

Co-membership connectivity model

In addition to the existence of a uniform random spanning tree over the subgroup, our co-membership connectivity model generation is conditioned under the following topological constraint: we consider each pair of connected subgroups, say i and j , and select a fraction of edges in the complete bipartite graph over i and j . For each of these selected edges, we randomly select one of the two individuals, say the individual in i , and we turn this individual into a member of the subgroup j by adding edges from this individual to almost all members of v . We illustrate an algorithm realization in Fig. 2.5.

The co-membership model can be generated as a realization of $\text{SBM}(n, p, W^C)$, conditioned under the edge bundles initiated from a single node in one of the corresponding subgroups. Again \mathcal{E}_T denotes the edge set of the random tree, p is calculated by Algorithm 1, and W^C is given by:

$$W_{ij}^C = \begin{cases} 1 - \epsilon, & \text{if } i = j, \\ \frac{\alpha_{ij}}{n^2 p_i p_j} = \frac{\alpha_{ij}}{s_i s_j}, & \text{if } i \neq j \text{ and } ij \in \mathcal{E}_T, \\ 0, & \text{otherwise,} \end{cases} \quad (2.3)$$

where W^C contains a tree structure, $\alpha_{ij} = \alpha_{ji} \geq 3$ for all i, j , and α_{ij} scales with either s_i or s_j ($\alpha_{ij} \approx s_i$ or $\alpha_{ij} \approx s_j$).

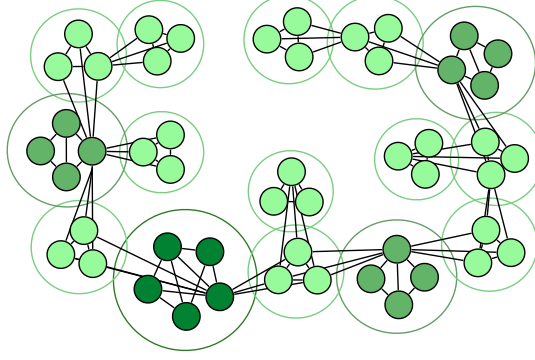


Figure 2.5: Example of 50 individuals in a co-membership connected network.

Liaison hierarchy connectivity model

Here, applying Algorithm 1 we first generate the subgroups as dense Erdős-Rényi graphs. Then we partition the subgroups into sets of 2 or 3, and (i) assign a liaison to each of sets and (ii) recursively assign a new liaison to groups of 2 or 3 liaisons until we reach the root at the top of the hierarchy. The resulting graph is a hierarchical tree structure with random branching factors of 2 and 3. A detailed description is provided in Algorithm 3 in the appendix, and Fig. 2.6 illustrates a realization of this model.

2.3 Results

Realistic networks are usually not exclusively based on a single modality of subgroup connectivity. Our comparative analysis of connectivity modalities is oriented to the question of the implications of a shift away from one modality toward another modality. For

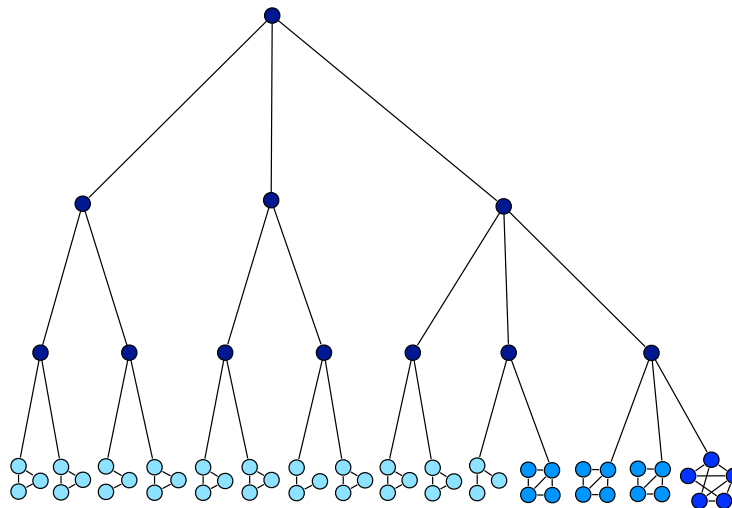


Figure 2.6: Example of 50 individuals in subgroups joined by a liaison hierarchy generated by Algorithm 3.

example, a modality shift from a liaison hierarchy toward direct bridges among subgroups, or from bridges among subgroups to intergroup edge bundles, or from intergroup edge bundles to co-memberships.

In Fig. 2.7 we present a comparison of the average shortest paths and average degrees of our generated networks as a function of network size for each of the four multi-group connectivity modalities. Each sample point on the curves is based on 100 realizations on networks with sizes that increase in step sizes of 50 up to 2,000 nodes. In analyses that increase the sample point size to 1,500 over a range of sizes up to 500, there is no marked change in the trajectories. In general, the confidence interval bands are narrow. Here, and elsewhere, red refers to the bridge model, purple to the edge bundle model, green to the co-membership model, and blue to the liaison hierarchy model. Fig. 2.7a shows that the liaison hierarchy increasingly distinguishes itself from the three modalities as network size increases. Its displayed trajectory is conditional on the liaison structure design. Average shortest paths are insensitive to redundancies. Hence, the lack of distinctions among the other three modalities is not surprising. Fig. 2.7b shows that the four modalities

are systematically ordered with respect to their average degrees: (co-membership) $>$ (edge-bundle) $>$ (bridge) $>$ (liaison) with respect to their average degrees.

Spectral radius and propagation processes

Propagation phenomena appear in various disciplines, such as spread of infectious diseases, transmission of information, diffusion of innovations, cascading failures in power grids, and spread of wild-fires in forests. Based on the application, the objective can vary from avoiding epidemic outbreaks and eradicating the disease in a population to facilitating the spread of an ideology or product over a network in marketing campaigns. In this subsection we provide a comparison of the system behavior under the simple and well-studied epidemic models proposed in the literature for our four proposed network models.

Let $x(t) = (x_1(t), \dots, x_n(t))^T$ denote the infection probabilities of each node at time t and $A \in \mathbb{R}^{n \times n}$ denote the adjacency matrix of the contact graph. Let $\beta > 0$ be the infection rate, and $\gamma > 0$ be the *recovery rate* to the susceptible state. Then the linearization of the *SI (Susceptible-Infected)* and *SIS (Susceptible-Infected-Susceptible)* network propagation models about the no-infection equilibrium point $\mathbb{0}_n$ on a weighted digraph are given by, respectively,

$$\dot{x} = \beta Ax, \tag{2.4}$$

$$\dot{x} = (\beta A - \gamma I_n)x. \tag{2.5}$$

The following results are well known (see the classic works [2, 9, 10] and the recent review [68]). In the SI model the epidemic initially experiences exponential growth with rate $\beta\lambda_{\max}$. In the SIS model near the onset of an epidemic outbreak, the exponential growth rate is $\beta\lambda_{\max} - \gamma$ and the outbreak tends to align with the dominant eigenvector.

In Fig. 2.8 we plot the spectral radius of the networks as a function of network size 50-2,000 for the four models. In Table 2.1 we evaluate the differences among these curves controlling a network's size (N), average degree (Degree), and (0,1) indicator variables for the edge-bundle, co-membership, and liaison modalities with the bridge modality taken as the baseline. Similar findings were obtained with 660K observations on a reduced range of network sizes 24-655. The average degree of a network has a positive effect on the speed of viral propagation. Controlling for network size and average degree, relative to the propagation speeds in the bridge modality, propagation speeds in the edge-bundle and liaison modalities are greater and those of the co-membership modality are less. The elevated curve for co-membership modality in Fig. 2.8 is based on its systematically higher average degrees.

Table 2.1: Nonlinear regression results for spectral radius, controlling for network size and average degree, and indicator variables for the connectivity modalities with bridge modality as baseline (15,200 networks, $R^2 = 0.833$)

	coeff.	s.e.	p-value
Constant	-2.8103	0.12916	<.0001
N	0.0038847	5.2749e-05	<.0001
Degree	5.0734	0.088421	<.0001
Edge-bundle	0.2012	0.019035	<.0001
Co-membership	-1.8589	0.062881	<.0001
Liaison	0.24287	0.023229	<.0001
N^2	-8.3082e-07	2.1709e-08	<.0001

Time to convergence in influence processes generating consensus with distributed linear averaging

Consensus algorithms play an important role in many multi-agent systems. They are usually defined as in French-DeGroot discrete-time averaging recursion

$$x(t+1) = Wx(t). \quad (2.6)$$

where W is row stochastic and $x(t) \in \mathbb{R}^n$ is the vector of individuals' opinions at time t . For primitive stochastic matrices the solution to (2.6) satisfies

$$\lim_{k \rightarrow \infty} x(k) = (v^T x(0)) \mathbf{1}_n \quad (2.7)$$

where v is the left dominant eigenvector of W satisfying $v_1 + \dots + v_n = 1$. Convergence time to consensus may be defined as $\tau_{\text{asym}} = \frac{1}{\log(1/r_{\text{asym}})}$ and it gives the asymptotic number of steps for the error to decrease by the factor $1/e$, where r_{asym} denotes the asymptotic convergence factor. It is well known, e.g., see [8], Chapter 10, that convergence to consensus is exponentially fast as ρ_2^t , where ρ_2 is the second largest eigenvalue of W in magnitude. We construct W from A as follows:

$$W = (D + I_n)^{-1}(A + I_n), \quad (2.8)$$

where $D = \text{diag}(A\mathbf{1}_n)$ denotes the diagonal matrix of all the nodes' out-degrees, with $d_{ii} = \sum_{j=1}^n a_{ij} \forall i$. Equation 2.8 gives positive weights w_{ii} that are equal to the w_{ij} weights of i 's neighbors in A .

In Fig. 2.9, we plot the average convergence-times of the networks as a function of network size 50-2,000 for the four models. In Table 2.2 we evaluate the differences among these curves controlling a network's size (N), average degree (Degree), and (0,1) indicator variables for the edge-bundle, co-membership, and liaison modalities with the bridge modality taken as the baseline. Similar findings were obtained with 660K observations on a reduced range of network sizes 24-655. The convergence times of the bridge modality are larger than those of the three other modalities, and the liaison modality has the fastest convergence times. Higher average degrees lower times to convergence. Controlling for network size and average degree, the convergence times of the edge-bundle modality are

faster than those of the co-membership modality.

Table 2.2: Nonlinear regression results for convergence time, controlling for network size and average degree, and indicator variables for the connectivity modalities with bridge modality as baseline (15,200 networks, $R^2 = 0.637$)

	coeff.	s.e.	p-value
Constant	6991.1	590.12	<.0001
N	11.558	0.241	<.0001
Degree	-3300.9	403.98	<.0001
Edge-bundle	-4652.9	86.969	<.0001
Co-membership	-2993.9	287.29	<.0001
Liaison	-7790.3	106.13	<.0001
N^2	-0.0018372	9.9184e-05	<.0001

Consensus processes subject to white Gaussian noise

The general form of a French-DeGroot influence process with white Gaussian noise is:

$$x(t+1) = Wx(t) + e(t) \quad (2.9)$$

where $e(t)$ is a random vector with zero mean and covariance Σ_e having independent entries. In the presence of noise, the states of the agents will be brought close to each other, but will not fully align to exact consensus. The resulting noisy consensus is referred to as *persistent disagreement*. For strongly connected and aperiodic graphs, the consensus dynamics (2.6) correspond to an irreducible and aperiodic Markov chain. The matrix W then corresponds to the transition probability matrix and its normalized left dominant eigenvector π corresponds to the stationary distribution vector of the chain. The results on the steady-state disagreement by Jadbabaie & Olshevsky [73] apply to reversible Markov chains which with the choice of weights on our adjacency matrix will be met. For the Markov chain with reversible transition matrix W and with uncorrelated

noise, the mean square asymptotic error δ_{ss} can be measured by:

$$\delta_{ss} = \pi^T H D_\pi \Sigma_e D_\pi \mathbf{1}_n, \quad (2.10)$$

where $D_\pi = \text{diag}(\pi)$, and H is the matrix of hitting times for the Markov chain. The algorithm by Kemeny & Snell [74] is applied to compute H .

In Fig. 2.10, we plot the steady-state mean deviation from consensus, given by (2.10), on the networks as a function of network size 50-2,000 for the four models. In Table 2.3 we evaluate the differences among these curves controlling a network's size (N), average degree (Degree), and (0,1) indicator variables for the edge-bundle, co-membership, and liaison modalities with the bridge modality taken as the baseline. Similar findings were obtained with 660K observations on a reduced range of network sizes 24-655. The steady-state mean deviations for the bridge modality are larger than those of the three other modalities. Higher average degrees lower steady-state mean deviations from consensus. Although the modalities have distinguishable effects, again we note that average degree differences are “boiled into” the modality models, so that when average degree is controlled, the relative ordering of modalities is altered. The edge-bundle and liaison modalities have greater noise reduction properties than the co-membership modality.

Table 2.3: Nonlinear regression results for steady-state mean deviation from consensus, controlling for network size and average degree, and indicator variables for the connectivity modalities with bridge modality as baseline (15200 networks, $R^2 = 0.768$)

	coeff.	s.e.	p-value
Constant	30.894	0.84085	<.0001
N	0.031003	0.0003434	<.0001
Degree	-9.1312	0.57562	<.0001
Edge-bundle	-16.807	0.12392	<.0001
Co-membership	-10.502	0.40935	<.0001
Liaison	-14.052	0.15122	<.0001
N^2	-9.1291e-06	1.4133e-07	<.0001

2.4 Discussion

We have proposed simple, synergistic, and stochastic algorithms to generate four modalities of multi-group connectivity and have compared their implications. These algorithms are a variant of what is known as planted partition or stochastic block models, under some further topological constraints including that the intergroup connectivity is shaped by an underlying tree. Models 1-3 are nested in the following sense: for appropriate parameters, 1) graphs generated by the bridge connectivity structure are subgraphs of those generated by the edge bundles, and 2) graphs generated by the edge bundle connectivity structure could be subgraphs of those generated by the co-membership. However, moving from the edge bundles to co-memberships, we introduce an additional constraint, that is, edge bundles of the spanning tree are initiated from the same node in one of neighboring subgroups in the co-membership model. The work touches on two central traditions in network analysis: models of network structure and models of dynamical processes that unfold on networks composed of multiple small groups with dense within-group edges. In a connected network, any two such groups might be intersecting (with one or more individuals who are members of both) or disjoint. Two disjoint subgroups may be linked by a bridge, or by multiple edges, or by individuals who are not members of any dense group. We consider networks that can be strictly characterized in terms of one of these types of inter-group connectivity. The touchstone for our analysis is the work that has been conducted on multiple-group connectivity based on bridges. Here we elaborate the analysis with a comparison of implications of group-connectivity based on (i) a minimal set of bridges, (ii) a minimal block-model structure in which pairs of groups are linked by multiple edges, (iii) a minimal set of group membership intersections, and (iv) a hierarchical tree of group-independent agents (intermediary liaisons.) No doubt there are many ways to construct realizations of each type of connectivity. No doubt there

are many process metrics that might be examined. We compare structures in terms of network process metrics. We focus on metrics of two processes—epidemic propagation and consensus formation. These metrics are sensitive to network topology. We emphasize that the results of these comparative analyses are not merely due to the different numbers of links being added to isolated clusters. The regression results controlling for the network sizes and average node degrees affirm this claim. We constrain topology to four broad classes of markedly non-random clustered networks. Our contribution is to show the feasibility of a principled approach to a comparative analysis that we believe is currently lacking with respect to these distinguishable topological classes.

Our findings on the speed of viral propagation show that the speeds differ depending on the form of multi-group connectivity. The average degree of a network has a positive effect on the speed of viral propagation. If the average degrees differences, shown in Fig. 2.7b, are characteristic features of the modalities, then Fig. 2.8 shows the net effect of each modality. Controlling for network size and average degree, our regression analysis in Table 2.1 evaluates the independent contributions of average degree and modality type. If it were possible to construct modality types with identical average degrees, then the regression results suggest that the bridge, edge-bundle, and liaison modalities do not substantially differ in their speeds of viral propagation, and that the co-membership modality dampens the speed of viral propagation.

Our findings on the times to convergence to consensus show that convergence times differ depending on the form of multi-group connectivity. The average degree of a network has a negative effect on convergence times, that is, higher average degrees are associated with faster convergence to consensus. If the average degrees differences, shown in Fig. 2.7b, are characteristic features of the modalities, then Fig. 2.9 shows the net effect of each modality. The bridge modality has slower convergence times than all other modalities. If it were possible to construct modality types with identical average degrees, then

the regression results in Table 2.2 suggest somewhat similar results. As in Fig. 2.9, the convergence times in the bridge modality are greater than all other modalities, and the liaison modality has the fastest convergence times. The regression on the edge-bundle and co-membership modalities indicates that, for a given average degree and network size, convergence is faster for edge-bundles than co-membership modalities.

Finally, our findings for levels of steady-state stochastic deviations from consensus in the presence of noise show that the mean deviations differ depending on the form of multi-group connectivity. The average degree of a network has a negative effect on steady-deviation, that is, higher average degrees are associated with smaller deviations (more reduction of noise). If the average degrees differences, shown in Fig. 2.7b, are characteristic features of the modalities, then Fig. 2.10 shows the net effect of each modality. The bridge modality has greater deviations (less reduction of noise) than all other modalities. If it were possible to construct modality types with identical average degrees, then the regression results in Table 2.3 suggest somewhat similar results. As in Fig. 2.9, the levels of noise reduction in the bridge modality are less than in all other modalities. The regression on the edge-bundle, co-membership and liaison modalities indicate that edge-bundles are associated with the greatest reduction of noise.

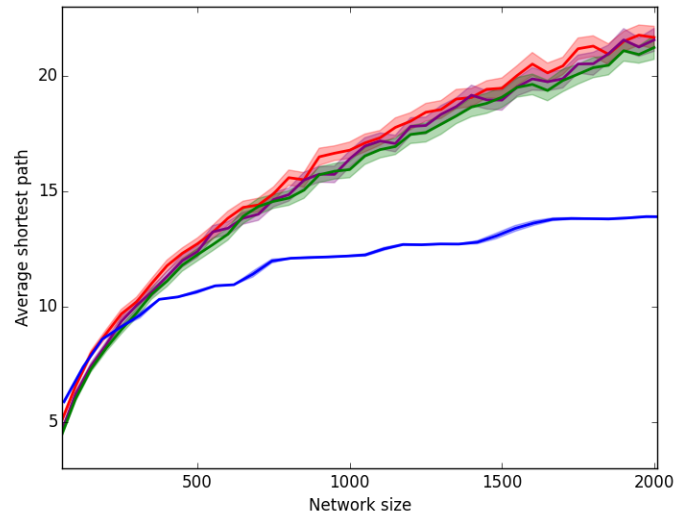
The important caveat on our findings is that they are conditional on positions taken in the models with which we generated realizations of each modality; see Algorithms 1-2 in the appendix. In addition, although it is reasonable that differences of average degree are associated with different modalities, we have not derived bounds on average degree for each modality (this may be an intractable problem). Furthermore, our analysis of multi-group connectivity modalities involves a uniform modality, whereas real networks with multiple subgroups are likely to be connected with mixed modalities including instances of bridges, edge-bundles, co-memberships, and liaison nodes who are not members of any group. We believe that these obvious limitations are out-weighted by the insights

obtained from an analysis of artificial network topologies with controllable features. In the set of findings of this chapter, we were particularly struck by (1) the implications on network process metrics of the social cohesion entailed in edge-bundle and co-membership modalities of multi-group connectivity, and (2) by the strong effects on process metrics of network differences of average degree arising from the multiple modalities.

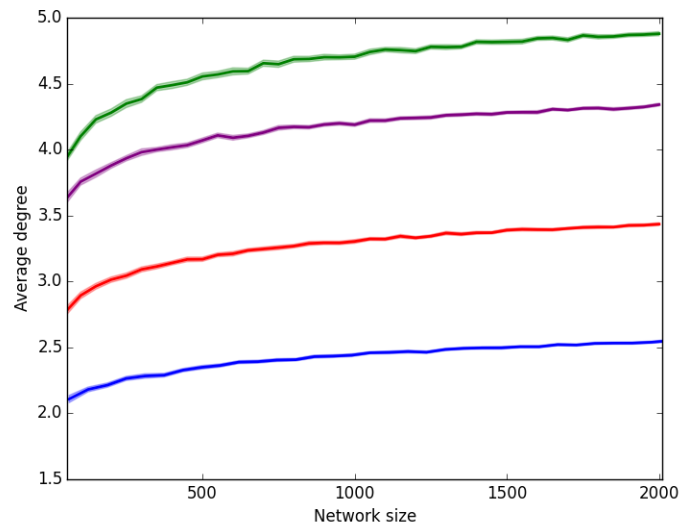
An interesting future research direction is to propose sufficiently predictive indicators that enable one to categorize an arbitrary graph into any of the four connectivity structures discussed in this chapter. In other words, we are interested in the following question: “given an empirically observed graph, can one provide a computationally efficient algorithm to identify subgroups and classify them into these different connectivity structures?” We find the results on the following literature relevant: recovery of the communities in the prolific community detection literature [75, 76], graph clustering [77], and graph modularity [78]. Stochastic block models are widely recognized generative models for community detection and clustering in graphs and they provide a ground truth for identifying subgroups. [79] surveys recent developments for necessary and sufficient conditions for community recovery and community detection in SBMs.

2.5 Permissions and Attributions

The content of chapter 2 and appendix A is the result of a collaboration with Pushkarini Agharkar and Noah E. Friedkin. The authors thank professor Ambuj K. Singh for his valuable comments and suggestions. This material is based upon work supported by, or in part by, the U.S. Army Research Laboratory and the U.S. Army Research Office under grant numbers W911NF-15-1-0577.



(a) Plot of average shortest path



(b) Plot of average degree

Figure 2.7: In each plot red refers to the bridge model, purple to the edge bundle model, green to the co-membership model, and blue to the liaison hierarchy model

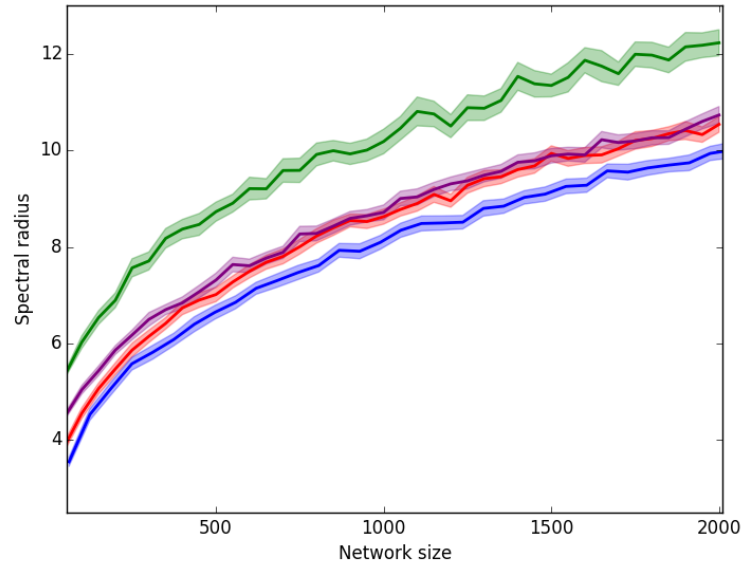


Figure 2.8: Plot of spectral radius

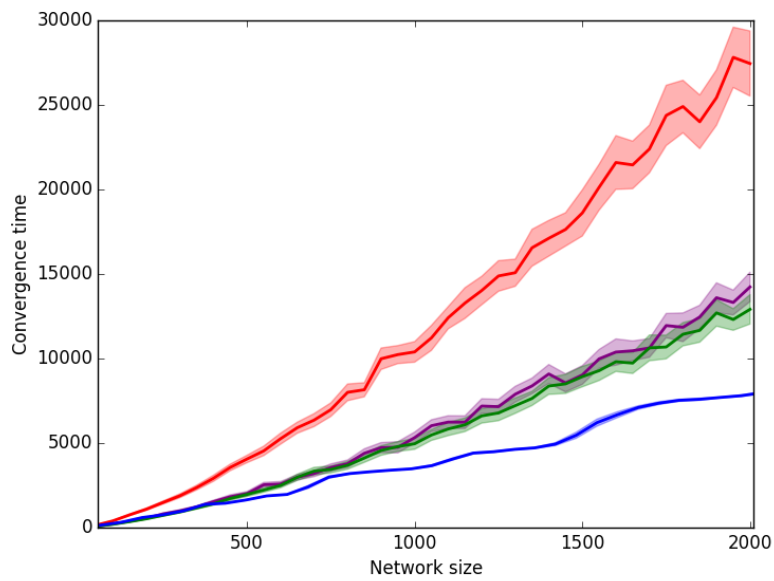


Figure 2.9: Plot of convergence time for the four network models with equal neighboring weights

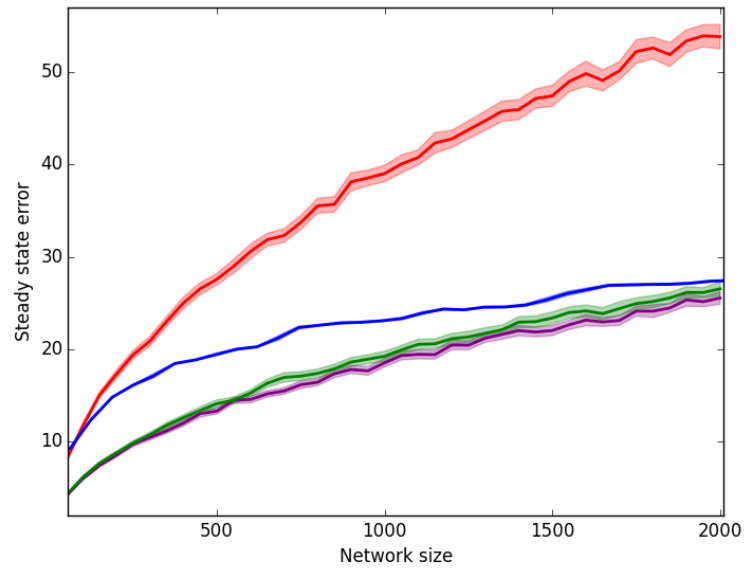


Figure 2.10: Plot of δ_{ss} of graph A for the four network models with equal neighboring weights

Chapter 3

Stable and Efficient Structures in Multigroup Network Formation

3.1 Introduction

3.1.1 Motivation and problem description

To study the coordination and control features of a group task, the multiple groups' performances must be fitted together. An enduring postulate in organization science is that coordination and control cannot be achieved strictly by the authority structure, but must also entail informal communication and influence networks that link the members of different task-oriented groups; we focus on formation of such network structures. As the size of a connected social network increases, multigroup formations that are distinguishable clusters of individuals become a characteristic and important feature of network topology. The connectivity of multigroup networks may be based on edge bundles connecting multiple individuals in two disjoint groups, bridges connecting two individuals in two disjoint groups, or co-memberships. A large-scale network may include instances

of all of these connectivity modalities. We set up populations of multiple groups and propose a dynamic model for formation of these intergroup connectivity structures.

Our economic dynamical model explains and predicts whether a network evolves into different coordination and control structures. Medium and large scale organizations adopt these multigroup structures to tackle complex nested tasks. Among the multitude of possible coordination and control structures, we study formation of multigroup connectivity structures shown in Fig. 3.1, which are familiar constructs in the field of social network science. For this purpose we apply a game-theoretic framework in which strategic agents

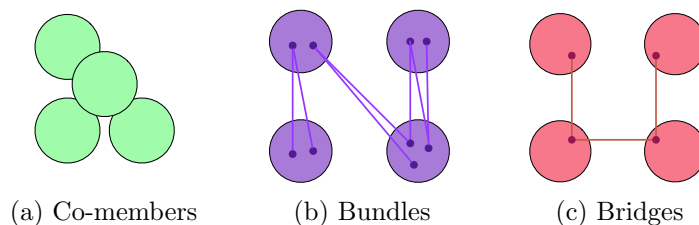


Figure 3.1: Schematic illustration of the three possible control and coordination structures

take actions based on the rate or importance of coordination problems. In other words, a value is assigned to the coordination problem between any two distinct groups, so that all control and coordination problems among groups are described by a square non-negative matrix, as illustrated in Fig. 3.2. In our setting, agents are myopic, self-interested, and have thorough knowledge of graph topology and the utility they acquire from any other agent.

3.1.2 Related literature

Bridge, edge bundle, and co-membership connectivity models have been studied extensively in [80], where implications of these structures are investigated and generative models are proposed for each. These prototypical structures can mitigate coordination

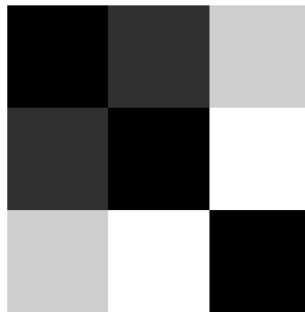


Figure 3.2: F = frequency/importance of intergroup coordination problem

and control loss in an organization. Coordination and control importance of bridge connected structure, in which communication between subgroups are based on single contact edges, is the emphasis of the [46, 48], and [49] models. Coordination and control importance of the redundant ties structure, in which multiple redundant contact edges connect pairs of groups, is the emphasis of [45], Chapter 8, [52], and [53]. Co-membership intersection structures, in which subgroups have common members, is the emphasis of the linking-pin model by Likert [41], as well as [56] and [57]. [81] and [82] propose a community detection algorithm for overlapping networks.

Jackson and Wolinsky introduced a strategic network formation model in their seminal paper [83]. They studied pairwise stability, where bilateral agreement is required for link formation. Homogeneity and common knowledge of current network to all players are two assumptions in this model. Jackson and Watts studied strategic network formation in a dynamic framework in [84]. The network formation model we present in this work is closely related to [83] and [84]. Jackson and Rogers examined an economic model of network formation in [85] where agents benefit from indirect relationships. They showed that small-world features necessarily emerge for a wide set of parameters.

In [86], Bala and Goyal proposed a dynamic model to study Nash and strict Nash stability. In their model, starting from any initial network, each player with some positive

probability plays a best response (or randomizes across them when there is more than one); otherwise the player exhibits inertia. A Markov chain on the state space of all networks is defined whose absorbing states are strict Nash networks. The authors proved that starting from any network, the dynamic process converges to a strict Nash network (i.e., the empty network or a center-sponsored star) with probability 1.

In [87], Olaizola and Valenciano extended the model in [86] and studied network formation under linking constraints. An exogenous link-constraining system specifies the admissible links. Players in the same component of the link-constraining network have common knowledge of that component. This model collapses to the unrestricted setting in [86] (when the underlying constraining network is complete graph). The set of Nash networks is a subset of Bala and Goyal's unrestricted Nash network sets.

In the network formation game by Chasparis and Shamma in [88] and [89], agents form and sever unidirectional links with other nodes, and stable networks are characterized through the notion of Nash equilibrium. Pagan and Dörfler [90] studied network formation on directed weighted graphs and considered two notions of stability: Nash equilibrium to model purely selfish actors, and pairwise-Nash stability which combines the selfish attitude with the possibility of coordination among agents. McBride dropped the common knowledge assumption and studied the effects of limited perception (each player perceives the current network only up to a certain distance) in [91]. Song and van der Schaar [92] studied a dynamic network formation model with incomplete information.

Community networks and their growth into potential socially robust structures is studied in [93]. Bringmann et al. analyzed the evolution of large networks to predict link creation among the nodes in [94]. [95] studied link inference problem in heterogeneous information networks by proposing a knapsack-constrained inference method.

3.1.3 Statement of contribution

We consider a strategic network formation game described by a cost of maintaining links, a benefit of having connections, and an importance of coordination problems among pre-specified groups. Our setup is a heterogeneous generalization of the famous connection model. For this game, we study the resulting multi-group structures that are pairwise stable and socially efficient.

For this game, we also introduce a formation dynamics whereby link formations require mutual consent and link removals can be initiated unilaterally. We study the conditions that give rise to formation of multigroup structures, as well as conditions which cause the multigroup structures be stable and/or efficient. Our contributions are as follows:

We introduce certain threshold functions and provide bounds based on these functions to study pairwise stable and efficient structures. We also investigate the convergence of Formation Dynamics. For our analysis, we first focus on the structure of each group and formation of intra-connections. We particularly study the conditions which result in each group being a clique, and present results on pairwise stability, efficiency, and convergence of these cliques.

We then focus on the interconnections among those cliques. We present results on the pairwise stability and convergence to disjoint union of cliques for multigroup structures of arbitrary sizes. The rest of the analysis for density of interconnections is divided into two sections: two-group connectivity structures and multigroup connectivity structures.

For the two group structures, we provide a complete characterization of full ranges of parameters for stability and efficiency. We present results on the pairwise stability and efficiency of minimally connected, redundantly connected, and maximally connected structures. We identify the ranges of parameter in which the efficient and the pairwise

stable structure overlap and those in which they have a conflict.

We then investigate the multigroup structures. We study the pairwise stability of minimally connected cliques along arbitrary interconnection structures. We show that for the special case of the interconnection being a star graph, it is possible to identify the boundaries of parameters for stability of all interconnections being minimally connected. We also present results on formation of redundancies and for efficiency.

3.1.4 Preliminaries

Each undirected graph is identified with the pair $(\mathcal{V}, \mathcal{E})$. The set of graph nodes $\mathcal{V} \neq \emptyset$ represents individuals or groups of individuals in a social network. $|\mathcal{V}| = n$ is the size of the network. The pair (i, j) is called an edge and it indicates the interaction between the two individuals i and j . The set of graph edges \mathcal{E} represents the social interactions or ties among all individuals. Throughout this chapter, since the individuals are unchangeable, we refer to the network $(\mathcal{V}, \mathcal{E})$ simply as \mathcal{E} .

The density of a graph is given by the ratio of the number of its observed to possible edges, $\frac{2|\mathcal{E}|}{n(n-1)}$. In a complete graph every pair of distinct nodes is connected by an edge. We denote the complete graph of size n by K_n . A clique is a subset of vertices of a graph in which every two distinct vertices are adjacent. We say two graphs are adjacent if they differ in precisely one edge. A path of length k is a sequence of nodes $i_1 i_2 \dots i_k$ such that $\{(i_s, i_{s+1})\} \in \mathcal{E}$. A walk of minimum length between two nodes is the shortest path. $d_{ij}(\mathcal{E})$ denotes the distance between nodes i and j , which is defined as the length of the shortest path beginning at i and ending at j .

3.2 Multigroup Network Formation Model

Consider a society of n individuals \mathcal{V} , divided into m groups. The set of m groups is denoted by $\{1, \dots, m\}$, $m \leq n$. $P = \{P_1, \dots, P_m\}$ represents the partitioning of individuals into the groups and is a set partition of size n , i.e., $\mathcal{V} = \bigcup_{\gamma=1}^m P_\gamma$, and $\bigcap_{\gamma=1}^m P_\gamma = \emptyset$. We use the shorthand notation $s_\gamma = |P_\gamma|$ denoting the size of group γ . Throughout this chapter, we assume that $s_\gamma \geq 3$ for all $\gamma \in \{1, \dots, m\}$.

Group coordination importance matrix (data): is given as $F \in \mathbb{R}^{m \times m}$, where $0 \leq F_{\alpha\beta} \leq 1$ for $\alpha, \beta \in \{1, \dots, m\}$ represents importance/frequency of coordination problem between groups α and β . We assume F is a symmetric matrix with diagonal entries equal to 1.

Individual coordination importance matrix: $\hat{F} \in \mathbb{R}^{n \times n}$, is obtained from F and the partition P , i.e., $\hat{F} = f(F, P)$. We construct \hat{F} as follows:

$$\hat{F}_{ij} = \begin{cases} F_{\alpha\beta}, & i \in P_\alpha, j \in P_\beta, i \neq j \\ 0, & i = j. \end{cases}$$

For the setting where groups are all of equal size s , one can write

$$\hat{F} = F \otimes \mathbb{1}_s \mathbb{1}_s^T - I_n$$

At edge set \mathcal{E} , the payoff function for individual $i \in \mathcal{V}$ is

$$U_i(\mathcal{E}) = \sum_{k=1}^n \hat{F}_{ik} \delta^{d_{ik}(\mathcal{E})} - \sum_{k \in N_i(\mathcal{E})} c, \quad (3.1)$$

where $d_{ik}(\mathcal{E})$ is the number of steps from individual i to k , $\delta < 1$ is the one-hop benefit, and c is the cost of each link. The value of network \mathcal{E} is defined as the sum of all

individuals' payoffs, i.e., $v(\mathcal{E}) = \sum_{i=1}^n U_i(\mathcal{E})$, and it indicates the social welfare. For a given society \mathcal{V} and value function v , \mathcal{E}^* is an *efficient structure* if its social welfare(value) is maximized over all possible edge sets on \mathcal{V} , i.e., $\mathcal{E}^* = \arg \max_{\mathcal{E}} v(\mathcal{E})$. Given the pair (i, j) in network \mathcal{E} , we say that individual i *benefits from edge* $\{(i, j)\}$ if $U_i(\mathcal{E} \cup \{(i, j)\}) > U_i(\mathcal{E} \setminus \{(i, j)\})$.

Formation Dynamics: Time periods are represented with countable infinite set $\mathbb{N} = \{1, 2, \dots, t, \dots\}$. In each period, a pair (i, j) is uniformly randomly selected and is added to, or removed from, the network \mathcal{E} according to the following rules:

- if $\{(i, j)\} \notin \mathcal{E}$, then it is added when its addition is marginally beneficial to the pair of individuals (i.e., either both individuals benefit or one individual is indifferent and the other benefits); the edge (i, j) is not added when its addition causes a drop in the payoff of either or both individuals or both individuals are indifferent towards it; and
- if $\{(i, j)\} \in \mathcal{E}$, then (i, j) is removed when its removal benefits at least one of the two individuals; no action is taken when both sides are either indifferent or benefit from the existence of the edge.

Definition 3.2.1 (*Pairwise Stability*) A network \mathcal{E} is pairwise stable if,

for all $\{(i, j)\} \in \mathcal{E}$,

$$U_i(\mathcal{E}) \geq U_i(\mathcal{E} \setminus \{(i, j)\}) \text{ and } U_j(\mathcal{E}) \geq U_j(\mathcal{E} \setminus \{(i, j)\});$$

and for all $\{(i, j)\} \notin \mathcal{E}$,

$$\text{if } U_i(\mathcal{E}) < U_i(\mathcal{E} \cup \{(i, j)\}), \text{ then } U_j(\mathcal{E}) > U_j(\mathcal{E} \cup \{(i, j)\}).$$

Remark 3.2.2 According to Definition 3.2.1, if the edge (i, j) belongs to the pairwise stable network, removing it results in a loss for i or j ; and if the edge (i, j) does not

belong to the pairwise stable network, adding it makes no difference or causes loss for i or j .

Definition 3.2.3 \mathcal{E}' defeats \mathcal{E} if either $\mathcal{E}' = \mathcal{E} \setminus \{(i, j)\}$ and $U_i(\mathcal{E}') > U_i(\mathcal{E})$, or $\mathcal{E}' = \mathcal{E} \cup \{(i, j)\}$ and $U_i(\mathcal{E}') \geq U_i(\mathcal{E})$ and $U_j(\mathcal{E}') \geq U_j(\mathcal{E})$ with at least one inequality holding strictly.

Lemma 3.2.4 A network is pairwise stable if and only if it does not change under Formation Dynamics.

Proof: To prove necessity, we refer to Remark 3.2.2. According to the definition, if a network is pairwise stable, no network can defeat it, i.e., no links can be added to or severed from it. To show sufficiency, note that a network not being changed by Formation Dynamics, implies that:

- (i) adding a link makes no difference or causes loss for at least one individual;
- (ii) removing a link results in loss for at least one individual.

Therefore, the network is pairwise stable. ■

According to Lemma 3.2.4, if there exists some time t^* such that from t^* on, no additional links are added to or severed from a network by Formation Dynamics, then the network has reached the pairwise stable structure.

We define the following terms that we will frequently use throughout this chapter indicating the density of the interconnections among the groups.

Definition 3.2.5 We say that a society of individuals consists of the disjoint union of groups if there exists no interconnection among any pairs of groups. For a connected pair, we say it is

- (i) *minimally connected* if there exists exactly one interconnection among the pair;
- (ii) *redundantly connected* if there exist at least two interconnections among the pair;
- (iii) *maximally connected* if all of the possible interconnections among the pair of groups exist.

Fig. 3.3 represents a schematic illustration of the terms discussed above.

Remark 3.2.6 *A minimally connected pair corresponds to the bridge connection (Fig. 3.1c), redundantly connected to the ridge connection (Fig. 3.1b), and maximally connected to a full co-membership connection (Fig. 3.1a.)*

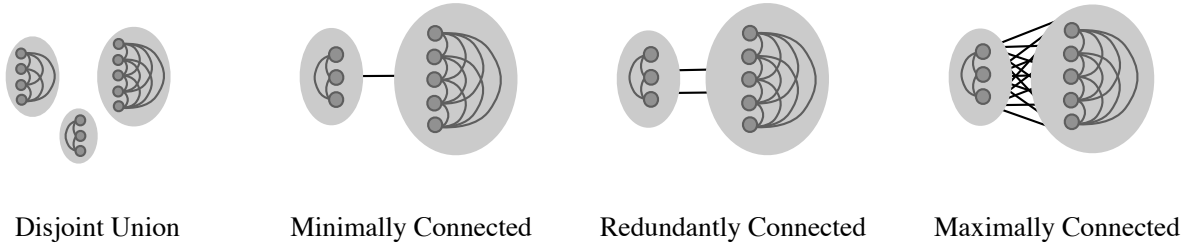


Figure 3.3: Schematic illustration of interconnection densities

We next define the Price of Anarchy (PoA) as a measure of how the efficiency of a system degrades due to the selfish behavior of its individuals. It is calculated as follows:

$$PoA = \frac{\max_{\mathcal{E}} v(\mathcal{E})}{\min_{p.w.stable \mathcal{E}} v(\mathcal{E})}.$$

Throughout this chapter we use the following threshold functions $y_1(s, \delta)$, $y_2(s, \delta)$,

and $y_3(\delta)$ defined by

$$y_1(s, \delta) = \delta + (s - 1)\delta^2,$$

$$y_2(s, \delta) = \delta - \delta^2 + (s - 1)\delta^2 - (s - 1)\delta^3 = (1 - \delta)y_1(s),$$

$$y_3(\delta) = \delta - \delta^2.$$

In what follows we will often suppress the argument δ in the interest of simplicity.

Under the conditions $0 < \delta < 1$ and $s \geq 3$, we claim that,

$$0 < y_3 < y_2(s) < y_1(s).$$

The proof is as follows: it is easy to see that $y_2(s) < y_1(s)$. To verify $y_3 < y_2(s)$, we rewrite $y_2(s)$ as $(\delta - \delta^2)(1 + \delta(s - 1)) = y_3(1 + \delta(s - 1)) > y_3$. Plots of these three threshold functions for $0 < \delta < 1$, where $s = 3$ are depicted in Fig. 3.4. In what follows we

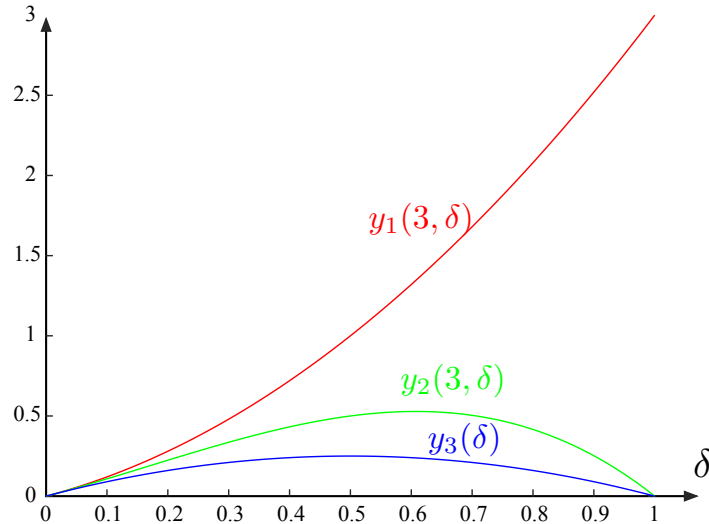


Figure 3.4: Plots of y_1 , y_2 , and y_3 for $s = 3$.

provide bounds based on these functions to study pairwise stable and efficient structures, and investigate the convergence of the Formation Dynamics when possible.

3.3 Results on Formation of Disjoint Cliques

We first study the inner structure of each group in a pairwise stable network. Throughout this chapter, we assume that the dynamics does not start with an initial state containing any interconnection. We define the invariant set of all subgraphs of disjoint cliques as $S = \left\{ \bigcup_{\gamma=1}^m \mathcal{E}_\gamma \mid \mathcal{E}_\gamma \subset \mathcal{E}_{K_{s_\gamma}} \right\}$ where \mathcal{E}_γ indicates the inner-network of group P_γ .

Theorem 3.3.1 (Formation of Cliques: Pairwise Stability, Efficiency, Convergence)

Consider n individuals partitioned into groups P_1, \dots, P_m . Then, each one of these m groups is a clique in the pairwise stable and in the efficient structure if and only if $c < y_3$. Moreover, starting from any state in the invariant set S , each group P_α will form a s_α -size clique along Formation Dynamics (introduced in Section 3.2).

Proof: We first provide the proof of sufficiency for pairwise stability: for any individual $i \in P_\alpha$, a direct link with individual j , ($j \neq i$) from the same group provides a profit of $\delta - c$. Without a direct link, this profit is equal to $\delta^{d_{ij}}$ where $d_{ij} > 1$ is the distance between i and j in $\mathcal{E} \setminus \{(i, j)\}$. Since $\delta - \delta^2 > c$, we have $\delta - c > \delta^2 > \dots > \delta^n$; meaning that all agents prefer direct links to any indirect link. Thus, if agents i and j in group P_α are not directly connected, they will form a link and each will gain at least $(\delta - c) - \delta^{d_{ij}} > 0$, i.e.,

$$\text{for all } \{(i, j)\} \notin \mathcal{E}, \quad i, j \in P_\alpha, \quad i \neq j$$

$$U_i(\mathcal{E}) < U_i(\mathcal{E} \cup \{(i, j)\}), \text{ and } U_j(\mathcal{E}) < U_j(\mathcal{E} \cup \{(i, j)\}).$$

Moreover, no node has an incentive to break any link since its payoff strictly decreases if it do so, i.e.,

$$\begin{aligned} & \text{for all } \{(i, j)\} \in \mathcal{E}, \quad i, j \in P_\alpha, \quad i \neq j, \\ & U_i(\mathcal{E}) > U_i(\mathcal{E} \setminus \{(i, j)\}), \text{ and } U_j(\mathcal{E}) > U_j(\mathcal{E} \setminus \{(i, j)\}). \end{aligned}$$

Thus, each group forms a clique and no intra-connection is removed after being formed, and according to Lemma 3.2.4, these m groups are cliques in the pairwise stable structure. To prove necessity, assume we have a pairwise stable clique. For P_α to remain a clique, all pairs of nodes belonging to the same group should prefer to keep one-hop links rather than having links with larger lengths, and thus $\delta - c > \delta^2 > \delta^3 > \dots$. This proves the claim that each group P_α is a clique if and only if $c < \delta - \delta^2$. Convergence of dynamics to cliques can be obtained directly from the same argument.

We now continue by first proving that if $c < \delta - \delta^2$, in the efficient structure each group is a clique. From the analysis above, when $c < \delta - \delta^2$, we have:

$$\begin{aligned} & v(\mathcal{E} \cup \{(i, j)\}) - v(\mathcal{E} \setminus \{(i, j)\}) \\ & \geq U_i(\mathcal{E} \cup \{(i, j)\}) + U_j(\mathcal{E} \cup \{(i, j)\}) \\ & \quad - U_i(\mathcal{E} \setminus \{(i, j)\}) - U_j(\mathcal{E} \setminus \{(i, j)\}) \\ & \geq 2(\delta - c - \delta^2) > 0 \end{aligned}$$

which holds for each pair (i, j) belonging to the same group, meaning that each group is a clique in the efficient structure. We next prove necessity for efficiency: assume \mathcal{E} is the efficient structure and each group is a clique, i.e., $\{(i, j)\} \in \mathcal{E}$ for any two individuals

i, j , ($i \neq j$) from the same group. Then, we have:

$$\begin{aligned}
 v(\mathcal{E}) - v(\mathcal{E} \setminus \{(i, j)\}) \\
 &= U_i(\mathcal{E}) + U_j(\mathcal{E}) - U_i(\mathcal{E} \setminus \{(i, j)\}) - U_j(\mathcal{E} \setminus \{(i, j)\}) \\
 &= 2(\delta - c - \delta^2) > 0,
 \end{aligned}$$

which results in $c < y_3$. ■

Note: Theorem 3.3.1 implies that formation of cliques requires $c < 1/4$.

Theorem 3.3.2 (Pairwise Stable Structures and Convergence: Disjoint Union of Cliques)

Consider n individuals partitioned into groups P_1, \dots, P_m of sizes s_1, \dots, s_m respectively. Assume that $c < y_3$. Then, the unique pairwise stable structures consists of disjoint union of cliques equal to the groups P_1, \dots, P_m if and only if $F_{\alpha\beta} \leq \max_{s \in \{s_\alpha, s_\beta\}} \frac{c}{y_1(s)}$ for all $\alpha, \beta \in \{1, \dots, m\}$, $\alpha \neq \beta$. Moreover, starting from any state in the invariant set S , Formation Dynamics (introduced in Section 3.2) converges to this pairwise stable structure.

Proof: We first prove sufficiency. Since no interconnection exists in the invariant set S , for any network $\mathcal{E} \in S$, suppose two individuals $i \in P_\alpha$ and $j \in P_\beta$ are picked to decide whether to add the corresponding interconnection or not. We know that $U_i(\mathcal{E} \cup \{(i, j)\}) \leq F_{\alpha\beta}y_1(s_\beta) - c$ and $U_j(\mathcal{E} \cup \{(i, j)\}) \leq F_{\alpha\beta}y_1(s_\alpha) - c$, where equalities hold when both groups form cliques. Since $F_{\alpha\beta} \leq \max_{s \in \{s_\alpha, s_\beta\}} \frac{c}{y_1(s)}$, at least one of $U_i(\mathcal{E} \cup \{(i, j)\}) \leq 0$ and $U_j(\mathcal{E} \cup \{(i, j)\}) \leq 0$ holds. Therefore, the interconnection $\{(i, j)\}$ does not belong to pairwise stable structure and it does not form. From Theorem 3.3.1, we know that unique stable state consists of the disjoint union of cliques equal to the groups $\{1, \dots, m\}$. Suppose that all groups form cliques at a time t^* . From then on, no link will be added or removed. According to Lemma 3.2.4, the pairwise stable structure consists of the disjoint union of cliques equal to the groups $\{1, \dots, m\}$, and the network converges to this unique stable state.

To prove necessity, take any two individuals $i \in P_\alpha$ and $j \in P_\beta$. Since $\{(i, j)\}$ does not belong to pairwise stable structure, we have at least one of $U_i(\mathcal{E} \cup \{(i, j)\}) \leq 0$ and $U_j(\mathcal{E} \cup \{(i, j)\}) \leq 0$ holds, and therefore, $F_{\alpha\beta} \leq \max_{s \in \{s_\alpha, s_\beta\}} \frac{c}{y_1(s)}$. ■

3.4 Two Group Connectivity Structure

In this section we study pairwise stable and efficient structures when individuals are partitioned into two groups.

3.4.1 Pairwise Stability

In what follows we give the sufficient and necessary condition for pairwise stable structures.

Theorem 3.4.1 (Pairwise Stability and Convergence with Two Groups) *Consider n individuals partitioned into groups P_1, P_2 of sizes s_1 and s_2 respectively. Then, under the assumption $c < y_3$, the network has*

- (i) *a unique pairwise stable structure consisting of minimally connected cliques if and only if*

$$\max_{s \in \{s_1, s_2\}} \frac{c}{y_1(s)} \leq F_{12} < \max_{s \in \{s_1, s_2\}} \frac{c}{y_2(s)};$$

- (ii) *a unique pairwise stable structure consisting of exact k ($2 \leq k \leq \min\{s_1, s_2\}$) interconnections if and only if*

$$\begin{aligned} \max_{s \in \{s_1, s_2\}} \frac{c}{y_2(s) - (k-2)\delta y_3} \\ < F_{12} < \max_{s \in \{s_1, s_2\}} \frac{c}{y_2(s) - (k-1)\delta y_3}. \end{aligned} \quad (3.2)$$

(iii) a unique pairwise stable structure consisting of maximally connected cliques if and only if

$$\frac{c}{y_3} < F_{12} \leq 1.$$

Moreover, starting from any state in the invariant set S , the Formation Dynamics (introduced in Section 3.2) converges to the corresponding pairwise stable structure.

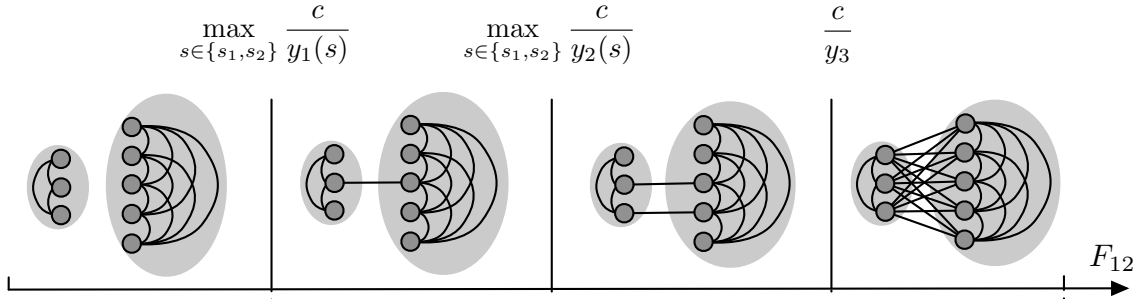


Figure 3.5: An illustration of the four ranges of parameter space in Theorems 3.3.2 and 3.4.1.

Proof:

From Theorem 3.3.2, we know that at least one interconnection will be formed under Formation Dynamics if and only if $F_{12} \geq \max_{s \in \{s_1, s_2\}} \frac{c}{y_1(s)}$. Without loss of generality, suppose that \mathcal{E} contain two cliques and at least one interconnection between them. Assume that agents i and j , respectively from P_1 and P_2 , are connected in \mathcal{E} .

Take agents \hat{i} from P_1 and \hat{j} from P_2 . For $\hat{i} \neq i, \hat{j} = j$, we have $U_{\hat{i}}(\mathcal{E} \cup \{(\hat{i}, j)\}) = (s_1 - 1)\delta + F_{12}\delta + (s_2 - 1)F_{12}\delta^2 - s_1c$ and $U_{\hat{i}}(\mathcal{E} \setminus \{(\hat{i}, j)\}) = (s_1 - 1)(\delta - c) + F_{12}\delta^2 + (s_2 - 1)F_{12}\delta^3$, implying $U_{\hat{i}}(\mathcal{E} \cup \{(\hat{i}, j)\}) > U_{\hat{i}}(\mathcal{E} \setminus \{(\hat{i}, j)\}) \iff F_{12} > \frac{c}{y_2(s_2)}$. From $U_j(\mathcal{E} \cup \{(\hat{i}, j)\}) = (s_2 - 1)\delta + 2F_{12}\delta + (s_2 - 2)F_{12}\delta^2 + (s_2 + 1)c$ and $U_j(\mathcal{E} \setminus \{(\hat{i}, j)\}) = (s_2 - 1)\delta + F_{12}\delta + (s_2 - 1)F_{12}\delta^2 + s_2c$, we obtain: $U_j(\mathcal{E} \cup \{(\hat{i}, j)\}) > U_j(\mathcal{E} \setminus \{(\hat{i}, j)\}) \iff F_{12} > \frac{c}{y_3}$. Then, from $y_2(s) > y_3 > 0$, we conclude that an additional interconnection $\{(\hat{i}, j)\}$ is added

and maintained if and only if $F_{12} > \frac{c}{y_3}$. Similarly, an additional interconnection $\{(i, \hat{j})\}$ is added and maintained if and only if $F_{12} > \frac{c}{y_3}$. For $\hat{i} \neq i, \hat{j} \neq j$, using a similar argument, we obtain that $U_{\hat{i}}(\mathcal{E} \cup \{(\hat{i}, \hat{j})\}) > U_{\hat{i}}(\mathcal{E} \setminus \{(\hat{i}, \hat{j})\}) \iff F_{12} > \frac{c}{y_2(s_2)}$ and $U_{\hat{j}}(\mathcal{E} \cup \{(\hat{i}, \hat{j})\}) > U_{\hat{j}}(\mathcal{E} \setminus \{(\hat{i}, \hat{j})\}) \iff F_{12} > \frac{c}{y_2(s_1)}$; which means that an additional interconnection $\{(\hat{i}, \hat{j})\}$ is added and maintained if and only if $F_{12} > \max_{s \in \{s_1, s_2\}} \frac{c}{y_2(s)}$ (strictly holds when $s_1 = s_2$). Thus, we conclude that at least two interconnections are added and maintained if and only if $F_{12} > \min \left\{ \frac{c}{y_3}, \max_{s \in \{s_1, s_2\}} \frac{c}{y_2(s)} \right\} = \max_{s \in \{s_1, s_2\}} \frac{c}{y_2(s)}$ (strictly holds when $s_1 = s_2$.) Therefore, the network contains precisely one interconnection if and only if $\max_{s \in \{s_1, s_2\}} \frac{c}{y_1(s)} < F_{12} < \max_{s \in \{s_1, s_2\}} \frac{c}{y_2(s)}$. Moreover, from the moment when two group form cliques and this unique interconnection builds, the network will not change. According to Lemma 3.2.4, this concludes the proof of statement (i).

To prove (iii), assume that $F_{12} > \max_{s \in \{s_1, s_2\}} \frac{c}{y_2(s)}$. We have shown above that \mathcal{E} contains at least two interconnections between two cliques. As a result, for any agent \hat{i} from P_1 and \hat{j} from P_2 , the distance between \hat{i} and \hat{j} in $\mathcal{E} \setminus \{(\hat{i}, \hat{j})\}$ is equal to either 2 or 3. If it is equal to 2, then $U_{\hat{i}}(\mathcal{E} \cup \{(\hat{i}, \hat{j})\}) - U_{\hat{i}}(\mathcal{E} \setminus \{(\hat{i}, \hat{j})\}) = U_{\hat{j}}(\mathcal{E} \cup \{(\hat{i}, \hat{j})\}) - U_{\hat{j}}(\mathcal{E} \setminus \{(\hat{i}, \hat{j})\}) = F_{12}(\delta - \delta^2) - c$; and if it is equal to 3, then $U_{\hat{i}}(\mathcal{E} \cup \{(\hat{i}, \hat{j})\}) - U_{\hat{i}}(\mathcal{E} \setminus \{(\hat{i}, \hat{j})\}) = U_{\hat{j}}(\mathcal{E} \cup \{(\hat{i}, \hat{j})\}) - U_{\hat{j}}(\mathcal{E} \setminus \{(\hat{i}, \hat{j})\}) = F_{12}(\delta - \delta^3) - c$. Interconnection $\{(\hat{i}, \hat{j})\}$ is added and maintained if and only if $U_{\hat{i}}(\mathcal{E} \cup \{(\hat{i}, \hat{j})\}) - U_{\hat{i}}(\mathcal{E} \setminus \{(\hat{i}, \hat{j})\}) > 0$ and $U_{\hat{j}}(\mathcal{E} \cup \{(\hat{i}, \hat{j})\}) - U_{\hat{j}}(\mathcal{E} \setminus \{(\hat{i}, \hat{j})\}) > 0$. Thus, we conclude that $\{(\hat{i}, \hat{j})\}$ is added and maintained if and only if $F_{12} > \max \left\{ \frac{c}{\delta - \delta^2}, \frac{c}{\delta - \delta^3} \right\}$. Since $\max \left\{ \frac{c}{\delta - \delta^2}, \frac{c}{\delta - \delta^3} \right\} = \frac{c}{\delta - \delta^2}$ for $0 < \delta < 1$, $\{(\hat{i}, \hat{j})\}$ is added and maintained if and only if $F_{12} > \frac{c}{\delta - \delta^2} = \frac{c}{y_3}$. Therefore, the network will not be changed when all agents link with each other. By Lemma 3.2.4, this concludes the proof of (iii).

From statements (i) and (iii), we know that the pairwise stable structure contains at least 2 but not fully numbers of interconnections if $\max_{s \in \{s_1, s_2\}} \frac{c}{y_2(s)} < F_{12} < \frac{c}{y_3}$. Suppose that $(i_1, j_1), \dots, (i_{k-1}, j_{k-1})$ are $k - 1$ interconnections between P_1 and P_2 . Take agents

\hat{i} from P_1 and \hat{j} from P_2 . Similar to the analysis in the proof of statement (i), we have the following two cases:

(i) For $\hat{i} \notin \{i_1, \dots, i_{k-1}\}, \hat{j} \notin \{j_1, \dots, j_{k-1}\}$, we have

$$\begin{aligned} & U_{\hat{i}}(\mathcal{E} \cup \{(\hat{i}, j)\}) - U_{\hat{i}}(\mathcal{E} \setminus \{(\hat{i}, j)\}) \\ &= F_{12}(y_2(s_2) - (k-2)\delta y_3), \text{ and} \\ & U_{\hat{j}}(\mathcal{E} \cup \{(\hat{i}, j)\}) - U_{\hat{j}}(\mathcal{E} \setminus \{(\hat{i}, j)\}) \\ &= F_{12}(y_2(s_1) - (k-2)\delta y_3), \end{aligned}$$

implying

$$\begin{aligned} & U_{\hat{i}}(\mathcal{E} \cup \{(\hat{i}, j)\}) > U_{\hat{i}}(\mathcal{E} \setminus \{(\hat{i}, j)\}), \text{ and} \\ & U_{\hat{j}}(\mathcal{E} \cup \{(\hat{i}, j)\}) > U_{\hat{j}}(\mathcal{E} \setminus \{(\hat{i}, j)\}) \\ \iff & F_{12} > \max_{s \in \{s_1, s_2\}} \frac{c}{y_2(s) - (k-2)\delta y_3}. \end{aligned}$$

(ii) For $\hat{i} \in \{i_1, \dots, i_{k-1}\}, \hat{j} \notin \{j_1, \dots, j_{k-1}\}$ or $\hat{i} \notin \{i_1, \dots, i_{k-1}\}, \hat{j} \in \{j_1, \dots, j_{k-1}\}$, we have

$$\begin{aligned} & U_{\hat{i}}(\mathcal{E} \cup \{(\hat{i}, j)\}) > U_{\hat{i}}(\mathcal{E} \setminus \{(\hat{i}, j)\}) \text{ and} \\ & U_{\hat{j}}(\mathcal{E} \cup \{(\hat{i}, j)\}) > U_{\hat{j}}(\mathcal{E} \setminus \{(\hat{i}, j)\}) \\ \iff & F_{12} > \frac{c}{y_3}. \end{aligned}$$

Therefore, we conclude then k -th interconnection is added and maintained if and only if $F_{12} > \max_{s \in \{s_1, s_2\}} \frac{c}{y_2(s) - (k-2)\delta y_3}$. Likewise, the $(k+1)$ -th interconnection is added and maintained if and only if $F_{12} > \max_{s \in \{s_1, s_2\}} \frac{c}{y_2(s) - (k-1)\delta y_3}$. It follows that the unique pair-wise stable structure has exact k ($2 \leq k \leq \min\{s_1, s_2\}$) interconnections if and only if $\max_{s \in \{s_1, s_2\}} \frac{c}{y_2(s) - (k-2)\delta y_3} < F_{12} < \max_{s \in \{s_1, s_2\}} \frac{c}{y_2(s) - (k-1)\delta y_3}$. This concludes the proof of (ii).

Finally, we complete the proof of Theorem 3.4.1 by proving the convergence statement.

Since $c < y_3$, from Theorem 3.3.1 we know that the network structure, regardless of the density of intra-group connections, consists of cliques of sizes s_1 and s_2 . From above analysis, starting from invariable set S , intra-connections will increase one by one until one more intra-connection can not bring increasing of benefit for two players. Then, it follows from Lemma 3.2.4 that the network can not be changed from then on, i.e., the network will converge to the corresponding pairwise stable structure under the formation dynamics in Section 3.2. ■

Theorem 3.4.1 implies that if F_{12} equals the boundaries, i.e., $\max_{s \in \{s_1, s_2\}} \frac{c}{y_2(s)}$, $\max_{s \in \{s_1, s_2\}} \frac{c}{y_2(s) - \delta y_3}$, $\max_{s \in \{s_1, s_2\}} \frac{c}{y_3}$, ..., $\max_{s \in \{s_1, s_2\}} \frac{c}{y_3}$, the pairwise stable structure is not unique. To show this, we provide the following example for a society consisting of 8 individuals.

Example 3.4.2 Suppose that individuals are partitioned into groups $P_1 = \{1, 2, 3\}$ and $P_2 = \{4, 5, 6, 7, 8\}$. Let $c = 0.2$, $\delta = 0.5$ and $F_{12} = \max_{s \in \{s_1, s_2\}} \frac{c}{y_2(s)} = 0.4$. Assume at time 0, each of the two groups have a line structure, illustrated in Fig 3.6. Now consider the following two processes:

Process (A) At first, individuals 2 and 6 are chosen to play the game and interconnection (2, 6) is formed. Then, individuals 3 and 7 are chosen to play the game, and interconnection (3, 7) is also formed. After that, all possible intra-connections are considered and formed. Finally, the network contains two interconnections and reaches pairwise stability.

Process (B) At first, all possible intra-connections are considered and formed. Then individuals 2 and 6 are chosen to play the game and interconnection (2, 6) is formed. As a result, the network contains only 1 interconnection and reaches pairwise stability.

Fig. 3.5 illustrates the scenarios specified in Theorems 3.3.2 and 3.4.1 for F_{12} .

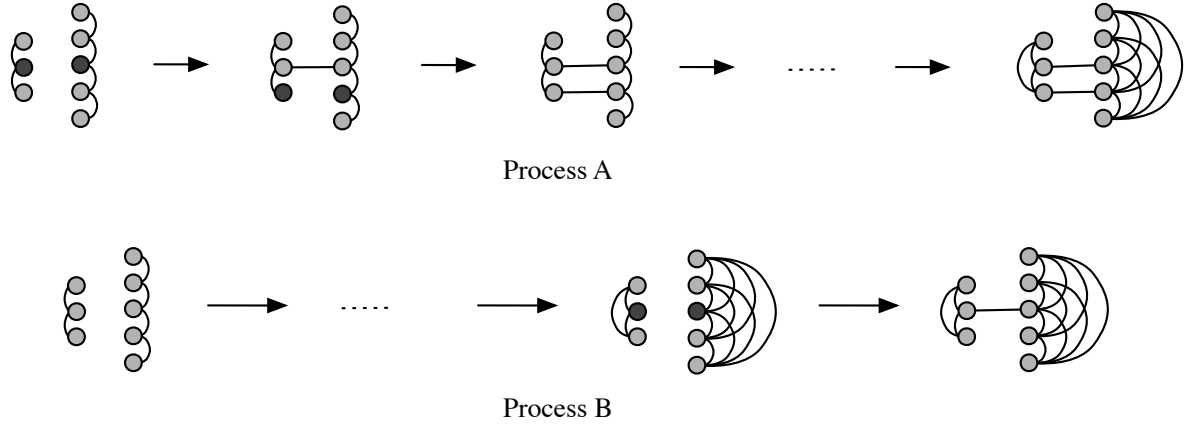


Figure 3.6: An illustration of two processes in Example 3.4.2. At each step, the darker dots are chosen to play the game.

Remark 3.4.3 *As the difference between group sizes $|s_2 - s_1|$ increases, the bound for formation of bridges increases, and thus communication between groups becomes harder. To see why this is true, for a society of $n = s_1 + s_2$ individuals, without loss of generality, we assume that $s_1 \leq s_2$. We know $\max_{s \in \{s_1, s_2\}} \frac{c}{y_1(s)} = \frac{c}{\min_{s \in \{s_1, s_2\}} y_1(s)} = \frac{c}{y_1(\min\{s_1, s_2\})}$, and since $\max_{s \in \{s_1, s_2\}} \frac{c}{y_1(s)}$ is a monotonically decreasing function of s , as s_1 increases, $|s_2 - s_1|$, and therefore, $\max_{s \in \{s_1, s_2\}} \frac{c}{y_1(s)}$ decreases, and communication is facilitated. As illustrated in Fig. 3.7, for a society of fixed size, as the sizes of the two groups becomes closer to each other, the number of interconnections increases.*

3.4.2 Efficiency

We now study the efficiency of two group structure.

Theorem 3.4.4 (Efficiency with Two groups) *Consider n individuals partitioned into groups P_1, P_2 of sizes s_1 and s_2 respectively. Under the assumption that $c < y_3$, the efficient structure consists of:*

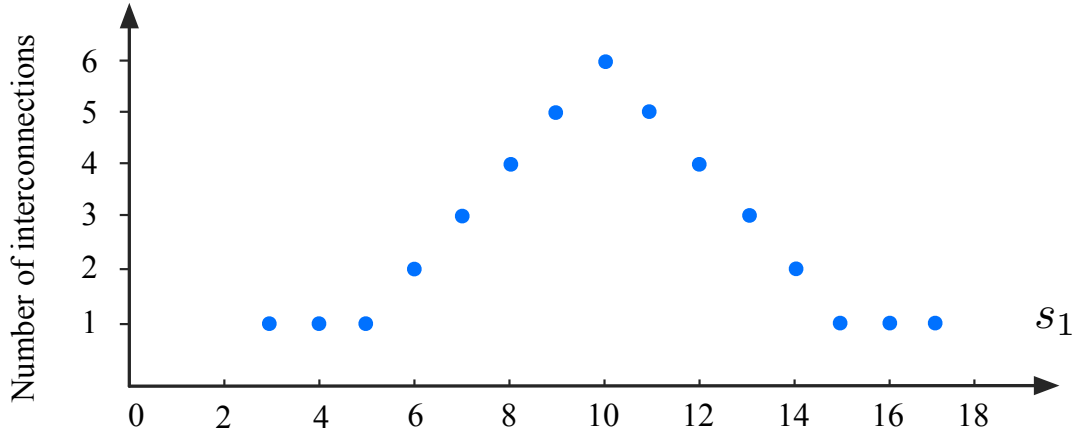


Figure 3.7: Plots of no. of interconnections with fixed $F_{12} = 0.25$ and $n = 20$ as a function of groups size s_1 , $\delta = 0.5$, $c = 0.2$. Note that $s_2 = n - s_1$, and thus the plot is symmetric about the line $s_1 = \frac{n}{2}$ and maximized at $s_1 = \frac{n}{2}$.

(i) *disjoint union of cliques if and only if*

$$0 \leq F_{12} \leq \frac{c\delta}{y_1(s_1)y_1(s_2)};$$

(ii) *minimally connected cliques if and only if*

$$\frac{c\delta}{y_1(s_1)y_1(s_2)} \leq F_{12} \leq \frac{2c}{y_2(s_2) + y_2(s_1) + (s_1 + s_2 - 4)\delta y_3};$$

(iii) *redundantly connected cliques if and only if*

$$\frac{2c}{y_2(s_2) + y_2(s_1) + (s_1 + s_2 - 4)\delta y_3} \leq F_{12} \leq \frac{c}{y_3};$$

(iv) *maximally connected cliques if and only if*

$$\frac{c}{y_3} \leq F_{12} \leq 1.$$

Proof: From Theorem 3.3.1, we know that addition of an intra-connection results in increasing the payoff of both individuals involved in that link, as well as the social welfare, and removal of any intra-connection causes loss for both individuals and decreases social welfare. As a result, the efficient structure consists of two cliques. Suppose $i \in P_1$ and $j \in P_2$. Let $\mathcal{E}_0 = \mathcal{E}_{K_{s_1}} \cup \mathcal{E}_{K_{s_2}}$ be the union of two cliques of sizes s_1 and s_2 . We have

$$\begin{aligned}
 & U_k(\mathcal{E}_0 \cup \{(i, j)\}) - U_k(\mathcal{E}_0) \\
 &= \begin{cases} F_{12}(\delta + (s_2 - 1)\delta^2) - c, & k = i; \\ F_{12}(\delta + (s_1 - 1)\delta^2) - c, & k = j; \\ F_{12}(\delta^2 + (s_2 - 1)\delta^3), & k \in P_1, k \neq i; \\ F_{12}(\delta^2 + (s_1 - 1)\delta^3), & k \in P_2, k \neq j. \end{cases} \quad (3.3)
 \end{aligned}$$

It follows that

$$\begin{aligned}
 v((\mathcal{E}_0 \cup \{(i, j)\})) - v(\mathcal{E}_0) &= 2F_{12}[\delta + (s_1 - 1)\delta^2 + (s_2 - 1)\delta^2 \\
 &\quad + (s_1 - 1)(s_2 - 1)\delta^3] - 2c.
 \end{aligned}$$

\mathcal{E}_0 is the efficient structure if and only if $v((\mathcal{E}_0 \cup \{(i, j)\})) - v(\mathcal{E}_0) \leq 0$, which is equivalent to:

$$\begin{aligned}
 F_{12} &\leq \frac{c}{\delta + (s_1 - 1)\delta^2 + (s_2 - 1)\delta^2 + (s_1 - 1)(s_2 - 1)\delta^3} \\
 &= \frac{c\delta}{y_1(s_1)y_1(s_2)}.
 \end{aligned}$$

This concludes the proof of (i).

Now let $\mathcal{E}_1 = \mathcal{E}_0 \cup \{(i, j)\}$. As elaborated above, $v(\mathcal{E}_1) - v(\mathcal{E}_0) \geq 0$ if and only if

$$\begin{aligned} F_{12} &\geq \frac{c}{\delta + (s_1 - 1)\delta^2 + (s_2 - 1)\delta^2 + (s_1 - 1)(s_2 - 1)\delta^3} \\ &= \frac{c\delta}{y_1(s_1)y_1(s_2)}. \end{aligned}$$

Suppose $\hat{i} \in P_1$ and $\hat{j} \in P_2$. For the case of $\hat{i} \neq i$ and $\hat{j} \neq j$, we have

$$U_k(\mathcal{E}_1 \cup \{(\hat{i}, \hat{j})\}) - U_k(\mathcal{E}_1) = \begin{cases} F_{12}y_2(s_2) - c, & k = \hat{i} \\ F_{12}y_2(s_1) - c, & k = \hat{j} \\ 0, & k = i, j \\ F_{12}(\delta^2 - \delta^3), & \text{otherwise.} \end{cases}$$

For the case of $\hat{i} = i$ and $\hat{j} \neq j$, we have

$$\begin{aligned} &U_k(\mathcal{E}_1 \cup \{(i, \hat{j})\}) - U_k(\mathcal{E}_1) \\ &= \begin{cases} F_{12}(\delta - \delta^2) - c, & k = i, \\ F_{12}y_2(s_1) - c, & k = \hat{j}, \\ 0, & k \in P_2 \text{ and } k \neq \hat{j}, \\ F_{12}(\delta^2 - \delta^3), & k \in P_1 \text{ and } k \neq i. \end{cases} \end{aligned}$$

For the case of $\hat{i} \neq i$ and $\hat{j} = j$, we have

$$\begin{aligned}
 & U_k(\mathcal{E}_1 \cup \{(\hat{i}, j)\}) - U_k(\mathcal{E}_1) \\
 &= \begin{cases} F_{12}(\delta - \delta^2) - c, & k = j, \\ F_{12}y_2(s_2) - c, & k = \hat{i}, \\ 0, & k \in P_1 \text{ and } k \neq \hat{i}, \\ F_{12}(\delta^2 - \delta^3), & k \in P_2 \text{ and } k \neq j. \end{cases}
 \end{aligned}$$

It follows that

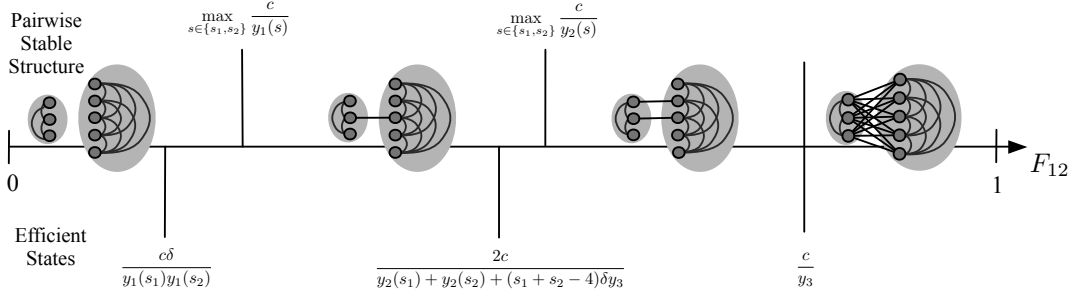
$$\begin{aligned}
 & v(\mathcal{E}_1 \cup \{(\hat{i}, j)\}) - v(\mathcal{E}_1) \\
 &= \begin{cases} F_{12}[y_2(s_2) + y_2(s_1) + (s_1 + s_2 - 4)(\delta^2 - \delta^3)] - 2c, \\ \quad \hat{j} \neq j, \hat{i} \neq i, \\ 2F_{12}y_2(s_1) - 2c, \hat{i} = i, \hat{j} \neq j, \\ 2F_{12}y_2(s_2) - 2c, \hat{i} \neq i, \hat{j} = j. \end{cases}
 \end{aligned}$$

Since $y_2(s)$ is a monotonically increasing function of s and

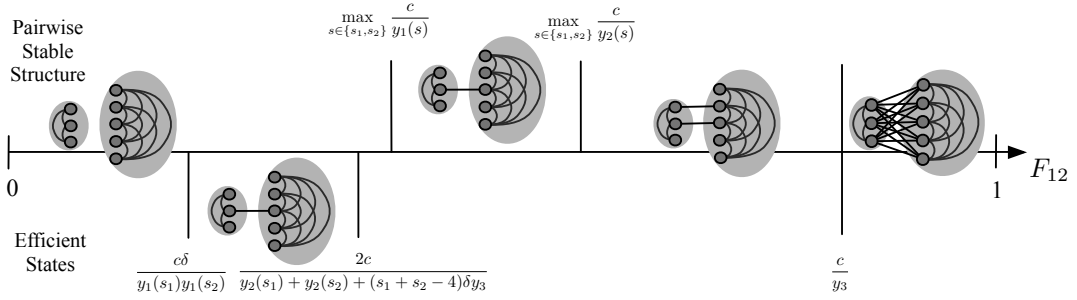
$$\begin{aligned}
 & \frac{2c}{y_2(s_2) + y_2(s_1) + (s_1 + s_2 - 4)(\delta^2 - \delta^3)} \\
 &= \frac{c}{y_2(s_1) + (s_2 - 2)(\delta^2 - \delta^3)} \\
 &= \frac{c}{y_2(s_2) + (s_1 - 2)(\delta^2 - \delta^3)},
 \end{aligned}$$

we have

$$\begin{aligned}
 & \frac{2c}{y_2(s_2) + y_2(s_1) + (s_1 + s_2 - 4)(\delta^2 - \delta^3)} \\
 & < \min_{s \in \{s_1, s_2\}} \frac{c}{y_2(s)}.
 \end{aligned}$$



(a) Ranges of parameter space for high value benefit ($\delta \geq \max_{s \in \{s_1, s_2\}} \frac{s-3}{n-3}$)



(b) Ranges of parameter space for low value benefit ($\delta < \max_{s \in \{s_1, s_2\}} \frac{s-3}{n-3}$)

Figure 3.8: An illustration of the ranges of parameter space in Theorems 3.4.1 and 3.4.4. The intervals indicated above the horizontal line refer to bounds of pairwise stability and those below the horizontal line refer to bounds of efficiency.

We then conclude that $v(\mathcal{E}_2 \cup \{(\hat{i}, \hat{j})\}) - v(\mathcal{E}_2) \leq 0$ if and only if $F_{12} \leq \frac{2c}{y_2(s_2) + y_2(s_1) + (s_1 + s_2 - 4)\delta y_3}$.

Statement (ii) follows accordingly.

Assume $F_{12} \geq \max_{s \in \{s_1, s_2\}} \frac{c}{y_2(s)}$. From statement (ii), we know that the efficient structure has at least two interconnections. For any agent \hat{i} from P_1 and \hat{j} from P_2 , as elaborated in the proof of Theorem 3.4.1, one has

$$v(\mathcal{E} \cup \{(\hat{i}, \hat{j})\}) - v(\mathcal{E} \setminus \{(\hat{i}, \hat{j})\}) \geq 2[F_{12}(\delta - \delta^2) - c],$$

which concludes statements (iii) and (iv). ■

From the properties of $y_1(s)$, $y_2(s)$, and y_3 , we have:

(i) if $\delta \geq \max_{s \in \{s_1, s_2\}} \frac{s-3}{n-3}$, then

$$\begin{aligned} \frac{c\delta}{y_1(s_1)y_1(s_2)} &< \max_{s \in \{s_1, s_2\}} \frac{c}{y_1(s)} \\ &\leq \frac{2c}{y_2(s_2) + y_2(s_1) + (s_1 + s_2 - 4)\delta y_3} \\ &< \max_{s \in \{s_1, s_2\}} \frac{c}{y_2(s)}; \end{aligned}$$

(ii) if $\delta < \max_{s \in \{s_1, s_2\}} \frac{s-3}{n-3}$, then

$$\begin{aligned} \frac{c\delta}{y_1(s_1)y_1(s_2)} &< \frac{2c}{y_2(s_2) + y_2(s_1) + (s_1 + s_2 - 4)\delta y_3} \\ &< \max_{s \in \{s_1, s_2\}} \frac{c}{y_1(s)} \\ &< \max_{s \in \{s_1, s_2\}} \frac{c}{y_2(s)}. \end{aligned}$$

From Theorems 3.4.1 and 3.4.4, we can directly obtain the conditions for the equivalence between pairwise stability and efficiency.

Corollary 3.4.5 *Consider n individuals partitioned into groups, P_1 and P_2 of sizes s_1 and s_2 respectively. Under the assumption $c < y_3$, the efficient structure has equal or more interconnections than the pairwise stable structure. Moreover, the efficient structure is the pairwise stable structure if*

$$(i) \text{ for } \delta \geq \max_{s \in \{s_1, s_2\}} \frac{s-3}{n-3},$$

$$\begin{aligned} F_{12} \in & \left[0, \frac{c\delta}{y_1(s_1)y_1(s_2)} \right] \\ & \bigcup \left[\max_{s \in \{s_1, s_2\}} \frac{c}{y_1(s)}, \frac{2c}{y_2(s_2) + y_2(s_1) + (s_1 + s_2 - 4)\delta y_3} \right] \\ & \bigcup \left[\frac{c}{y_3}, 1 \right], \text{ or} \end{aligned}$$

$$(ii) \text{ for } \delta < \max_{s \in \{s_1, s_2\}} \frac{s-3}{n-3},$$

$$F_{12} \in \left[0, \frac{c\delta}{y_1(s_1)y_1(s_2)} \right] \bigcup \left[\frac{c}{y_3}, 1 \right],$$

We illustrate the compatibility (and incompatibility) between the pairwise stable and efficient structures in Fig. 3.8. The intersections of efficient and pairwise stable structures are highlighted.

Corollary 3.4.6 *Consider n individuals partitioned into groups P_1 and P_2 of sizes s_1 and s_2 , respectively. Under the assumption $c < y_3$, if the efficient structure is not pairwise stable, then the efficient structure has more interconnections than the pairwise stable structure.*

Proof: If the efficient structure is not pairwise stable, it implies that it can be changed by Formation Dynamics. Suppose that it has less interconnections than pairwise stable structure. Then, adding interconnections can make it pairwise stable, which means that both players involved in the interconnection benefit from this interconnection. Then the social welfare increases which is conflict with the fact that the structure is efficient. Thus, the efficient structure has more interconnections than the pairwise stable structure. ■

Remark 3.4.7 For the two intervals $\frac{c\delta}{y_1(s_1)y_1(s_2)} < F_{12} < \max_{s \in \{s_1, s_2\}} \frac{c}{y_1(s)}$ and $\frac{2c}{y_2(s_2) + y_2(s_1) + (s_1 + s_2)} < F_{12} < \max_{s \in \{s_1, s_2\}} \frac{c}{y_2(s)}$, the pairwise stable structure is not efficient. For $\max_{s \in \{s_1, s_2\}} \frac{c}{y_2(s)} \leq F_{12} < \frac{c}{y_3}$, the pairwise stable structure might not be efficient. This is because individuals are rational and selfish (i.e., they only care about their own payoffs.) Therefore, total social utility might drop when an individual tries to maximize its own payoff. Specifically,

(i) when $\frac{c\delta}{y_1(s_1)y_1(s_2)} < F_{12} < \max_{s \in \{s_1, s_2\}} \frac{c}{y_1(s)}$, an individual experiences loss by having an interconnection, although that interconnection could bring profit for other individuals and, therefore, result in an increase of total utility. The individual refuses to add or maintain this interconnection.

(ii) when $\frac{2c}{y_2(s_2) + y_2(s_1) + (s_1 + s_2 - 4)\delta y_3} < F_{12} < \frac{c}{y_3}$, as mentioned in the proof of Theorem 3.4.4, there exists at least one interconnection $\{(i, j)\}, i \in P_1, j \in P_2$. For the two individuals $\hat{i} \in P_1$ and $\hat{j} \in P_2$ ($\hat{i} \neq i, \hat{j} \neq j$), an interconnection causes loss for the player from the larger group, but brings profit for all other individuals, which results in removal of the interconnection or rejection in adding it and, therefore, in total utility loss.

Fig. 3.9 shows the number of interconnections and social welfare for both efficient and stable structures for two cliques of sizes 3 and 5, where the value of $\delta = 0.5$ and $c = 0.2$.

Note that:

(i) As shown in Fig. 3.9a, when $F_{12} = \frac{c}{y_3}$ which evaluates to 0.8 for the choice of our parameters, there exist non unique pairwise stable and efficient structures, and the number of interconnections for those structures vary between 3 and 15.

(ii) As shown in Fig. 3.9a and Fig. 3.9b, for $F_{12} \in (0.67, 0.2) \cup (0.23, 0.53)$, the pairwise stable structure is not efficient and thus the social welfare of efficient structures is always greater than that of pairwise stable structures. Fig. 3.10 shows plot of

PoA as a function of F_{12} . We observe that the slope for $F_{12} \in (0.67, 0.2)$ is the highest. This is because in this interval, the pairwise stable structure does not have any interconnection, whereas the efficient structure has one interconnection. This link brings large value for the overall network and makes a large difference in social welfare of two kinds of structures.

We next discuss the evolution of intra vs. interconnections according to Formation Dynamics, when starting from an empty graph.

Remark 3.4.8 (Formation of intra- vs. interconnections) *Starting from an empty (or sparse) graph, initially the speed of formation of intra-connections is generally higher than that of interconnections. Fig. 3.11 illustrates the fact that at the beginning of the formation dynamics, a certain amount of intra-connections is required to produce enough incentives for both groups to communicate through an interconnection.*

3.5 Multigroup Connectivity Structure

In what follows we analyze the more general case of having more than two groups. Consider n individuals partitioned into groups P_1, \dots, P_m , and the payoff function defined above with 1-benefit $\delta < 1$ and edge cost c , and functions y_1 , y_2 , and y_3 . From Theorem 3.3.1 we know that each group forms a clique when $y_3 > c$. We introduce the undirected graph $\mathcal{T} = (\mathcal{V}_P, \mathcal{E}_{\mathcal{T}})$, whose nodes represent groups and $(\alpha, \beta) \in \mathcal{E}_{\mathcal{T}}$ if there exists at least one connection between P_α and P_β .

Theorem 3.5.1 (Sufficiency Condition for Minimally Connected Cliques) *Consider n individuals partitioned into groups P_1, \dots, P_m of sizes s_1, \dots, s_m respectively. Assume that $c < y_3$ and \mathcal{T} is connected. Then, there exists a pairwise stable structure consisting of minimally connected cliques along \mathcal{T} , if*

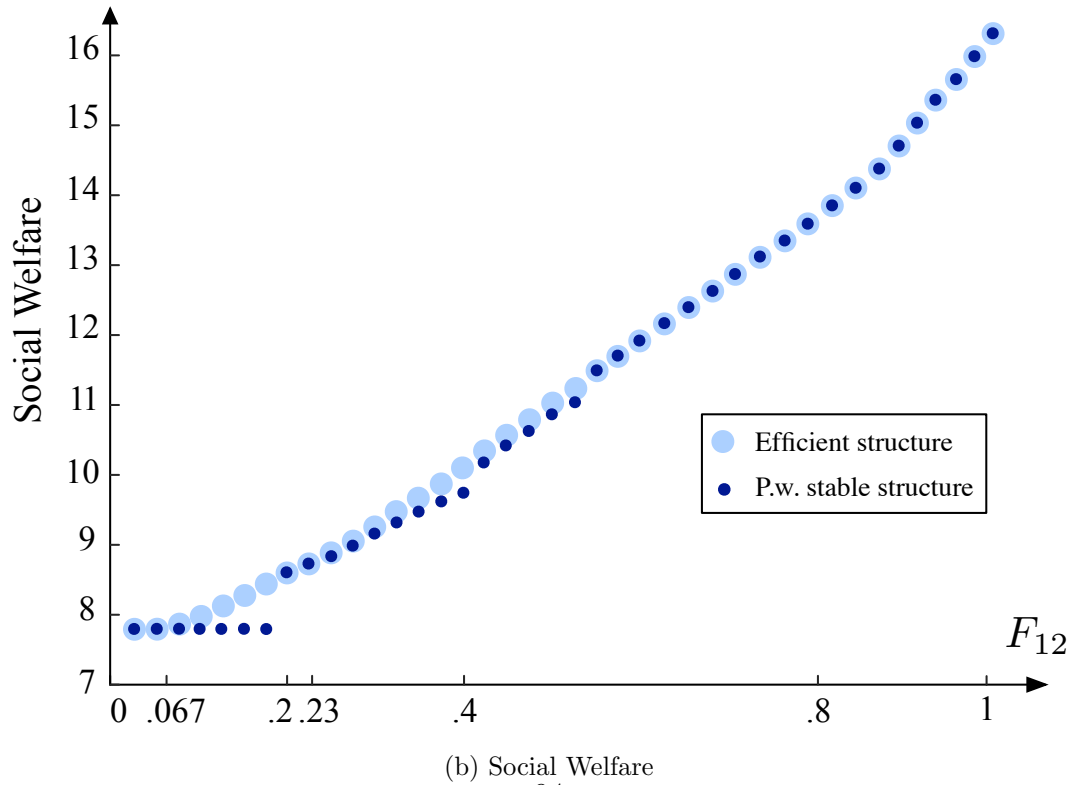
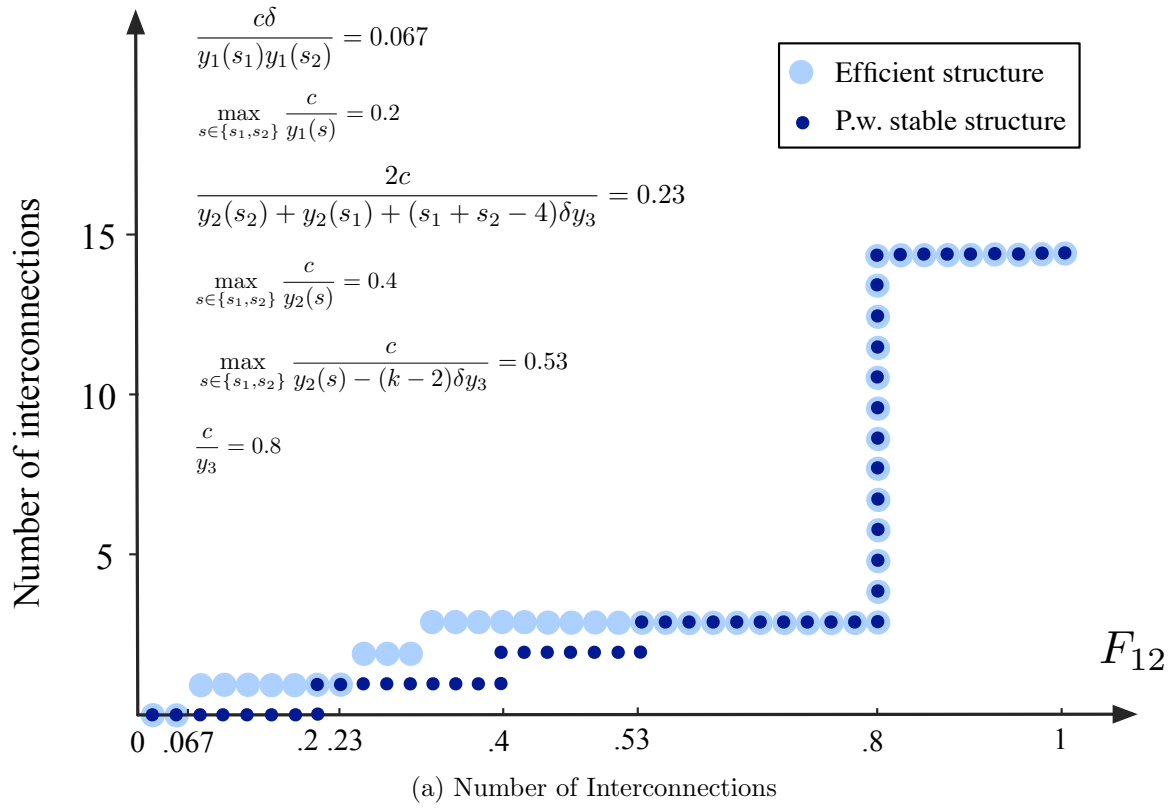


Figure 3.9: Plots of no. of interconnections and social welfare as a function of F_{12} for two groups of sizes 3 and 5, $\delta = 0.5$, $c = 0.2$.

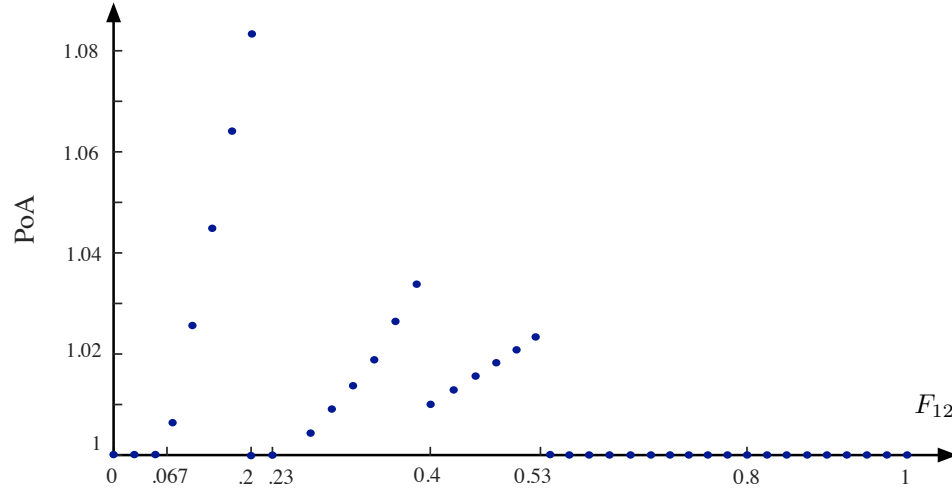


Figure 3.10: Plot of price of anarchy as a function of F_{12} for two groups of sizes 3 and 5, $\delta = 0.5$, $c = 0.2$.

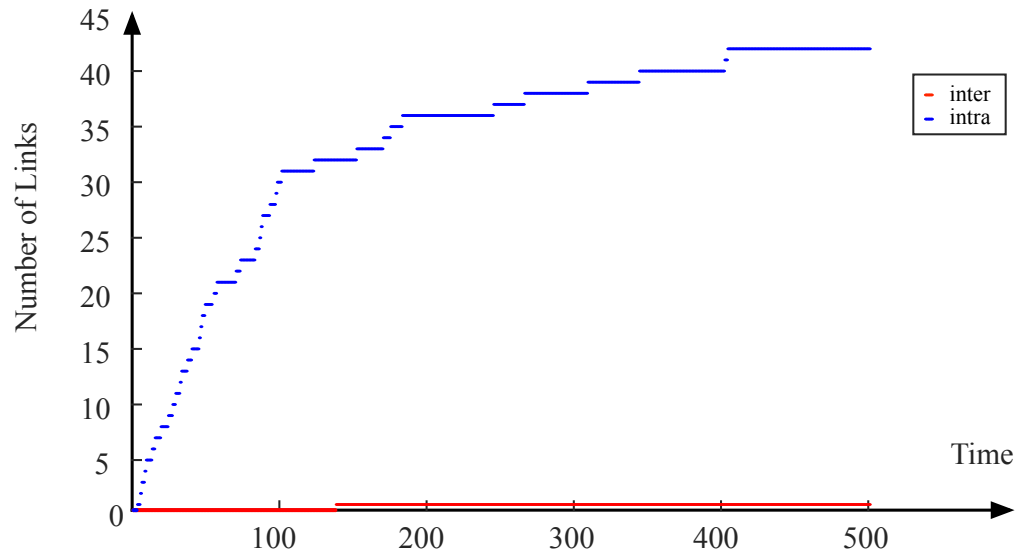


Figure 3.11: Time evolution of the number of inter- and intra-connections for two cliques of size 7.

(i) for all $(\alpha, \beta) \in \mathcal{E}_{\mathcal{T}}$, $\alpha, \beta \in \{1, \dots, m\}$,

$$\begin{aligned} \sum_{\lambda \neq \alpha, \lambda=1}^m F_{\alpha\lambda}(\delta^{d'_{\alpha\lambda}} - \delta^{d_{\alpha\lambda}})(1 + (s_{\lambda} - 1)\delta) &> c, \\ \sum_{\lambda \neq \beta, \lambda=1}^m F_{\beta\lambda}(\delta^{d'_{\beta\lambda}} - \delta^{d_{\beta\lambda}})(1 + (s_{\lambda} - 1)\delta) &> c, \\ F_{\alpha\beta} &< \max_{s \in \{s_{\alpha}, s_{\beta}\}} \frac{c}{y_2(s)}; \text{ and} \end{aligned} \quad (3.4)$$

(ii) for all $(\alpha, \beta) \notin \mathcal{E}_{\mathcal{T}}$, $\alpha, \beta \in \{1, \dots, m\}$,

$$\begin{aligned} \sum_{\lambda \neq \alpha, \lambda=1}^m F_{\alpha\lambda}(\delta^{d'_{\alpha\lambda}} - \delta^{d_{\alpha\lambda}})(1 + (s_{\lambda} - 1)\delta) &< c, \\ \text{or } \sum_{\lambda \neq \beta, \lambda=1}^m F_{\beta\lambda}(\delta^{d'_{\beta\lambda}} - \delta^{d_{\beta\lambda}})(1 + (s_{\lambda} - 1)\delta) &< c, \end{aligned} \quad (3.5)$$

where $d'_{\mu\lambda} = d_{\mu\lambda}(\mathcal{E}_{\mathcal{T}} \cup \{(\alpha, \beta)\})$ and $d_{\mu\lambda} = d_{\mu\lambda}(\mathcal{E}_{\mathcal{T}} \setminus \{(\alpha, \beta)\})$.

Proof: Suppose the network \mathcal{E}_0 (consisting of disjoint cliques) be connected along \mathcal{T} and satisfy

- (i) if $(\alpha, \beta) \in \mathcal{E}_{\mathcal{T}}$, there is only one inter-link between P_{α} and P_{β} ;
- (ii) for every group P_{α} , only one agent i_{α} has inter-links.

For any pair of (α, β) , let $\mathcal{E}'' = \mathcal{E}_0 \cup \{(i_{\alpha}, i_{\beta})\}$ and $\mathcal{E}' = \mathcal{E}_0 \setminus \{(i_{\alpha}, i_{\beta})\}$. it is easy to find that

$$U_i(\mathcal{E}'') - U_i(\mathcal{E}') = \sum_{k=1, k \neq \alpha}^m F_{k\alpha} \sum_{l \in P_k} (\delta^{d_{il}(\mathcal{E}'')} - \delta^{d_{il}(\mathcal{E}')} - c).$$

Therefore, we have

$$U_{i_{\alpha}}(\mathcal{E}'') - U_{i_{\alpha}}(\mathcal{E}') = \sum_{\lambda \neq \alpha, \lambda=1}^m F_{\alpha\lambda}(\delta^{d'_{\alpha\lambda}} - \delta^{d_{\alpha\lambda}})(1 + (s_{\lambda} - 1)\delta) - c$$

and

$$U_{i_\beta}(\mathcal{E}'') - U_{i_\alpha}(\mathcal{E}') = \sum_{\lambda \neq \beta, \lambda=1}^m F_{\beta\lambda}(\delta^{d'_{\beta\lambda}} - \delta^{d_{\beta\lambda}})(1 + (s_\lambda - 1)\delta) - c.$$

Therefore, for $(\alpha, \beta) \in \mathcal{E}_T$, it follows from (3.4) that \mathcal{E}'' defeats \mathcal{E}' . Similar to the proof of Theorem 3.4.1, since $F_{\alpha\beta} < \max_{s \in \{s_\alpha, s_\beta\}} \frac{c}{y_2(s)}$, there only exists one inter-link between P_α and P_β . For $(\alpha, \beta) \notin \mathcal{E}_T$, (3.5) implies that there exist no inter-link between P_α and P_β .

By Theorem 3.2.4, since network \mathcal{E}_0 can not be changed under dynamics, we can conclude that network \mathcal{E}_0 is stable. ■

Remark 3.5.2 *Theorem 3.5.1 answers the question: given a certain matrix F and graph structure \mathcal{E} is \mathcal{E} pairwise stable or not?*

Corollary 3.5.3 *For the special case of interconnection structure being a star, with P_γ as the central group, the sufficient condition of Theorem 3.5.1 can be simplified as follows:*

(i) for all $\alpha \in \{1, \dots, m\}$, $(\alpha \neq \gamma)$

$$F_{\alpha\gamma} > \max_{s \in \{s_\alpha, s_\gamma\}} \frac{c}{y_1(s)}; \text{ and}$$

(ii) for all $(\alpha, \beta) \in \{1, \dots, m\}$, $(\alpha, \beta \neq \gamma)$,

$$F_{\alpha\beta} < \max_{s \in \{s_\alpha, s_\beta\}} \frac{c}{y_2(s)}.$$

In the following example, we illustrate that due to randomness in choosing the pair of players, Formation Dynamic does not always converge to a unique stable structure even for the same initial network structure and matrix F .

Example 3.5.4 Consider the case where we have $\frac{c}{y_1(s)} < F_{\alpha\beta} < \frac{c}{y_2(s)}$ for all α, β , and that $\delta < \frac{\sqrt{5}-1}{2}$. We have five equal size groups named $\{1, 2, \dots, 5\}$. Two different processes are shown in Fig. 3.12.

Process (A) For the process shown in Fig. 3.12a the order of pair selection is as follows: $(1, 2) \rightarrow (1, 3) \rightarrow (1, 4) \rightarrow (1, 4) \rightarrow (1, 5)$. Note that by $(1, 2)$ we mean an individual selected from group 1 paired with an individual from group 2, which results in the star graph being the convergent pairwise stable structure.

Process (B) Now, consider the process shown in Fig. 3.12b for which the order of pairs of groups selected is as follows: $(2, 3) \rightarrow (1, 2) \rightarrow (1, 3) \rightarrow (1, 4) \rightarrow (3, 5) \rightarrow (2, 4) \rightarrow (4, 5)$. At the very last step, we have:

$$\begin{aligned} & U_i(\mathcal{E} \cup \{4, 5\} - U_i(\mathcal{E} \setminus \{4, 5\})) \\ &= F_{45}(y_1(s)) - F_{45}(\delta^3 y_1(s)) \\ &\quad + F_{35}(\delta y_1(s)) - F_{35}(\delta^2 y_1(s)) - c. \end{aligned}$$

Since $F_{35}, F_{45} < \frac{c}{y_1(s)}$ and $\delta < \frac{\sqrt{5}-1}{2}$, we conclude that

$$F_{45}(1 - \delta^3) + F_{35}(\delta - \delta^2) > \frac{c}{y_1(s)}.$$

Consequently, we obtain

$$U_i(\mathcal{E} \cup \{4, 5\} - U_i(\mathcal{E} \setminus \{4, 5\})) > 0$$

which means that the connection $(4, 5)$ is formed. Now since we have $F_{\alpha\beta} < \frac{c}{y_2(s)}$, no connected triad and thereby, no additional links will be formed. Also no link will be removed. Therefore, the final structure in Fig. 3.12b, which is a ring, is stable.

Example 3.5.4 shows that, based on the order of the sequence of selected pairs, we can have two or possibly more convergent stable structures, and therefore, the convergence results cannot be generalized and the convergent structure is not always unique.

From Theorem 3.3.1 we know that each group forms a clique. We now analyze the interconnections among those cliques. Theorem 3.5.5 addresses the redundancy of interconnections.

Theorem 3.5.5 (Formation of Redundancies) *Consider n individuals partitioned into groups P_1, \dots, P_m of sizes s_1, s_2, \dots, s_m . Suppose that $c < y_3$. Then, under Formation Dynamics,*

(i) *redundant interconnections between P_α and P_β will be formed and never removed,*

$$\text{if } F_{\alpha\beta} > \max_{s \in \{s_\alpha, s_\beta\}} \frac{c}{y_2(s)}, \text{ and}$$

(ii) *maximal interconnections between P_α and P_β will be formed and never removed, if*

$$\frac{c}{y_3} < F_{\alpha\beta} \leq 1.$$

Fig. 3.13 illustrates the scenarios for $F_{\alpha\beta}$'s. The horizontal axis corresponds to the values of $F_{\alpha\beta}$ where $\{\alpha\beta\}$ belongs to the edge-set of the spanning tree, and the vertical axis corresponds to all other $F_{\alpha\beta}$'s.

Theorem 3.5.6 (Efficiency) *For n individuals partitioned into groups according to P , the efficient structure requires the same node to be chosen from each clique to provide bridges to other cliques, i.e., for a fixed interconnection structure and number of nodes, choosing the same representative from each clique increases the social welfare.*

Proof: Suppose that the density and the structure of interconnections are fixed. It is easy to see that by choosing the same representative from each clique, the distance between individuals from different cliques would be shortened, resulting in the term δ_{ij}^d in equations (3.1) being larger. Therefore, the social welfare will increase. ■

However, this structure is unlikely to be pairwise stable since the representative would bear a high cost for maintaining these interconnections. Figure 3.15 illustrates two networks with the same interconnection structures where one network has higher social welfare due to each group having only one representative.

3.6 Conclusion

This chapter proposes the first strategic network formation model that, given a matrix specifying the frequency of a coordination problem among groups, identifies the conditions that result in multigroup formation. The model deviates from the seminal papers on strategic network formation in that it accounts for heterogeneous frequency of control problems arising among the individuals and investigates pairwise stability and efficiency of multigroup connectivity structures, as well as convergence of the formation dynamics.

In our model link formations occur bilaterally and thus many of the classical game-theoretic concepts do not apply to our framework. In particular, to study equilibrium structures, we utilize the concept of pairwise stability. A key challenge in our problem stems from the fact that not many tools are available for rigorous analysis or that they cannot be applied to the case of heterogeneous coordination problems among groups.

We identified the ranges of parameters where pairwise stable and efficient structures do and do not coincide and concluded that, for two-group structures, the efficient structures always has the same or a larger number of links than the pairwise stable ones. We also considered the price of anarchy and observed that the highest value occurs for the case when pairwise stable structures consist of disjoint union of cliques and the efficient structure has one link. Similar to the classical models, at the two ends of the spectrum of link values there is an overlap between efficient and stable structures.

We presented the conditions that result in the formation dynamics starting from

an invariant set converge to cliques, and provided rigorous results for the number of interconnections in two-group structures. However, exact identification of the boundaries that result in certain number of interconnections among arbitrary number of groups with arbitrary size and interconnection structure is out of scope of this chapter.

We note that by providing a full characterization of pairwise stability and efficiency for a two-group model, we focus on local topologies versus global topologies, as the individual interconnections can capture valuable information about the whole network and that all interconnections have subsets of two groups. This can be interpreted into taking the distance only for the people in one's group or in the next immediate group in the utility function.

3.7 Permissions and Attributions

The content of chapter 3 is the result of a collaboration with professor Jingying Ma. The authors thank professors Ambuj K. Singh and Noah E. Friedkin for their valuable comments and suggestions. This material is based upon work supported by, or in part by, the U.S. Army Research Laboratory and the U.S. Army Research Office under grant numbers W911NF-15-1-0577, and the National Natural Science Foundation of China under grant 61963032.

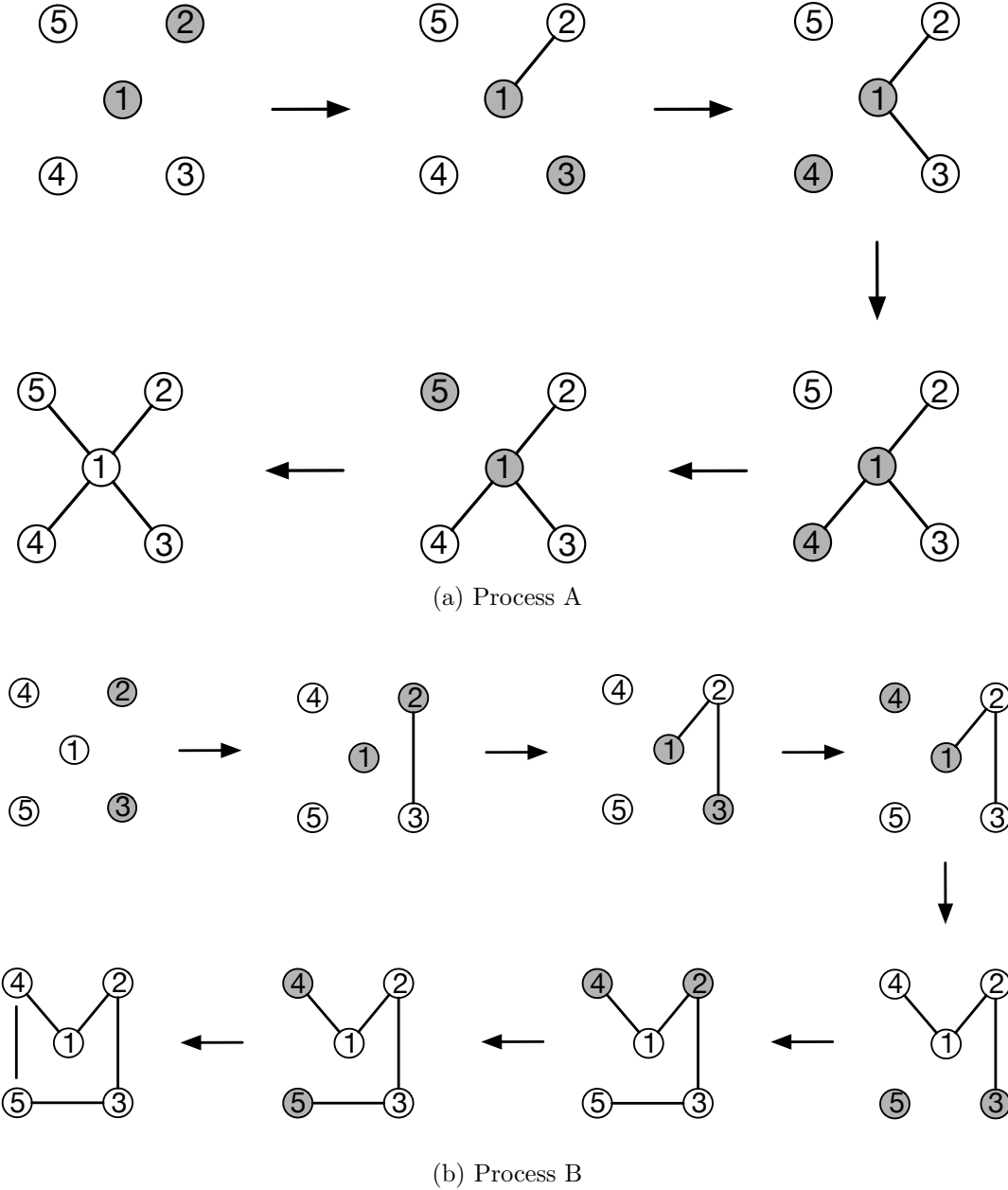


Figure 3.12: The processes of Example 3.5.4. At each step, shaded nodes represent the groups which the selected individuals belong to, and the outcome of the game (action taken regarding link addition, link removal, or indifference) is represented in the next.

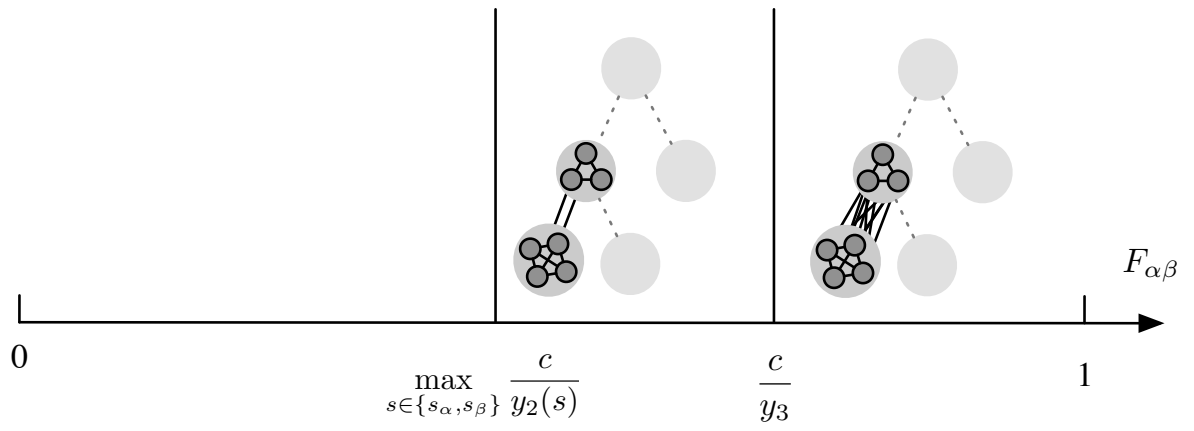
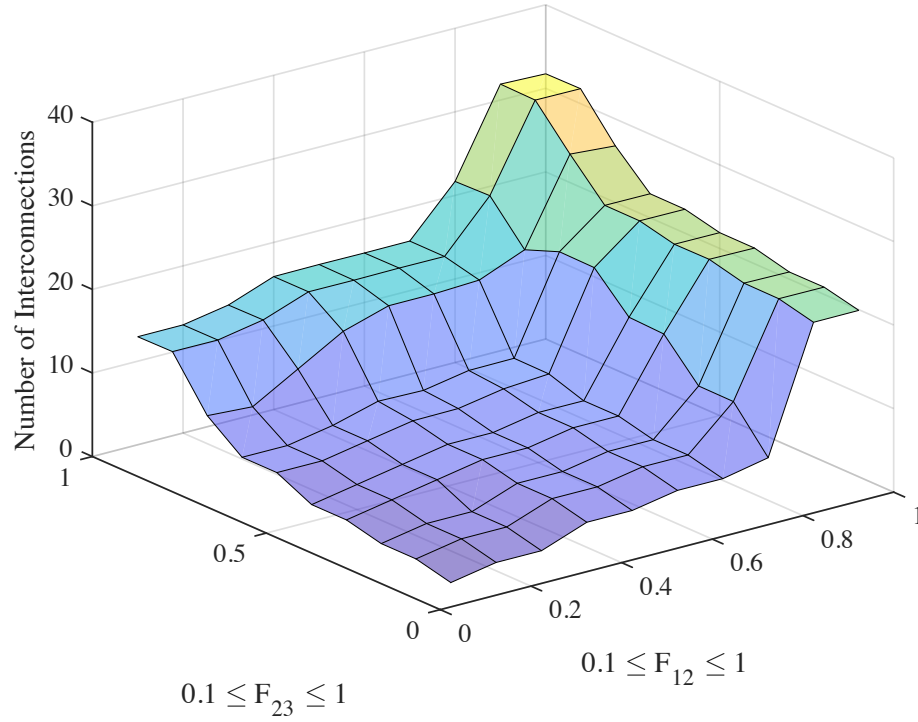
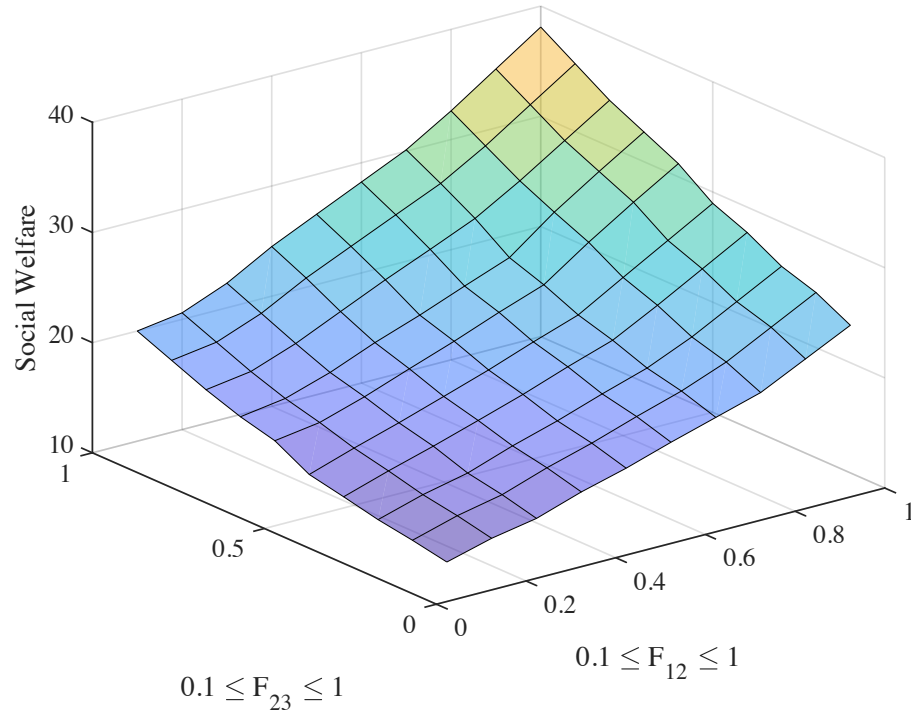


Figure 3.13: An illustration of ranges of parameter space in Theorem 3.5.5

Number of Interconnections for Three Groups of Sizes 3, 4, and 5

(a) Number of Interconnections

Social Welfare for Three Groups of Sizes 3, 4, and 5

(b) Social Welfare

Figure 3.14: Three groups of sizes 3, 4, and 5, $\delta = 0.5$, $c = 0.2$

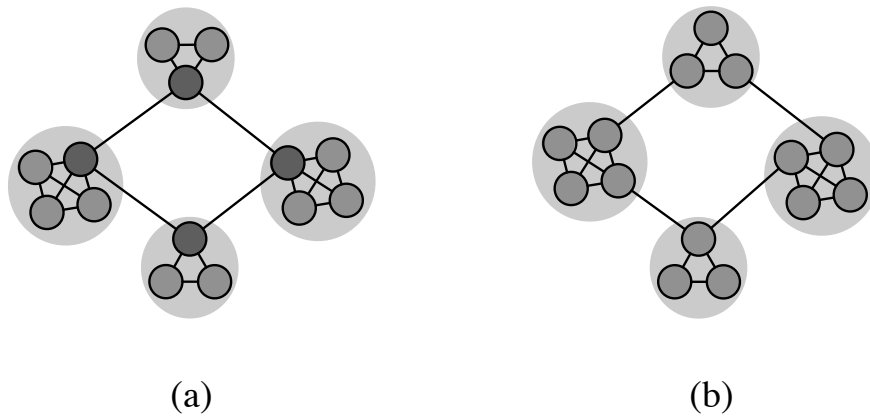


Figure 3.15: In network a) each clique has only one representative, whereas in figure b) some cliques have multiple representatives.

Appendix A

Algorithm Specifications

In this appendix we present a detailed pseudocode description for three relevant algorithms. Specifically, we present pseudocode for generating relative subgroup sizes, for the sub-problem of generating a sequence of realizations of a random variable subject to a fixed sum, and for the liaison generative model.

Algorithm 1 Generating sequence of relative subgroup sizes

Input: n = number of nodes

Parameters: $\alpha = 3$ exponent of power law

Output: sequence of relative subgroup sizes p

- 1: Define a random variable X taking values over $\{3, 4, \dots, n\}$, with probability mass function $P[X = x] \propto 1/x^3$ to denote the random size of the subgroups
 - 2: Invoke Algorithm 2 to incrementally and greedily generate a sequence of realizations for X , denoted by $\{S_1, \dots, S_k\}$, satisfying the constraint $S_1 + \dots + S_k = n$
 - 3: **for** $i = 1 : k$ **do**
 - 4: $p_i \leftarrow S_i/n$
 - 5: **end for**
 - 6: **return** p
-

Algorithm 2 Generating a sequence of realizations of a given random variable with fixed sum

Input: a discrete variable X taking values in $\{x_{\min}, \dots, x_{\max}\}$ with given pmf, number: n

Output: $S = \{S_1, \dots, S_k\}$ a sequence of realizations of X , adjusted in a greedy incremental way such that $S_0 + \dots + S_k = n$

```
1:  $S \leftarrow \{\}$ ,  $n_{\text{tmp}} \leftarrow n$ 
2: while  $n_{\text{tmp}} \geq x_{\min}$  do
3:    $\bar{x} \leftarrow$  realization of  $X$ 
4:   if  $\bar{x} \leq n_{\text{tmp}}$  then
5:      $S \leftarrow S \cup \{\bar{x}\}$ ,
6:      $n_{\text{tmp}} \leftarrow n_{\text{tmp}} - \bar{x}$ 
7:   end if
8: end while
9: for  $i = 1 : n_{\text{tmp}}$  do
10:  Randomly select an number  $S^*$  in the sequence  $S$  satisfying  $S^* < x_{\max}$ 
11:   $S^* \leftarrow S^* + 1$ 
12: end for
13: return  $S$ 
```

Algorithm 3 Liaison hierarchy connectivity

Input: collection of subgroups generated using Algorithm 1

Parameters: branching factor of each liaison = 2 or 3

Output: graph composed of subgroups plus hierarchy interconnections

```
1: Define a random variable  $L$  taking values over  $\{2, 3\}$ , with pmf  $P[L = l] \propto 1/l^3$  to
   denote the random branching factor of liaisons
2:  $n_l \leftarrow$  no. of subgroups
3: while  $n_l > 1$  do
4:   invoke Algorithm 2 to generate a sequence of realizations for  $L$ , denoted by
      $\{S_1, \dots, S_k\}$ , satisfying the constraint  $S_1 + \dots + S_k = n_l$ 
5:   for  $i = 1 : k$  do
6:     Generate a liaison with branching factor  $S_i$ 
7:     Incrementally connect the liaison to  $S_i$  unattended subgroups, if any exist, or
       unattended liaisons, after attending to all subgroups
8:   end for
9:    $n_l \leftarrow k$ 
10: end while
11: Assign one liaison to the top of the hierarchy
12: return hierarchical tree with the subgroups as the leaves
```

Bibliography

- [1] H. W. Hethcote, *The mathematics of infectious diseases*, *SIAM Review* **42** (2000), no. 4 599–653.
- [2] A. Lajmanovich and J. A. Yorke, *A deterministic model for gonorrhea in a nonhomogeneous population*, *Mathematical Biosciences* **28** (1976), no. 3 221–236.
- [3] H. W. Hethcote, *An immunization model for a heterogeneous population*, *Theoretical Population Biology* **14** (1978), no. 3 338–349.
- [4] F. D. Sahneh, C. Scoglio, and P. Van Mieghem, *Generalized epidemic mean-field model for spreading processes over multilayer complex networks*, *IEEE/ACM Transactions on Networking* **21** (2013), no. 5 1609–1620.
- [5] N. Azizan Ruhi and B. Hassibi, *SIRS epidemics on complex networks: Concurrence of exact Markov chain and approximated models*, in *IEEE Conf. on Decision and Control*, pp. 2919–2926, Dec., 2015.
- [6] R. Pastor-Satorras, C. Castellano, P. V. Mieghem, and A. Vespignani, *Epidemic processes in complex networks*, *Reviews of Modern Physics* **87** (2015) 925–979.
- [7] C. Nowzari, V. M. Preciado, and G. J. Pappas, *Analysis and control of epidemics: A survey of spreading processes on complex networks*, *IEEE Control Systems* **36** (2016), no. 1 26–46.
- [8] F. Bullo, *Lectures on Network Systems*. Kindle Direct Publishing, 1.3 ed., July, 2019. With contributions by J. Cortés, F. Dörfler, and S. Martínez.
- [9] L. J. S. Allen, *Some discrete-time SI, SIR, and SIS epidemic models*, *Mathematical Biosciences* **124** (1994), no. 1 83–105.
- [10] Y. Wang, D. Chakrabarti, C. Wang, and C. Faloutsos, *Epidemic spreading in real networks: An eigenvalue viewpoint*, in *IEEE Int. Symposium on Reliable Distributed Systems*, (Florence, Italy), pp. 25–34, Oct., 2003.
- [11] H. J. Ahn and B. Hassibi, *Global dynamics of epidemic spread over complex networks*, in *IEEE Conf. on Decision and Control*, (Florence, Italy), pp. 4579–4585, Dec., 2013.

- [12] P. Van Mieghem, J. Omic, and R. Kooij, *Virus spread in networks*, *IEEE/ACM Transactions on Networking* **17** (2009), no. 1 1–14.
- [13] A. Fall, A. Iggidr, G. Sallet, and J.-J. Tewa, *Epidemiological models and Lyapunov functions*, *Mathematical Modelling of Natural Phenomena* **2** (2007), no. 1 62–68.
- [14] A. Khamis, T. Başar, and B. Ghahserifard, *Stability of epidemic models over directed graphs: A positive systems approach*, *Automatica* **74** (2016) 126–134.
- [15] F. Chung, L. Lu, and V. Vu, *Spectra of random graphs with given expected degrees*, *Proceedings of the National Academy of Sciences* **100** (2003), no. 11 6313–6318.
- [16] C. Castellano and R. Pastor-Satorras, *Thresholds for epidemic spreading in networks*, *Physical Review Letters* **105** (2010) 218701.
- [17] N. Schwartz and L. Stone, *Exact epidemic analysis for the star topology*, *Physical Review E* **87** (2013) 042815.
- [18] M. Ogura and V. M. Preciado, *Second-order moment-closure for tighter epidemic thresholds*, 2017. arXiv preprint.
- [19] H. Guo, M. Li, and Z. Shuai, *A graph-theoretic approach to the method of global Lyapunov functions*, *Proceedings of the American Mathematical Society* **136** (2008), no. 8 2793–2802.
- [20] M. Youssef and C. Scoglio, *An individual-based approach to SIR epidemics in contact networks*, *Journal of Theoretical Biology* **283** (2011), no. 1 136–144.
- [21] K. J. Sharkey, *Deterministic epidemiological models at the individual level*, *Journal of Mathematical Biology* **57** (2008) 311–331.
- [22] K. J. Sharkey, I. Z. Kiss, R. R. Wilkinson, and P. L. Simon, *Exact equations for SIR epidemics on tree graphs*, *Bulletin of Mathematical Biology* **77** (2015) 614–645.
- [23] M. Mesbahi and M. Egerstedt, *Graph Theoretic Methods in Multiagent Networks*. Princeton University Press, 2010.
- [24] M. E. J. Newman, *Networks: An Introduction*. Oxford University Press, 2010.
- [25] D. Easley and J. Kleinberg, *Networks, Crowds, and Markets: Reasoning About a Highly Connected World*. Cambridge University Press, 2010.
- [26] A. Barrat, M. Barthélemy, and A. Vespignani, *Dynamical Processes on Complex Networks*. Cambridge University Press, 2008.
- [27] F. Brauer and C. Castillo-Chavez, *Mathematical Models in Population Biology and Epidemiology*. Springer, 2012.

- [28] F. Blanchini and S. Miani, *Set-Theoretic Methods in Control*. Springer, 2015.
- [29] C. D. Meyer, *Matrix Analysis and Applied Linear Algebra*. SIAM, 2001.
- [30] D. Krackhardt, *Cognitive social structures*, *Social Networks* **9** (1987), no. 2 109–134.
- [31] M. Ogura and V. M. Preciado, *Stability of spreading processes over time-varying large-scale networks*, *IEEE Transactions on Network Science and Engineering* **3** (2016) 44–57.
- [32] P. E. Paré, C. L. Beck, and A. Nedić, *Epidemic processes over time-varying networks*, *IEEE Transactions on Control of Network Systems* (2017). to appear.
- [33] C. Nowzari, V. M. Preciado, and G. J. Pappas, *Optimal resource allocation for control of networked epidemic models*, *IEEE Transactions on Control of Network Systems* **4** (2017) 159–169.
- [34] E. Ramírez-Llanos and S. Martínez, *A distributed dynamics for virus-spread control*, *Automatica* **76** (2017) 41–48.
- [35] S. Goyal, H. Heidari, and M. Kerans, *Competitive contagion in networks*, *Games and Economic Behavior* (2014). in press.
- [36] P. E. Paré, J. Liu, C. L. Beck, A. Nedić, and T. Başar, *Multi-competitive viruses over static and time-varying networks*, in *American Control Conference*, pp. 1685–1690, 2017.
- [37] W. Mei and F. Bullo, *Competitive propagation: Models, asymptotic behavior and quality-seeding games*, *IEEE Transactions on Network Science and Engineering* **4** (2017), no. 2 83–99.
- [38] W. Wang and X. Zhao, *An epidemic model in a patchy environment*, *Mathematical Biosciences* **190** (2004) 97–112.
- [39] V. Colizza, A. Barrat, M. Barthélemy, and A. Vespignani, *The role of the airline transportation network in the prediction and predictability of global epidemics*, *Proceedings of the National Academy of Sciences* **103** (2005), no. 7 2015–2020.
- [40] J. Arino and P. van den Driessche, *A multi-city epidemic model*, *Mathematical Population Studies* **10** (2010) 175–193.
- [41] R. Likert, *The Human Organization: Its Management and Values*. McGraw-Hill, 1967.
- [42] O. E. Williamson, *Corporate Control and Business Behavior: An Inquiry into the Effects of Organization Form on Enterprise Behavior*. Prentice Hall, 1970.

- [43] N. E. Friedkin and E. C. Johnsen, *Control loss and Fayol's gangplanks*, *Social Networks* **24** (2002), no. 4 395–406.
- [44] M. Crozier, *The Bureaucratic Phenomenon*. University of Chicago Press, Chicago, 1964.
- [45] N. E. Friedkin, *A Structural Theory of Social Influence*. Cambridge University Press, 1998.
- [46] M. S. Granovetter, *The strength of weak ties*, *American Journal of Sociology* **78** (1973), no. 6 1360–1380.
- [47] D. F. Schwartz and E. D. Jacobson, *Organizational communication network analysis: The liaison communication role*, *Organizational Behavior and Human Performance* **18** (1977), no. 1 158–174.
- [48] M. Tortoriello and D. Krackhardt, *Activating cross-boundary knowledge: The role of simmelian ties in the generation of innovations*, *Academy of Management Journal* **53** (2010), no. 1 167–181.
- [49] W. Stam and T. Elfring, *Entrepreneurial orientation and new venture performance: The moderating role of intra-and extraindustry social capital*, *Academy of Management Journal* **51** (2008), no. 1 97–111.
- [50] M. Granovetter, *The strength of weak ties: A network theory revisited*, *Sociological Theory* **1** (1983), no. 1 201–233.
- [51] W. R. Evans and W. D. Davis, *High-performance work systems and organizational performance: The mediating role of internal social structure*, *Journal of Management* **31** (2005), no. 5 758–775.
- [52] N. E. Friedkin, *Horizons of observability and limits of informal control in organizations*, *Social Forces* **62** (1983), no. 1 54–77.
- [53] H. C. White, S. A. Boorman, and R. L. Breiger, *Social structure from multiple networks. I. Blockmodels of roles and positions*, *American Journal of Sociology* **81** (1976), no. 4 730–780.
- [54] S. A. Boorman and H. C. White, *Social structure from multiple networks. II. Role structures*, *American Journal of Sociology* **81** (1976), no. 6 1384–1446.
- [55] E. N. Sawardecker, M. Sales-Pardo, and L. A. N. Amaral, *Detection of node group membership in networks with group overlap*, *The European Physical Journal B* **67** (2009), no. 3 277–284.

- [56] B. Cornwell and J. A. Harrison, *Union members and voluntary associations: Membership overlap as a case of organizational embeddedness*, *American Sociological Review* **69** (2004), no. 6 862–881.
- [57] S. P. Borgatti and D. S. Halgin, *Analyzing affiliation networks*, *The Sage Handbook of Social Network Analysis* (2011) 417–433.
- [58] J. R. Galbraith, *Organization design: An information processing view*, *Interfaces* **4** (1974), no. 3 28–36.
- [59] E. V. Reynolds and J. D. Johnson, *Liaison emergence: Relating theoretical perspectives*, *Academy of Management Review* **7** (1982), no. 4 551–559.
- [60] A. V. Singhal, A. Jha, and A. Gairola, *A networking solution for disaster management to address liaison failures in emergency response*, *Risk Analysis IX* **47** (2014) 401.
- [61] P. W. Holland, K. Laskey, and S. Leinhardt, *Stochastic blockmodels: First steps*, *Social Networks* **5** (1983), no. 2 109–137.
- [62] S. E. Fienberg and S. S. Wasserman, *Categorical data analysis of single sociometric relations*, *Sociological Methodology* **12** (1981) 156–192.
- [63] Y. J. Wang and G. Y. Wong, *Stochastic blockmodels for directed graphs*, *Journal of the American Statistical Association* **82** (1987), no. 397 8–19.
- [64] E. M. Airoldi, D. M. Blei, S. E. Fienberg, and E. P. Xing, *Mixed membership stochastic blockmodels*, *Journal of Machine Learning Research* **9** (2008) 1981–2014.
- [65] C. Aicher, A. Z. Jacobs, and A. Clauset, *Learning latent block structure in weighted networks*, *Journal of Complex Networks* **3** (2014) 221–248.
- [66] B. Karrer and M. E. J. Newman, *Stochastic blockmodels and community structure in networks*, *Physical Review E* **83** (2011).
- [67] D. J. Watts and S. H. Strogatz, *Collective dynamics of ‘small-world’ networks*, *Nature* **393** (1998) 440–442.
- [68] W. Mei, S. Mohagheghi, S. Zampieri, and F. Bullo, *On the dynamics of deterministic epidemic propagation over networks*, .
- [69] J. R. P. French Jr., *A formal theory of social power*, *Psychological Review* **63** (1956), no. 3 181–194.
- [70] M. H. DeGroot, *Reaching a consensus*, *Journal of the American Statistical Association* **69** (1974), no. 345 118–121.

- [71] M. O. Jackson, *Social and Economic Networks*. Princeton University Press, 2010.
- [72] P. Erdős and A. Rényi, *On Random Graphs, I, Publicationes Mathematicae (Debrecen)* **6** (1959) 290–297.
- [73] A. Jadbabaie and A. Olshevsky, *Scaling laws for consensus protocols subject to noise*, 2017.
- [74] J. G. Kemeny and J. L. Snell, *Finite Markov Chains*. Springer, 1976.
- [75] M. E. J. Newman and M. Girvan, *Finding and evaluating community structure in networks*, *Physical Review E* **69** (2004), no. 2 026113.
- [76] S. Fortunato, *Community detection in graphs*, *Physics Reports* **486** (2010), no. 3-5 75–174.
- [77] S. E. Schaeffer, *Graph clustering*, *Computer Science Review* **1** (2007), no. 1 27–64.
- [78] M. E. J. Newman, *Modularity and community structure in networks*, *Proceedings of the National Academy of Sciences* **103** (2006), no. 23 8577–8582.
- [79] E. Abbe, *Community detection and stochastic block models: Recent developments*, *Journal of Machine Learning Research* **18** (2017), no. 1 6446–6531.
- [80] S. Mohagheghi, P. Agharkar, F. Bullo, and N. E. Friedkin, *Multigroup connectivity structures and their implications*, *Network Science* (2019) 1–17.
- [81] X. Zhang, C. Wang, Y. Su, L. Pan, and H. Zhang, *A fast overlapping community detection algorithm based on weak cliques for large-scale networks*, *IEEE Transactions on Computational Social Systems* **4** (2017), no. 4 218–230.
- [82] J. Yang and J. Leskovec, *Community-affiliation graph model for overlapping network community detection*, in *IEEE International Conference on Data Mining*, (Brussels, Belgium), pp. 1170–1175, 2012.
- [83] M. O. Jackson and A. Wolinsky, *A strategic model of social and economic networks*, *Journal of Economic Theory* **71** (1996), no. 1 44–74.
- [84] M. O. Jackson and A. Watts, *The evolution of social and economic networks*, *Journal of Economic Theory* **106** (2002) 265–295.
- [85] M. O. Jackson and B. W. Rogers, *The economics of small worlds*, *Journal of the European Economic Association* **3** (2005) 617–627.
- [86] V. Bala and S. Goyal, *A noncooperative model of network formation*, *Econometrica* **68** (2000), no. 5 1181–1229.

- [87] N. Olaizola and F. Valenciano, *Network formation under linking constraints*, *Physica A: Statistical Mechanics and its Applications* **392** (2013) 5194–5205.
- [88] G. C. Chasparis and J. S. Shamma, *Network formation: Neighborhood structures, establishment costs, and distributed learning*, *IEEE Transactions on Cybernetics* **43** (2013), no. 6 1950–1962.
- [89] G. C. Chasparis and J. S. Shamma, *Efficient network formation by distributed reinforcement*, in *IEEE Conf. on Decision and Control*, (Cancun, Mexico), pp. 1690–1695, 2008.
- [90] N. Pagan and F. Dörfler, *Game theoretical inference of human behavior in social networks*, *Nature Communications* **10** (2019), no. 1 5507.
- [91] M. McBride, *Imperfect monitoring in communication networks*, *Economic Theory* **126** (2006) 97–119.
- [92] Y. Song and M. van der Schaar, *Dynamic network formation with incomplete information*, *Economic Theory* **59** (2015) 301–331.
- [93] L. Maccari, *Detecting and mitigating points of failure in community networks: A graph-based approach*, *IEEE Transactions on Computational Social Systems* **6** (2019), no. 1 103–116.
- [94] B. Bringmann, M. Berlingerio, F. Bonchi, and A. Gionis, *Learning and predicting the evolution of social networks*, *IEEE Intelligent Systems* **25** (2010), no. 4 26–35.
- [95] Y. Jia, Y. Wang, X. Jin, Z. Zhao, and X. Cheng, *Link inference in dynamic heterogeneous information network: A knapsack-based approach*, *IEEE Transactions on Computational Social Systems* **4** (2017), no. 3 80–92.